Response to Reviewer #1

We thank the reviewer for the valuable comments and suggestions that have helped us improve the paper. Our detailed responses (**Bold**) to the reviewers' questions and comments (*Italic*) are listed below.

P13, L1: Why the correlation of AOD between AERONET and CALIPSO is lower than that between AERONET and MODIS, any interpretations?

This is a good point. The correlation of AOD between AERONET and CALIPSO (r^2 =0.646, N = 70) is found lower than that between AERONET and MODIS (r^2 =0.845, N = 415). One reason is the insufficient data samples for AERONET-CALIPSO AOD comparison, which is also noted by Bibi et al. (2015). Another likely reason is that all these observations have their uncertainties which could make the correlations hardly expected. We have added this into our manuscript in P14 L6-8: "The lower correlation of AOD between AERONET and CALIPSO than that between AERONET and MODIS is likely related to the limited data samples for AERONET-CALIPSO AOD comparison, which is also noted by Bibi et al. (2015)**".**

Bibi, H., Alam, K., Chishtie, F., et al.: Intercomparison of MODIS, MISR, OMI, and CALIPSO aerosol optical depth retrievals for four locations on the Indo-Gangetic plains and validation against AERONET data, Atmospheric Environment, 111, 113-126, 2015.

P13, L7: Any explanation about the reason of "AOD becomes small, it seems that the correlation of AOD between MODIS and AERONET also decreases."

AOD retrieved from AERONET are accurate to within ±0.01 (Dubovik et al., 2000). When AOD becomes small, the relative errors in AOD from both MODIS and AERONET become large, which may be the reason that causes the correlation of AOD between MODIS and AERONET also decrease. We have added this discussion into Pg15 L3-6: "When AOD becomes small, the relative errors in AOD from both MODIS and AERONET become large, which may cause the correlation of AOD between MODIS and AERONET also decrease as demonstrated in Table 1.**".**

P13, L15-17: a lot of information contained in Table 1 and 2 needs more in-depth discussions.

We agree with the reviewer and made further descriptions and discussions in the manuscript, including

(1) The seasonal variations of AOD from different observations and the likely reason for their differences, which are added in P14 L9-19: "Table 1 further shows the inter-comparison results of AOD between AERONET and MODIS in spring (MAM), summer (JJA), fall (SON) and winter (DJF), which include their seasonal averaged AOD, squared correlation, absolute bias, relative bias and sample number. The absolute bias is calculated as the difference of seasonally averaged AOD from

AERONET and MODIS at the same time; and the relative bias is calculated as the ratio of the absolute bias to the seasonally averaged AERONET AOD. The seasonal averaged AOD are 0.49, 0.61, 0.30 and 0.19 respectively in four seasons for AERONET observations, and 0.66, 0.88, 0.39 and 0.21 for MODIS observations, which are highest in summer but lowest in winter. The corresponding sample numbers are 214, 103, 50 and 48 in four seasons. This seasonal variation pattern is also observed by Yu et al. (2009).**".**

(2) The correlation coefficient and RMSE error between MODIS and AERONET AOD observations, which are added into Pg14 L20-Pg15 L3: "The squared correlation (R^2) between MODIS and AERONET in Beijing are 0.81, 0.87, 0.69 and 0.34 in four seasons, of which the corresponding RMSEs are 0.23, 0.29, 0.15 and 0.08. Low correlation in winter may be caused by the shortage of data samples compared to other seasons.**".**

(3) An explanation for the lower RMSE value between MODIS and AERONET than that between CALIPSO and AERONET, which are in P15 L13-15: "For all seasons, RMSE are less for MODIS than CALIPSO compared to AERONET. As indicated earlier, this is likely related to the limited data samples for AERONET-CALIPSO AOD comparison".

P15, L1: add "for given PM2.5" before "the increase of RH can result in : : :.."
Corrected

P15, L2: add "for given AOD" before "the increase of PBLH can cause : : :: : :"
Corrected

P15, L18-21: This part of discussion need consider the impacts from horizontal atmosphere circulation in different seasons.

We highly appreciate this valuable comment. We have added the discussion about the impacts of horizontal atmospheric circulation in Pg19 L1-10: "Actually, PBLH and RH are influenced by the horizontal atmospheric circulation in different seasons, which contributes to the seasonal variations of $PM_{2.5}$ and AOD. Beijing is located in a mid-latitude East Asian monsoon region. In winter, heavy horizontal winds help the transportation of aerosols and result in a relatively low AOD, while low PBLH makes the surface $PM_{2.5}$ relatively high. By contrast, in summer, the high water vapor transported with the warm air from south makes both AOD and $PM_{2.5}$ relatively high, while high PBLH makes the surface $PM_{2.5}$ relatively low. These impacts from the horizontal atmospheric circulation make the seasonal variation of AOD is more significant than that for surface $PM_{2.5}$, as shown in Fig. 4b.**".**

P16, L20: the first row of Figure 6 seems redundant with Figure 5.

This is a good point. Actually, what Figure 6 shows in the first row is the diurnal variation of multi-year averaged RH and PBLH when all measurements of RH, PBLH, AOD, $PM_{2.5}$ are available. By contrast, Figure 5 shows the variation when RH and PBLH are available. Even so, the first row in Figure 6 does show

similar diurnal trends as those shown in Figure 6. We have modified the description to clarify these in P20 L12-14: "Figure 6 shows the diurnal variation of multi-year (2011-2015) averaged RH and PBLH, AOD and PM2.5, AODdry and PM2.5_column in four seasons when all four types of measurements are available.**" and indicated the similar seasonal variation in P18 L15-17: "**Fig. 6(a1-d1) show that PBLH and RH demonstrate a steady increase and decrease trend from 6:00 to 17:00 LT, respectively, which is almost the same as their diurnal variation demonstrated in Fig. 5.**".**

P17, L4: "0.01" should be "0.1"

Corrected.

P18, L14: The aerosol extinction capacity should "decrease" with increasing particle size.

The reviewer proposed a good question. In general, the aerosol extinction capacity depends on the size parameter ($2\pi*r/\lambda$). For size parameter between 0 and about 6, the extinction capacity increases with the size parameter. For solar visible radiation (such as λ=500 nm), the extinction capacity for aerosol particles generally increases with size for particles with radius less than 0.5 μm, which lies within fine and coarse modes. We have modified our description in P22 L11-Pg23 L1: "Theoretically, aerosol extinction capacity increases with particle size parameter ($x=2\pi r/\lambda$) and reaches a maximum value when size parameter is around 6. Therefore, for solar visible radiation (such as λ=500 nm), the extinction capacity for aerosol particles generally increases with size for particles with radius less than 0.5 μm, and then decreases when radius larger than 0.5 μm. Actually, for the wavelength of 550 nm, the extinction efficiency of fine-mode particles (peak radius ranging from ~0.11 to ~0.33 μm) is stronger than coarse-mode aerosols. Moreover, coarse particles, which may be not included in $PM_{2.5}$, can contribute a lot to the extinction at wavelengths in the visible, and thus to AOD. This is especially true for dust days dominated by coarse-mode aerosols, of which high AOD is more likely to be due to PM_{10} rather than $PM_{2.5}$. These make the lower η for coarse-mode than fine mode aerosol.**" .**

P19, L6: better be consistent, using "extinction capacity"?

Corrected

P19, L9-14: The information in Figure 9 is not thoroughly revealed yet: how will the size, the absorption/scattering capability impact? Can the conclusion be hold in all seasons?

We highly appreciate the reviewer's valuable comments here. We have added further analysis in depth and found the corresponding impacts which are shown in Pg23 L20-Pg24 L13: "However, there are large differences in the slope of regression functions among different aerosol types. For absorbing aerosols, the slope roughly decreases with increasing particle size from coarse, mixed to fine particles, with values of about 89, 111, 104 μg/m^3 in spring, 85, 122, 74 μg/m^3 in summer, 71, 163, 131 μg/m^3

in fall, and 44, 143, 158 μg/m^3 in winter. The slope is also generally larger for absorbing than non-absorbing aerosol. The slopes for mixed absorbing and non-absorbing aerosol are 111 and 65 μg/m^3 in spring, 122 and 40 μg/m^3 in summer, 163 and 109 μg/m^3 in fall, and 143 and 89 μg/m^3 in winter. And the slopes for fine absorbing and non-absorbing aerosol are 105 and 76 μg/m3 in spring, 74 and 65 μg/m^3 in summer, 131 and 96 μg/m^3 in fall, and 158 and 122 μg/m^3 in winter. Thus, same as shown in Fig. 8, the slope roughly decreases with particle size, with small values for coarse-mode aerosols and large values for fine-mode aerosols in four seasons, and the slope of non-absorbing aerosols is generally smaller than absorbing aerosols.**".**

P20, L1 & L3: "aerosol" to "aerosol and gas-phase pollutants". Because second order aerosol can form from gas-phase air pollutants.

Modified as suggested in Pg 24 L19-Pg25 L3.

P20, L20 – P21, L5: The effect of wind speed should work with wind direction, depending on the relative location of Beijing to the pollution source (i.e. upstream or downstream).

We highly agree with the reviewer's comment. Beijing is surrounded by Hebei province and mountains in the northern areas. When the winds come from south, Beijing is in the downstream location to the pollution source from Hebei and the pollutants could be further accumulated in Beijing due to the mountain blocking effect. By contrast, when the winds come from north, Beijing is in the upstream region relative to the pollution source in Hebei, and the cold air from north can disperse the air pollutants. Considering the wind speed and direction, the occurrence rate of heavy air pollution is higher for south wind than north wind, which is shown in Fig R1 (also current Figure 11). With the consideration that this study concentrates on the effect of the influential factors to the AOD-$PM_{2.5}$ relationship rather than the air pollution, we added corresponding descriptions in Pg 25 L11-Pg26 L2: "Different from the wind speed which will be analyzed in Figs. 12 and 13, the influence of wind direction to the AOD-$PM_{2.5}$ relationship is often combined with the effect of wind speed. Beijing is surrounded by Hebei province and mountains in the northern areas. When the winds come from south, Beijing is in the downstream location to the pollution source from Hebei and the pollutants could be further accumulated in Beijing due to the mountain blocking effect. By contrast, when the winds come from north, Beijing is in the upstream region relative to the pollution source in Hebei, and the cold air from north can disperse the air pollutants. As shown in Figure 11, with similar wind speed, the occurrence rate of heavy air pollution is much higher for cases with winds from the south than from the north. Moreover, the aerosol pollution events also decrease with increasing wind speed for cases with winds both from the north and the south.".

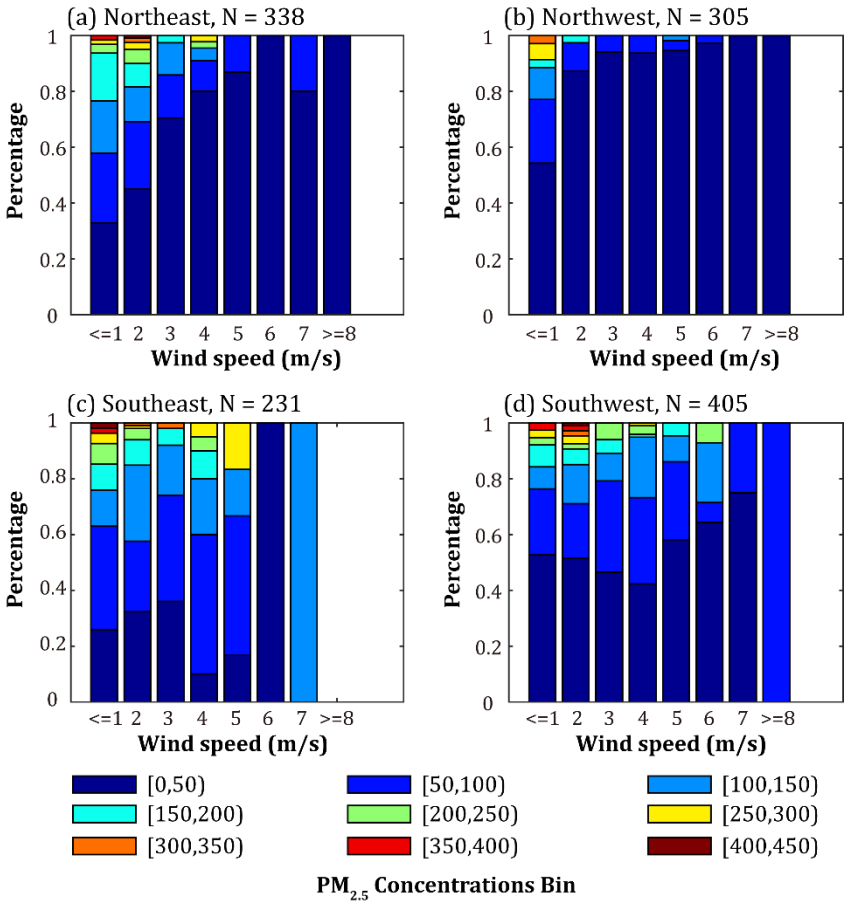

Fig. R1. The relative distribution of $PM_{2.5}$ within different value ranges at Beijing for different surface wind speed in different wind direction

P21, L8-9: Why AOD increase with increasing wind speed slower than 3m/s?

This is a good question. As indicated in the paper, the AOD variation is more complicated and less sensitive to surface wind speed, since the columnar AOD is affected by many factors and the surface wind speed is just a disturbing term to surface $PM_{2.5}$. Actually Fig 13(a) even shows that AOD increases with increasing wind speed when it is less than 3m/s, while the variation of the averaged AOD with the wind speed is small (0.50, 0.54 and 0.58 for wind speed 0, 1, 2m/s respectively as shown in Figure R2). Even though, we still can see a decreasing trend of AOD with wind speed in general. We have added corresponding discussions in Pg26 L15-Pg27 L1: "Although AOD and $PM_{2.5}$ are basically consistent in the decreasing trend with the increasing surface wind speed, AOD variation is more complicated and less sensitive to surface wind speed. Compared with the $PM_{2.5}$ variation range of 10~110 μg/m^3, the variation range of AOD is between 0.2 and 0.6. Moreover, there are even cases that AOD increases with wind speed, such as when wind speed is less than 3 m/s. This is likely associated with the fact that the columnar AOD is affected by many factors, and the surface wind speed is just a disturbing term to surface $PM_{2.5}$.".

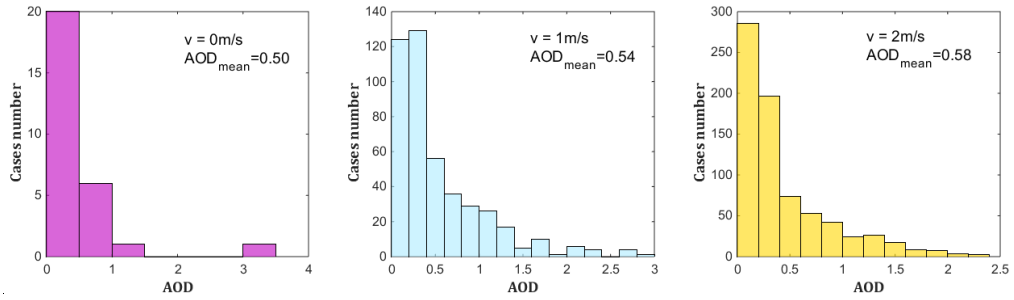

Fig. R2. The AOD histogram distribution in different wind speed (v=0, 1, 2m/s)

Response to Reviewer #2

We thank the reviewer for the detailed and valuable comments and suggestions that have helped us improve the paper. Our detailed responses (**Bold**) to the reviewers' questions and comments (*Italic*) are listed below.

Review of Zheng et al., "Analysis of influential factors for the relationship between $PM_{2.5}$ and AOD in Beijing" submitted for publication in ACP, May 2017.

General comments

The authors investigate the relationship between AOD and $PM_{2.5}$ using 5 years of data at a single site in Beijing. In particular, they investigate the influence of factors such as PBLH, RH, wind speed and direction and aerosol type. The rationale for this study is to explain the variability of the $PM_{2.5}$/AOD relationship because of the possible application of satellite observations of AOD for $PM_{2.5}$ monitoring.

In this study the authors use AOD from MODIS-Aqua (L2, C5.1 from the DB algorithm) and AERONET (L2 AOD, AE, FMF and SSA; these parameters were used to classify aerosol type) and aerosol profiles from CALIOP, together with hourly $PM_{2.5}$ data from the U.S. Department of State which are freely available from a website. However, no information is provided on how these data were measured and what parameter is reported (dry/wet aerosol). Also, a disclaimer on this website (http://www.stateair.net/web/assets/USDOS_AQDataFilesFactSheet.pdf) states that the data have not been validated or quality assured. Hence the authors should clarify what they have done to do this, and why these data were selected for their study over other possibly available $PM_{2.5}$ data.

We highly appreciate the detailed and invaluable comments of the reviewer for our study.

Regarding the data measurements and parameters used in this study, it has been briefly described in section 2.1 and a little more information about how they were measurements are added into Pg 7 line 6-18: "The $PM_{2.5}$ mass concentration was measured using the U.S federal reference method. This method first uses a size selective inlet to remove particles larger than 10 μm, then takes use of another filter to remove the particles larger than 2.5 μm. The air parcels before entering the $PM_{2.5}$ instruments undergo a dry process (RH<35%), which ensure that all $PM_{2.5}$ observations are obtained at dry condition. While this dataset has not been officially evaluated, a comparison of $PM_{2.5}$ measurements from U.S Department of State and from Beijing Municipal Environmental Protection Bureau at sites close to each other (1.6 km) in 2014 – 2016 shows great consistency with correlation coefficient of 0.94 and root mean square difference of 14.3 ug/m^3. Considering that the data measured by U.S. Department of State have longer time record, and have been widely used by many studies (Zheng et al., 2015; Jiang et al., 2015), they are adopted in this study.", **Pg 9 Line 4-5**: "Note that the AOD retrieved could have the

impacts of relative humidity which has not been excluded yet", **Pg 9 line 16** "… which has also been influenced by the relative humidity", a**nd Pg 9 line 15-21, and Pg10 line 15-17**: "…which is only retrieved for daytime, cloud-free and snow/ice-free conditions with an uncertainty confidence level of ~20%".

Regarding the use and data quality of $PM_{2.5}$ from the U.S. Department of State, the reviewer proposed a good question. We have noticed the disclaimer which states that this data has not been validated or quality assured before our study. There are two reasons why we use the hourly $PM_{2.5}$ data from the U.S. Department of State.

1) **The $PM_{2.5}$ observations at this station have a much longer record than those we can find at other sites, such as the sites operated by the Beijing Municipal Environmental Protection Bureau (MEP). The initial time for the observations by the US Department of State was on April 8, 2008 while the initial time for the data we can get from MEP was on May, 2013. We would like to use the observations as long as possible in our study. Actually, the time period of our study is from 2011 to 2015. Therefore, the hourly $PM_{2.5}$ data from the U.S. Department of State is better for the needs of our study.**
2) **This data has been widely used by many studies (e.g., Zheng et al., 2015; Jiang et al., 2015) and quickly evaluated in our early analysis (not provided in the paper). We did a quick examination by comparing the $PM_{2.5}$ observations from U.S Department of State and from Beijing Municipal Environmental Protection Bureau at sites close to each other (1.6 km) for the period from 2014 to 2016. As shown in Figure R1, the two observations show great consistency with each other: the correlation coefficient is as high as 0.94 and root mean square difference is ~14 μg/m^3. These two datasets are basically consistent. Data samples under rainy conditions (TP>0) have been removed to eliminate the influence of precipitation. So we believe that the U.S. Department of state data is reliable. This information has also been added into Pg7 L11-18: "**While this dataset has not been officially evaluated, a comparison of $PM_{2.5}$ measurements from U.S Department of State and from Beijing Municipal Environmental Protection Bureau at sites close to each other (1.6 km) in 2014 – 2016 shows great consistency with correlation coefficient of 0.94 and root mean square difference of 14.3 ug/m3. Considering that Ttheis data measured by U.S. Department of State haves relatively longer time record, and has been widely used by many studies (Zheng et al., 2015; Jiang et al., 2015), they are adopted in this study.**".**

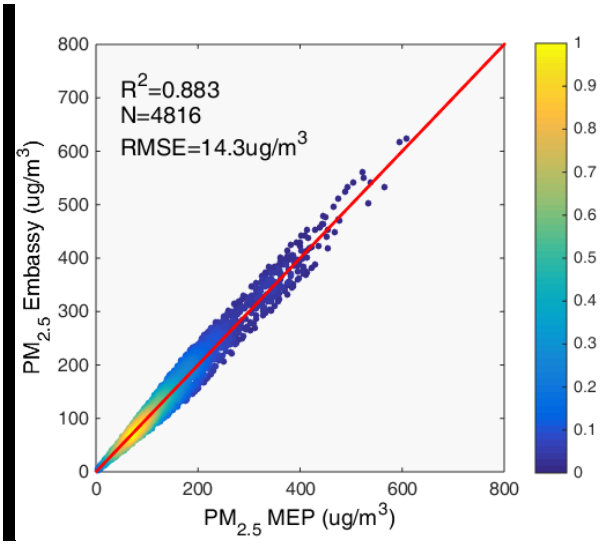

Figure R1. The intercomparison of $PM_{2.5}$ observations from U.S Department of State and from Beijing Municipal Environmental Protection Bureau (MEP)at sites close to each other (1.6 km) in 2014 – 2016.

TP, RH, wspd and WD. PBLH was extracted from ECMWF interim re-analysis data. This is a very comprehensive suite of experimental data. All of these are obtained at different times and with different spatial scales and, for ground-based measurements, at different locations. Hence the data sets need to be colocated in both space and time before any analysis can be undertaken. Although locations indicated in section 2 are within 1 degree, an inhomogeneous megacity environment, both as regards surface characteristics and aerosol sources, may result in substantial spatial variation of the aerosol characteristics. These points need to be addressed in the MS.

In principle, we agree with the reviewer that aerosol properties could vary a lot with location, particularly in a megacity. This is one contributing factor to the AOD-$PM_{2.5}$ relationship as indicated in this study. In general, to do a statistical analysis between aerosol properties and meteorology, we need make the datasets collocated in both time and space. Unfortunately, it is challenging to exactly collocated them in most cases.

This study actually uses the TP RH, wspd and WD from the MEP site observation, which is about 1.6 km away from the aerosol observation site. Differences in these meteorology (particularly near surface) do exist and cause uncertainties to our study, but we believe this is the best we can do at this moment. For the PBL, it is extracted from ECMWF reanalysis data which has a horizontal resolution of around 12.5 km, and may be different from that at the aerosol observation site. However, considering that PBLH varies slowly with space and the observation of PBLH generally has an uncertainty larger than 100 m, we think the PBLH from ECMWF could be a good estimate to that at aerosol observation site. Moreover, an early study by Guo et al. (2016) compared the site

observation of PBLH with ECMWF grid PBLH, which show good agreement. Of course, we agree with the reviewer that uncertainties could be introduced due to the mismatch of locations for these measurements. We have added partial description to indicate this in Pg8 L14-16: "We should admit that extra uncertainties could exist due to the distances between the MEP sit, U.S. Department of State site, and ECMWF grid, while they are close to each other.**".**

Overall, the manuscript shows the influence of various factor on the $PM_{2.5}$/AOD relationship, but presentation lacks clarity and many things are left unexplained as detailed in my comments below. I miss clear conclusions (only a summary is provided at the end) and how the findings can be combined to provide a relationship between $PM_{2.5}$ and AOD, if that would be possible even for a single site.

We feel sorry that we have not delivered our conclusion clearly and have made careful revisions based on the reviewer's comments as listed below. We have also made a little more description about our conclusions, while the build-up of a specific relationship between $PM_{2.5}$ and AOD is still not aimed or reached in this study. The addition in the summary part lies in Pg 31 L17-21: "With these findings, we need consider at least the impacts of PBLH, RH, Wind speed and wind direction, and use the AOD within PBL heights to build up better $PM_{2.5}$-AOD relationship. The impacts of these influential factors have been investigated while an optimal empirical $PM_{2.5}$-AOD relationship scheme has not been reached, which definitely need further study in future.**".**

In general, the figures would be more interesting if they were easier to read, in some cases the text is too small. Furthermore, although a comparison is made between MODIS and AERONET data, in the main part of the MS only AERONET and CALIPSO data are sued. Hence I do not understand why MODIS is included.

These are good questions. The figures have been modified in order for readers to easily read and follow.

We included MODIS in our intercomparison study based on the consideration that significant uncertainties could exist in the satellite observations of AOD which can cause errors in the derived $PM_{2.5}$-AOD relationship: using AOD from different sources, such as ground-based and satellite based observations, or even different satellite observations, we could have different $PM_{2.5}$-AOD relationships due to their different AOD observations.

Detailed comments

p4, lines 2-3 specify modifying: scattering and absorption?
Corrected

5, 3 usually it's not the extinction coefficient that is provided but the AOD, i.e. the integrated extinction over the whole column

In principle, many passive remote sensing instruments such as MODIS do provide AOD only rather than the extinction coefficient. However, the profile of mean extinction coefficient is being provided by some satellite products including CALIPSO level 2 aerosol profile products. This is why we provided the description here. We have slightly modified it in Pg 5 L1-4 as "Remote sensing observation generally provides the aerosol optical properties such as AOD and aerosol extinction coefficient, but not the aerosol mass or number concentration**".**

5, 10 spelling van Donkelaar (also elsewhere in the MS)
Corrected

5, 11-13 these statements need some references
Three references have been added to support these statements, which are (Paciorek et al., 2008; Li et al., 2017; Wang et al., 2017).

6, 18 what do you mean with 'and so on'? Either specify or remove
It has been changed in Pg6 L17-18: "The data used in this study are described as follows, including the data sources, their spatial and time resolutions, and the data period".

8, 11 Was AERONET version 2 or the new version 3 used?

We chose to use AERONET version 2 product rather than the new version 3, because AERONET version 3 inversion algorithm was in development and the data were not released before our study.

Actually, AERONET version 3 has not been widely used until now. It can only provide us with the level 1.5 AOD on the website (https://aeronet.gsfc.nasa.gov/new_web/units.html), which are automatically cloud cleared but may not have final calibration applied. These data are not quality assured. Also, some other parameters including single scattering albedo (SSA), absorption and extinction aerosol optical depth cannot be acquired now. AERONET version 2 has been used in many studies and the differences in retrieved quantities between versions 2 and 3 are expected to be smaller than between versions 1 and 2 (Sayer A M et al. 2014). This is another reason that we used AERONET version 2.

Reference: Sayer A M, Hsu N C, Eck T F, et al. AERONET-based models of smoke-dominated aerosol near source regions and transported over oceans, and implications for satellite retrievals of aerosol optical depth[J]. Atmospheric Chemistry and Physics, 2014, 14(20): 11493-11523.

9, 8 No, AOD is not extinction multiplied by layer depth, but the integral of the extinction over the whole layer. This is different when extinction is not constant with height, as is usually the case.
We agree with the reviewer that the AOD is the integral of the extinction over the

whole layer instead of a simple multiplication. CALIPSO level 2 aerosol profile products supply the extinction coefficient at different heights with a resolution of 60 or 120m in the vertical resolution. AOD at each layer is approximatively derived as the multiplication of the extinction coefficient and layer depth. Even though, we have modified the descriptions in Pg 10 L1-2 as "AOD at each layer is derived as the integration of the extinction coefficient within that layer".

9, 20 why was MODIS C5.1 used and not the newer C6?
We tried our best to use MODIS C6 instead of C5.1 at our initial study. However, it is very challenging for the new C6 MODIS data to get downloaded. After trying many times, we gave up. Instead, we kept using MODIS C5.1 by only selecting those data with "very good" quality.

10, 2 why was Deep Blue selected and not dark target? Or the merged DB/DT AOD product from C6?
Deep Blue instead of dark target was selected for AOD product because the AOD accuracy is highly dependent on the surface reflectance for dark target product. The merged DB/DT AOD product was not used simply because we didn't obtain the C6 product.

10, 14 is it the optical thickness per unit mass concentration, or inversely the mass concentration per unit AOD, as eq 1 says?
We thank the reviewer for helping pointing this mistake out. We have corrected it on Pg 11 L9-10: "where η ($\mu g/m^3$) indicates the near surface aerosol $PM_{2.5}$ mass concentration per unit aerosol optical thickness".

10, 16-19 it is not clear what extinction capability means: extinction per unit mass, or mass extinction coefficient? Or extinction efficiency? Or ….? Is it really true that for the same $PM_{2.5}$, the extinction is weaker for the same AOD? Or is it more complicated and does size distribution and RH have an influence?
We are sorry for the confusion. The extinction capability in this study actually means the mass extinction coefficient, we have explained this in Pg 11 L14-15: "Note that the extinction capability here denotes the aerosol mass extinction coefficient".

No, we do not mean that for the same $PM_{2.5}$, the extinction is weak for the same AOD. Instead, we believe that for the same $PM_{2.5}$, the larger the AOD, the larger the aerosol mass extinction coefficient which is defined as extinction capability here. Of course, if we go further into details, the aerosol extinction capability is definitely complicated which is dependent on multiple factors including size distribution and RH. These are what we have described in Pg 11 L10-15: "Its value depends on the aerosol type, aerosol size, RH, PBLH, and the vertical structure of aerosol distribution. At the same $PM_{2.5}$ mass concentration, the smaller the AOD, the weaker the extinction capability; and the larger the AOD, the stronger the

extinction capability. Note that the extinction capability here denotes the aerosol mass extinction coefficient".

11, 3 discrepancies or differences?
It should be 'differences" and we have corrected it.

11, 5 FMF is the fraction of the AOD due to fine particles (smaller than 1 micrometer); AE is exponent for the power law describing the wavelength dependence of the AOD
Many thanks to the reviewer for helping provide more accurate description. They have been modified as suggested.

11, 9 SSA is the ratio of the scattering coefficient to the extinction coefficient (=scattering + absorption)
It has been modified.

11, 12 replace According to with Following Lee et al. (2010)
Corrected

12, 2 what do you mean with "since the high percentage of"?

This is a good question. According to the classification method proposed by Lee et al. (2010), aerosols can be classified into six types based on fine mode fraction (FMF) and single scattering albedo (SSA). Fine absorbing aerosols (SSA<=0.95, FMF>0.6 and AE>1.2) constitute the largest proportion among all the types in Beijing, which are 36.5%, 42.6%, 51.1% and 60.3% in four seasons respectively.

To further study the absorptive properties of aerosols, fine absorbing aerosols are divided into heavily (SSA<=0.85), moderately (0.85<SSA<=0.9) and slightly (0.9<SSA<=0.95) absorbing aerosols in this study.

Even with these considerations, using "since the high percentage of …" might be not suitable. We have removed this sentence and changed our classification categories to eight types instead of six types as shown in Pg 12 L10-21.

12, 6 replace "the method" with "the classification method"
Corrected

13, 6 what does it mean when MODIS correlated best, considering the bias, i.e. considering that MODIS AOD is too high?
Tables 1 and 2: what parameter is listed in the first 2 columns? How is bias calculated?
This is a good question. It simply means that the correlations between MODIS and AERONET are better in spring and summer than in other seasons, without

considering any bias. To be more accurate, we have modified the description in Pg 14 L20- Pg15 L7: “The squared correlation (R^2) between MODIS and AERONET in Beijing are 0.81, 0.87, 0.69 and 0.34 in four seasons, of which the corresponding RMSE are 0.23, 0.29, 0.15 and 0.08. Low correlation in winter may be caused by the shortage of data samples compared to other seasons. When AOD becomes small, the relative errors in AOD from both MODIS and AERONET become large, which may cause the correlation of AOD between MODIS and AERONET also decrease as demonstrated in Table 1.”.

Table 1 and 2 compared paired AERONET and MODIS AOD, AERONET and CALIPSO in four seasons. Based on the satellite overpass time, the corresponding AERONET AOD averaged in time bins of within 30-min are compared to MODIS AOD and CALIPSO AOD respectively. The parameter in the first column is the averaged AERONET AOD, and the parameter in the second column is the averaged MODIS AOD (CALIPSO AOD) in Table 1 (Table 2). We have added the information into the Tables and described in Pg 14 L9-12: “Table 1 further shows the inter-comparison results of AOD between AERONET and MODIS in spring (MAM), summer (JJA), fall (SON) and winter (DJF), which include their seasonal averaged AOD, squared correlation, absolute bias, relative bias and sample number”

***Bias* in Table 1 is calculated as:**

$$Bias = MODIS\ AOD_{averaged} - AERONET\ AOD_{averaged}$$

***Bias* in Table 2 is calculated as:**

$$Bias = CALIPSO\ AOD_{averaged} - AERONET\ AOD_{averaged}$$

These calculation information have been added into Pg 14 L12-14: “The absolute bias is calculated as the difference of seasonally averaged AOD from AERONET and MODIS at the same time; and the relative bias is calculated as the ratio of the absolute bias to the seasonally averaged AERONET AOD.” **and Pg 15 L9-10**: “The bias shown in Table 2 is calculated in the same way as that in Table 1.”.

14, 1 suggest to change to: the hygroscopic growth factor f/(RH) is defined as the ratio ... ;
Corrected

Is it really the hygroscopic growth factor? This factor would relate to particle size, which indeed is one of the underlying factors, in addition to refractive index, influencing scattering; however, this article is about AOD, which is scattering and thus the scattering enhancement factor should be considered, see for instance Zieger et al., (2015) (Low hygroscopic scattering enhancement of boreal aerosol and the implications for a columnar optical closure study, Atmos. Chem. Phys., 15, 7247-7267, doi:10.5194/acp-15-7247-2015, 2015) and references therein for a

discussion on the subject and the f(RH) for different aerosol types in Europe.

The reviewer proposed good question. The hygroscopic growth of aerosols with increasing relative humidity (RH) affects aerosol direct radiative effects by changing aerosol optical properties due to increasing water uptake of hydrophilic compositions such as sulfate, nitrate, and some organic matters. The aerosol hygroscopicity varies by space and time because of different aerosol sources, types, and chemical components (Li J et al, 2014).

Therefore, the hygroscopic growth parameterization of different aerosol types are also different as the reviewer commented. For example, the hygroscopic growth factor of sulfate optical properties is expressed as a function of relative humidity (RH) in an exponential way:

$$f(RH) = \exp[c_1 + c_2 / (RH + c_3) + c_4 / (RH + c_5)]$$

Where *f*(*RH*) denotes the hygroscopic growth factor of aerosol scattering coefficient, c_1 to c_5 are five wavelength dependent fitting coefficients taken directly from the CCM3 radiation package. The values of these coefficients are 11.24, 0.304, 1.088, 177.6 and 15.37, respectively, at a wavelength of 550 nm.

However, the scheme of Im et al. (2001) can be applied to other aerosol types (such as carbonaceous aerosols, etc.), which is in a form of power law:

$$f(RH) = (1 - RH)^{-g}$$

Where *g* is an empirical fitting value, setting to 0.38.

Zieger et al., (2015) tried to study the the magnitude of the scattering enhancement factor *f*(*RH*) in the boreal forest region of northern Europe. Also, they compared AOD achieved from ground-based in situ and remote sensing aerosol measurements

In fact, the hygroscopic growth correction is unable to be perfectly achieved using only one parameterization formula. Nevertheless, due to the lack of the observations of chemical composition in Beijing, in our study, *f*(RH) is expressed in a simple function as Eq 2, which is also used in Li C et al, (2005). We have also changed our description from "… is defined as …**" to "**can be defined as …**".**

Reference:

Li C, Mao J, Lau A K H, et al. Application of MODIS satellite products to the air pollution research in Beijing[J]. Science in China Series D(Earth Sciences), 2005, 48: 209-219.

Li J, Han Z, Zhang R. Influence of aerosol hygroscopic growth parameterization on aerosol optical depth and direct radiative forcing over East Asia[J]. Atmospheric research, 2014, 140: 14-27.

14, 6-8 I don't understand this explanation since both the MODIS and AERONET AOD are derived in ambient conditions, and for the same air mass when well colocated. Hence hygroscopic growth cannot be the physical reason for larger MODIS AOD than AERONET AOD, since these should be the same. More likely these

are retrieval errors. Since in this MS CALIPSO AOD is the main source for analysis, should a similar discussion be made for CALIPSO?

We are sorry that we did not deliver the information clearly and caused confusion. The description here is a general information that the hygroscopic growth process can cause a larger value of AOD compared to dry conditions, not for the comparison between MODIS and AERONET, or between CALIPSO and AERONET, since all of them are affected by this process. We have modified the description to make our point more clear in Pg 16 L6-12: "The hygroscopic growth process has a significant contribution to AOD. Since $PM_{2.5}$ is often measured at a dry condition (< 40% in relative humidity), we often need consider the impacts of relative humidity to AOD in order to get a more reliable $PM_{2.5}$-AOD relationship. A dehydration adjusment can be applied to get the dry condition AOD, which is …**"**

14, 13 what is the consequence of this assumption? Uniform mixing would imply that dry aerosol particles, water vapour and potential temperature are well-mixed, but RH would in that case increase with height and thus all aerosol parameters that vary with RH. In addition, often a scale height is used to account for an aerosol gradient.

The reviewer proposed a very good question. It is true that the RH would have large variation with height – would increase with height. This could definitely affect the dehydration adjustment of AOD. Currently, we only use the surface RH to do the adjustment which could cause the dry condition AOD is actually somehow overestimated compared its true value. We have removed the assumption and added this discussion into our manuscript in Pg 17 L4-7: "In the atmosphere, the RH often increases with height within PBLH. This could definitely affect the dehydration adjustment of AOD in Eq. (3). Currently, we only use the surface RH to do the adjustment which could cause the dry condition AOD is actually somehow overestimated compared to its true value. **"**

14, 19 this assumption implies that there are no disconnected aerosol layers and thus may introduce errors in experimental conditions where these may occur, as revealed by lidar.

This is a good point. The assumption made here does imply that there are no disconnected aerosol layers and could introduce errors in experimental conditions. We have carried out 4 different field observations in east China region and found for most time, the $PM_{2.5}$ mass concentration varies little with height within PBLH. Liu et al. (2009) also have the similar findings based on their 17 in-situ aircraft measurements in spring of 2005 and 2006 over Beijing. Therefore, our assumption could be valid for most cases. Even though, we agree with the reviewer and have added a discussion in Pg 17 L10-13: "The calculation of column $PM_{2.5}$ mass concentration in Eq. (4) has implied that there are no disconnected aerosol layers and could introduce errors in experimental conditions, which was not considered in this study.**"**

Reference:

Liu P, Zhao C, Zhang Q, et al. Aircraft study of aerosol vertical distributions over Beijing and their optical properties[J]. Tellus B, 2009, 61(5): 756-767.

15, 2-3 I would agree that an increase of PBLH could result in the decrease of surface $PM_{2.5}$, in the absence of sources and sinks for $PM_{2.5}$, but that does not follow from eqs 3 and 4, unless $PM_{2.5}$ column would be assumed constant.

We agree with the reviewer and have made changes to our descriptions in Pg 17 L13-16: "Eqs. (3) and (4) imply that for given $PM_{2.5}$, the increase of RH can result in the increase of AOD and the decrease of η, and that for given AOD, the increase of PBLH can cause the decrease of near-surface $PM_{2.5}$ concentrations and the decrease of η."

15, 7 opposite trend, suggest to replace with anti-correlated;

Changed.

What are the colour bands in Fig 4a?

The colour bands in Fig. 4a are simply used to help readers see the anti-correlated temporal trends between PBLH and RH. The blue bands are for high PBLH and low RH, and the purple bands are for low PBLH and high PBLH, both of which indicate anti-correlated trends between PBLH and RH. Differently, the green (yellow) bands are for low (high) PBLH and low (high) RH, which indicates correlated trends of PBLH and RH. Clearly, there is generally an anti-correlated temporal trend between PBLH and RH. We have added the description about the colour bands into Pg17 L19-Pg18 L3: "In Fig. 4a, the blue bands are for high PBLH and low RH, and the purple bands are for low PBLH and high PBLH, both of which indicate anti-correlated trends between PBLH and RH. Differently, the green (yellow) bands are for low (high) PBLH and low (high) RH, which indicates correlated trends of PBLH and RH. Clearly, there is generally an anti-correlated temporal trend between PBLH and RH." **The colour bands have also been explained in the caption of Figure 4.**

15, 11 I assume that this is a typo and fig 4a is meant, but still don't understand the sentence

Yes, this is a typo and it is actually Fig. 4a. We are sorry that this sentence is kind of confusing. The main information we would like to deliver is that the effects of PBLH and RH should be considered when we study the $PM_{2.5}$-AOD relationship. We deleted this sentence. Instead, we added the following sentence in Pg 18, L10-14: "Without considering the variations of sources and sinks, PBLH is negatively correlated with $PM_{2.5}$, and RH is positively correlated with AOD. The anti-correlated trend between PBLH and RH shown in Fig. 4a imply that the effects of PBLH and RH on the $PM_{2.5}$-AOD relationship could be partially canceled out. However, it is still necessary to consider the effects of PBLH and RH for the study of $PM_{2.5}$-AOD relationship.**"**

16, top para: here AOD_{dry} is plotted where AOD_{dry} was obtained using the correction factor given by eq 2, which has to be explained. However, as mentioned above, RH is not constant with height, and hence f(RH) also varies with height. How was this accounted for? It seems that the good correlation between AOD_{dry} and $PM_{2.5}$ is somewhat fortuitous. Does this good agreement lead to the conclusion that $PM_{2.5}$ was measured dry (at low RH)? See also the discussions on vertical variation of aerosol profiles later in this MS. Figs 5 and 6 both show the diurnal variation of PBLH and RH, for different seasons averaged over many years, for the whole day in Fig. 5, and for 5-20 in Figure 6 (a-d). I would expect that the curves for each season are exactly the same for the overlapping time periods. Could the authors explain the differences?

The reviewers proposed good questions and here are our explanations.

(1) **Yes, we have added the explanation about the AOD_{dry} and discussed the potential issues in our adjustment due to potential errors in RH, which are in Pg 19 L12-14**: "Note that the AOD_{dry} is adjusted based on surface RH using Eqs. (2) and (3) and the vertical variation of RH has not been considered. As indicated earlier, the AOD_{dry} obtained here could be somehow overestimated compared to its true value.".

The impacts that we do not consider the vertical variation of RH has also been replied earlier and indicated in Pg 17 L4-7: "In the atmosphere, the RH often increases with height within PBLH. This could definitely affect the dehydration adjustment of AOD in Eq. (3). Currently, we only use the surface RH to do the adjustment which could cause the dry condition AOD is actually somehow overestimated compared to its true value."

(2) "$PM_{2.5}$ was measured at low RH**" is not a conclusion, but a fact. The air samples before enter by the $PM_{2.5}$ instruments undergo a dry process (RH<35%), which ensure that all $PM_{2.5}$ observations are obtained at dry condition. We have added this information into the data part in Pg 7 L9-11: "**The air parcels before enter by the PM2.5 instruments undergo a dry process (RH<35%), which ensure that all PM2.5 observations are obtained at dry condition.**"**

(3) While both Figs. 5 and 6(a) show the diurnal variation of PBLH and RH, they are for different data samples. What Figure 6 shows in the first row is the diurnal variation of multi-year averaged RH and PBLH when all measurements of RH, PBLH, AOD, $PM_{2.5}$ are available. By contrast, Figure 5 shows the variation once RH and PBLH are available.

17, 4-8 why is a linear relationship expected between AOD and $PM_{2.5}$, while the authors showed already in the above that there is not a good correlation, as also shown in Figs 6a2-d2? Why are these plots shown, why not only the corrected AOD_{dry}, since the necessity of that correction was discussed above? Furthermore, Figs 6a3-d3 do not show the R^2, they show time series which show that part of the time AOD_{dry} and $PM_{2.5}$ trace each other, but at other times not; furthermore, these plots show the offset, i.e. AOD_{dry} much larger than $PM_{2.5}$, which is in contrast to what was shown in Figure 4c, where the time series are much closer. Could the authors explain the differences? The $PM_{2.5}$ scales in Figs 4c and Fig 6 a3-d3 are much different but plotting on the same scales would make the discrepancy even larger.

These are very good comments and we highly appreciate them.
(1)

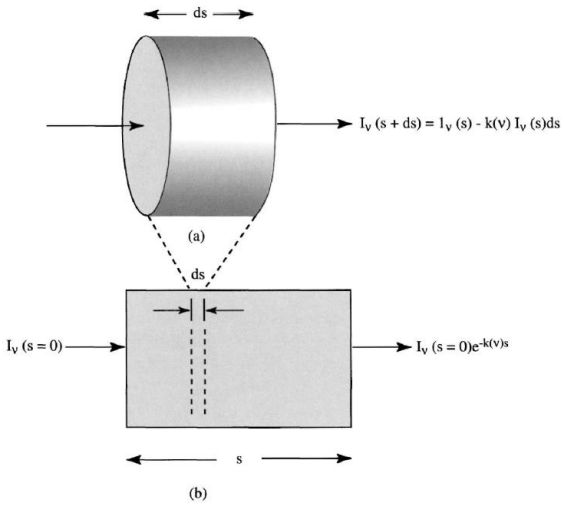

The Extinction Law (differential form)

$$k_m(v) = -\frac{dI_v}{I_v \rho ds} = -\frac{dI_v}{I_v dM}$$

Where $k_m(v)$ is mass extinction coefficient [$m^2 \times kg^{-1}$],
If k_m keeps constant along the light path s, we have

$$\tau_s(v) = k_m(v)\int_0^s \rho ds' = k_m(v)M$$

Based on above equation, we could expect a linear relationship between AOD and aerosol mass concentration.

(2) The purpose that we show these figures is to see if the correction of PBLH and RH can improve the $PM_{2.5}$-AOD relationship, or a further examination of the effect of PBLH and RH, by comparing the results shown in Fig. 6a2-d2 and in Fig. 6a3-d3. AOD_{dry} and $PM_{2.5\_column}$ have been shown in Fig. 6a3-d3, then we can examine their differences from those shown in Fig. 6a2-d2.

(3) Figs. 6a3-d3 do show the diurnal variation of the two examined variables, instead of scattering plots. The purpose is to see if they follow similar diurnal variation since both PBLH and RH have clear diurnal variation and the purpose of these figures is to examine the effect of PBLH and RH as indicated above. Even so, the squared correlation R^2 has been calculated and provided in the figure titles, which are 0.93, 0.84, 0.91 and 0.93 in four seasons respectively.

(4) There are offsets for the plots shown in Fig. 6. However, the two variables (AOD_{dry} and $PM_{2.5}$) are using different y-coordinates, left and right respectively. Moreover, they have different yrange values. Furthermore, the data (so aerosol types and meteorology conditions) used in Figure 4c and the sub panels in Figure

6 are different (month in a particular year vs seasonal average). All of these make it challenging to compare the results in Figure 4c and Figure 6 directly. Our purpose is also not for this kind of intercomparison. The much closer time series shown in Figure 4c is simply due to the yrange selections of AOD and $PM_{2.5}$. We could change the $PM_{2.5}$ scales in Figure 6 to make AOD and $PM_{2.5}$ lines closer. However, as said, the different data considered in Figure 4c and sub panels of Figure 6 make them hard to compare with each other.

17, 10-12 why only this narrow time frame (11-17 LT)? why does this limit the diurnal and seasonal variation on $PM_{2.5}$/AOD?

The narrow time frame adopted in this study is not used to limit the seasonal variation, but to limit the diurnal variation on $PM_{2.5}$/AOD. The reason is as follows. Atmospheric boundary layer generally increases from the morning, reaching the maximum at ~14:00 LT and decreases hereafter. Figure 5 in the manuscript shows that the PBLH is high around noon time and have weak changes. Also, RH has a low but weakly variable values also around noon time. So, we choose the time period between 11:00 and 17:00 local time to reduce the variability of PBLH and RH. By doing this way, we can guarantee a certain amount of data samples, and limit the influence of diurnal variation of PBLH and RH to $PM_{2.5}$/AOD. We have modified/corrected our description to make it more accurate in Pg 21 L4-8: "For this time period, the PBLH (RH) has high (low) values with weak variation, which make the impacts of PBLH and RH vary weakly with selected sample time in a season. By doing this, we try to keep a certain amount of data samples and limit the influence of diurnal variation of RH and PBLH on η."

17, 13 Is the classification based on the scheme described on p. 11? Please refer to that scheme, and if not provide a reference. In Figure 7 are 8 aerosol types are shown whereas on p. 11 there are only 6, so I suspect that the some other classification than that on p. 11 is used

Yes, the aerosol classification in section 3.2 is bsed on the scheme described on pg 11. The scheme actually classifies the aerosol into 8 instead of 6 types in this study. We have corrected our description in Pg 11 to show the classification methods in Pg 12 L10-21: "In this study, hourly averaged level 2 inversion products from AERONET at sites in Beijing are used, including FMF, AE and SSA data. Following Lee et al. (2010), aerosol is classified into eight types as follows: 1) Coarse non-absorbing (SSA>0.95, FMF<=0.4 and AE<=0.6), 2) Coarse absorbing (SSA<=0.95, FMF<=0.4 and AE<=0.6), 3) Mixed non-absorbing (SSA>0.95, 0.4<=FMF<0.6 and 0.6<=AE<1.2), 4) Mixed absorbing (SSA<=0.95, 0.4<=FMF<0.6 and 0.6<=AE<1.2), 5) Fine non-absorbing (SSA>0.95, FMF>0.6 and AE>1.2), 6) Fine highly-absorbing (SSA<=0.85, FMF>0.6 and AE>1.2), 7) Fine moderately-absorbing (0.85<=SSA<0.9, FMF>0.6 and AE>1.2), Fine slightly-absorbing (0.9<=SSA<0.95, FMF>0.6 and AE>1.2)."

18, 5 what is 'heavily non-absorbing aerosols'? This type neither occurs in Fig 7 nor

on p. 11.
Figures 7 and 8 present the same aerosol types, but with a different colour scheme. It would be much easier to read when the colour schemes are the same. Please change.
The "heavily non-absorbing aerosols' is a typo, we have corrected it as 'fine non-absorbing aerosol' in Pg 22 L1. Following the great suggestion, we have also modified Figure 8 to make its color scheme as the same as that used in Figure 7.

18, 14 extinction capacity? On p.10 extinction capability was used. Is that different? I don't understand either of these terms, see my comment on p. 10.
Yes, this is the same as that shown in Pg 10, which is the mass extinction coefficient. We have indicated this in the manuscript in Pg 11 L14-15: "Note that the extinction capability here denotes the aerosol mass extinction coefficient."

18, Fig 8 and Table 3 discussion: rather than only providing correlation coefficients, the authors should discuss the reasons for the observed differences. There are two fundamental reasons for the variation of the $PM_{2.5}$/AOD ratio: $PM_{2.5}$ does not include coarse particles while they do contribute to the extinction at wavelengths in the visible, and thus to AOD. In addition, the extinction efficiency peaks for a particle size which depends on the ratio between particle size and the wavelength.
Great comments and we highly appreciate the reviewer's help. Following this suggestion, we have modified our descriptions in Pg 22 L11-Pg23 L1: "Theoretically, aerosol extinction capacity increases with particle size parameter ($x=2\pi r/\lambda$) and reaches a maximum value when size parameter is around 6. Therefore, for solar visible radiation (such as λ=500 nm), the extinction capacity for aerosol particles generally increases with size for particles with radius less than 0.5 μm, and then decreases when radius larger than 0.5 μm. Actually, for the wavelength of 550 nm, the extinction efficiency of fine-mode particles (peak radius ranging from ~0.11 to ~0.33 μm) is stronger than coarse-mode aerosols. Moreover, coarse particles, which may be not included in $PM_{2.5}$, can contribute a lot to the extinction at wavelengths in the visible, and thus to AOD. This is especially true for dust days dominated by coarse-mode aerosols, of which high AOD is more likely to be due to PM_{10} rather than $PM_{2.5}$. These make the lower η for coarse-mode than fine mode aerosol."

19, 1-5 Figure 9 is too small to read the numbers, but it is clear that there are large differences in the slopes from one aerosol type to another, as also stated on line 9. Hence I don't understand where the numbers given on line 3 come from.
We have modified Figure 9 so that the numbers in the figure can be easier to read. The numbers given on line 3 comes from our analysis which is not shown in the manuscript. As shown in Figure R2, we carried out the linear regression analysis for all types of aerosols. The slopes of the linear regression functions ($PM_{2.5}=a\times AOD+b$) are 90.16, 56.9, 117.97 and 138.42 in four seasons respectively. We have modified our description in Pg23 L9-12: "We have also done the linear regression analysis for all types of aerosols which is not shown here, and found that the slopes of the linear regression functions ($PM_{2.5}=a\times AOD+b$) are 90.16, 56.9,

117.97 and 138.42 in four seasons respectively."

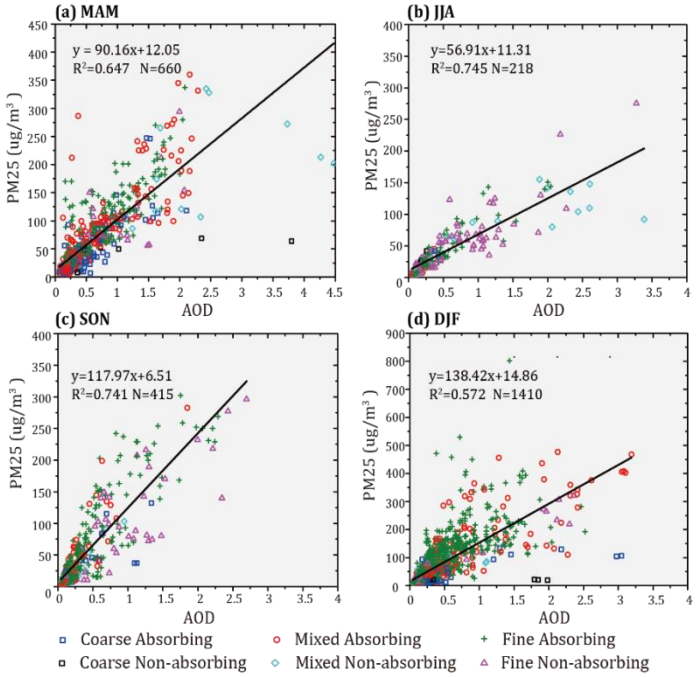

Figure R2. Scatterplots of AERONET AOD vs. $PM_{2.5}$ concentrations of different aerosol types in four seasons for the period of 2011 to 2015 in Beijing.

19, 6 why does high RH increase the extinction efficiency? Since the refractive index of water is lower than that of most other materials, would the condensation of water vapour lower the extinction efficiency?

The reviewer proposed a good question. The mass extinction coefficient of particles is dependent on the refractive index of the mater and its size parameter. While the refractive index of water is lower than that of most other materials, the hygroscopic growth of aerosol particles under high RH condition makes more particles with size parameters more close to 5 or 6, in other words, makes more particles with strong extinction coefficient. Thus, the high RH can increase the extinction capacity of aerosol.

19, 10 Similar as on line 3, I do not understand where these numbers come from. I cannot find them in Fig 9

These numbers are in the linear fitting regression equations which are shown in Figure 9 for different types of aerosols in four seasons. We have added them into Figure 9 and made modification to the figure and descriptions in Pg 23 L20 – Pg24 L13: "However, there are large differences in the slope of regression functions among different aerosol types. For absorbing aerosols, the slope roughly decreases with increasing particle size from coarse, mixed to fine particles, with values of about 89, 111, 104 μg/m^3 in spring, 85, 122, 74 μg/m^3 in summer, 71, 163, 131 μg/m^3 in fall, and 44, 143, 158 μg/m^3 in winter. The slope is also generally larger for absorbing than non-absorbing aerosol. The slopes for mixed absorbing and non-absorbing aerosol are

111 and 65 μg/m^3 in spring, 122 and 40 μg/m^3 in summer, 163 and 109 μg/m^3 in fall, and 143 and 89 μg/m^3 in winter. And the slopes for fine absorbing and non-absorbing aerosol are 105 and 76 μg/m3 in spring, 74 and 65 μg/m^3 in summer, 131 and 96 μg/m^3 in fall, and 158 and 122 μg/m^3 in winter. Thus, same as shown in Fig. 8, the slope roughly decreases with particle size, with small values for coarse-mode aerosols and large values for fine-mode aerosols in four seasons, and the slope of non-absorbing aerosols is generally smaller than absorbing aerosols. ”

19, 12 Figure 4 does not show that the slope decreases with particle size.
Many thanks to the reviewer. This is a typo, it is actually Figure 8 instead of Figure 4. We have corrected it.

19, 15 this conclusion is clear, if only looking at Figure 9. However, I do not understand how the discussion in this section supports this conclusion.
We agree with the reviewer and made changes to our discussion to support this conclusion in Pg 23 L20 to Pg 24 L13: “However, there are large differences in the slope of regression functions among different aerosol types. For absorbing aerosols, the slope roughly decreases with increasing particle size from coarse, mixed to fine particles, with values of about 89, 111, 104 μg/m^3 in spring, 85, 122, 74 μg/m^3 in summer, 71, 163, 131 μg/m^3 in fall, and 44, 143, 158 μg/m^3 in winter. The slope is also generally larger for absorbing than non-absorbing aerosol. The slopes for mixed absorbing and non-absorbing aerosol are 111 and 65 μg/m^3 in spring, 122 and 40 μg/m^3 in summer, 163 and 109 μg/m^3 in fall, and 143 and 89 μg/m^3 in winter. And the slopes for fine absorbing and non-absorbing aerosol are 105 and 76 μg/m3 in spring, 74 and 65 μg/m^3 in summer, 131 and 96 μg/m^3 in fall, and 158 and 122 μg/m^3 in winter. Thus, same as shown in Fig. 8, the slope roughly decreases with particle size, with small values for coarse-mode aerosols and large values for fine-mode aerosols in four seasons, and the slope of non-absorbing aerosols is generally smaller than absorbing aerosols.”

20, 13-15 this is a very surprising conclusion, regarding the location of Beijing with near-by mountains blocking the circulation, pollution advected form the south and clean air from the north, as well as the transport of desert dust aerosol in the spring. What leads to this conclusion? I don’t see it in Figure 10. And also the first 5 lines on top of p. 2 contradict this conclusion.
We highly agree with the reviewer. We made a more careful examination and found that conclusion is erroneous. We corrected them with more analysis in Pg 25 L11- Pg26 L2: “Different from the wind speed which will be analyzed in Figs. 11 and 12, the influence of wind direction to the AOD-$PM_{2.5}$ relationship is often combined with the effect of wind speed. Beijing is surrounded by Hebei province and mountains in the northern areas. When the winds come from south, Beijing is in the downstream location to the pollution source from Hebei and the pollutants could be further accumulated in Beijing due to the mountain blocking effect. By contrast, when the winds come from north, Beijing is in the upstream region relative to the pollution

source in Hebei, and the cold air from north can disperse the air pollutants. As shown in Figure 11, with similar wind speed, the occurrence rate of heavy air pollution is much higher for cases with winds from the south than from the north. Moreover, the aerosol pollution events also decrease with increasing wind speed for cases with winds both from the north and the south."

20, Fig 11 does not show haze occurrence but AOD and $PM_{2.5}$.
We agree with the reviewer that Figure 11 actually shows AOD and $PM_{2.5}$ instead of haze occurrence. We have modified our description in Pg 26 L3 – L13: "Figure 12 illustrates the relationship between the severity extent of aerosol amount denoted by AOD and $PM_{2.5}$ and surface wind speed. For good air quality with $PM_{2.5}$<50 μg/m^3, the occurrence rate increases with increasing wind speed, ranging from 39.3% (v<=1 m/s) to 92.9% (v>7 m/s). Differently, the occurrence of poor air quality with $PM_{2.5}$>150 μg/m^3 ranges from 20.92% (v<=1 m/s) to 0 (v>7 m/s). The weakening of surface wind speed reduces the transport of near-surface aerosol to the outside regions, leading to the build-up and continuance of heavy aerosol pollution condition in Beijing. On the contrary, the increase of surface wind speed, which may be due to the development of weather system like monsoon in Beijing, causes the disperse of aerosols, and then reduction of the heavy aerosol pollution occurrence rate."

22, 2 and fig 13: what is actually plotted: the axis annotation reads AOD, but AOD thus far was the column integrated extinction, i.e. independent of height. May be extinction is plotted? Should these profiles reflect that the PBLH varies with season, and thus also the aerosol vertical distribution vary with season? The strong decrease with height contradicts the assumption of a uniform mixing (p. 14).
The reviewer proposed very good questions here. Actually, what Figure 13 shows is similar to the extinction, instead of the columnar AOD. More correctly, the AOD in figure 13 is the integrated extinction at each atmospheric layer. In CALIPSO level 2 product, AOD_layer and AODcolumn could be calculated as

$$\begin{cases} AOD_h = k_h \times \Delta h \\ AOD_{column} = \sum_{h=0}^{H} AOD_h \end{cases}$$

Where AOD_h represents AOD at the altitude of h, k_h is the extinction coefficient at the altitude of h, Δh is layer depth and AOD_{column} is the AOD of the whole column.

We agree with the reviewer that the profile in Figure 13 actually partially reflect that the that PBLH varies with season. Moreover, the layer integrated values also depend on the aerosol type and size distribution in addition to $PM_{2.5}$, so it could vary with height within PBLH. We have removed Figure 13, 14 and corresponding descriptions in the revision version. By the way, the assumption of a uniform mixing in pg14 has been removed in this revision.

22, 9 as for Fig 13, I don't understand what is plotted here
Figure 14 has also been removed.

22, 18-21: same comments as for the top of the page. I don't understand what is shown here, and hence it is hard to comment. I also don't understand why in summer, with peak AOD at a height of 516 m, is concluded that most aerosol is below that height. Integration of the profiles below and above 500 m would give a number supporting this conclusion.
This figure and its corresponding descriptions have been removed. For your information, this figure is actually the probability density distribution function of layer integrated AOD with altitude in four seasons.

23, eq 5 This eq needs some more explanation. Apparently the authors assume here that CALIPSO AOD underestimates the true value (fig 3)? And therefore they scale to AERONET AOD?

What the reviewer understands is right. The quality-assured level 2.0 AERONET AOD data with a stated uncertainty of 0.015 were used as the "ground truth" (Holben et al., 1998). Compared with AERONET AOD, there exist errors in CALIPSO AOD measurements, which might be caused by cloud and near-surface noise. Thus, we use the CALIPSO vertical profile product to obtain the proportion of AOD at each layer to AOD of the whole column in the vertical direction. Combined with Aeronet AOD, AOD of different altitude can be acquired as accurately as possible. We have add he explanation in Pg 29 L5- 8: **"**As shown in Figure 3, the CALIPSO seems underestimate AOD compared to AEORNET. We here treat the AERONET AOD as more reliable or "ground truth" data, and use the CALIPSO vertical profile to scale the AERONET AOD for its vertical distribution.**".**

23, 15 how is top of atmosphere defined? Figure 15 would be easier to understand when the AOD was plotted on the same scale. Note that, $PM_{2.5}$ is plotted vs AOD, not AOD vs $PM_{2.5}$ as the caption says.

Here, the top of atmosphere is actually for the columnar atmosphere that the satellite can observe, which is about 705 km. We have modified it as "For heights of 500 m, 1000 m, PBLH and the whole atmospheric column, …**" in Pg 29 L11-13.**

Figure 15 has been modified by following the reviewer's suggestion. The title has been corrected as $PM_{2.5}$ vs AOD.

24, 1-3 this conclusion is clear and follows form Figure 13, and hence Fig 15 is obsolete, including the explanation on p.23; it also shows that the uniform-mixing assumption on p 14. is not valid for aerosol.

We agree with the reviewer. Currently, we have removed Figures 13 and 14 along with their descriptions. Instead, we kept using Figure 15 and its description.

The results shown in Figure 15 do indicate the varying extinction coefficient with heights within PBLH. This could be related with the changes of RH and particle size distribution with heights. We have removed the assumption used on Pg 14 by citing several aircraft observations which found that PM2.5 varies little with height within PBLH in Pg 16 L14-17: "Several aircraft observations studies (Liu et al., 2009; Zhang et al., 2009) have found that aerosol particles mainly concentrated within PBLH and that $PM_{2.5}$ mass concentration varies little with height within PBLH."**.**

Analysis of Influential Factors for the Relationship between $PM_{2.5}$ and AOD in Beijing

Caiwang Zheng[1,2], Chuanfeng Zhao[1,2,3]*, Yannian Zhu[1,2,43]*, Yang Wang[1,2], Xiaoqin Shi[1,2], Xiaolin Wu[1,2], Tianmeng Chen[1,2], Fang Wu[1,2], Yanmei Qiu[1,2]

1. State Key Laboratory of Earth Surface Processes and Resource Ecology, and College of Global Change and Earth System Science, Beijing Normal University, Beijing 100875, China

2. Joint Center for Global Change Studies, Beijing, 100875, China

3. Division of Geological and Planetary Sciences, California Institute of Technology, Pasadena, CA 91125, USA.

4. Meteorological Institute of Shaanxi Province, Xi' an, China

Correspondence to: Chuanfeng Zhao, czhao@bnu.edu.cn
Yannian Zhu, yannianzhu@gmail.com

Abstract: Relationship between aerosol optical depth (AOD) and $PM_{2.5}$ is often investigated in order to obtain surface $PM_{2.5}$ from satellite observation of AOD with a broad area coverage. However, various factors could affect the AOD-$PM_{2.5}$ regressions. Using both ground and satellite observations in Beijing from 2011 to 2015, this study analyzes the influential factors including the aerosol type, relative humidity (RH), atmospheric boundary layer height (PBLH), wind speed and direction, and the vertical structure of aerosol distribution. The ratio of $PM_{2.5}$ to AOD, which is defined as η, and the square of their correlation coefficient (R^2) have been examined. It shows that η varies from 54.32 to 183.14, 87.32 to 104.79, 95.13 to 163.52 and 1.23 to 235.08 μg/m^3 with aerosol type in four seasons respectively. η is smaller for scattering-dominant aerosols than for absorbing-dominant aerosols, and smaller for coarse mode aerosols than for fine mode aerosols. Both RH and PBLH affect the η value significantly. The higher the RH or~~, the larger the η, and~~ the higher the PBLH, the smaller the η. For AOD and $PM_{2.5}$ data with the correction of RH and PBLH compared to those without, R^2 of monthly averaged $PM_{2.5}$ and AOD at 14:00 LT increases from 0.63 to 0.76, and R^2 of multi-year averaged $PM_{2.5}$ and AOD by time of day increases from 0.01 to 0.93, 0.24 to 0.84, 0.85 to 0.91 and 0.84 to 0.93 in four seasons respectively. Wind direction is a key factor to the transport and spatial-temporal distribution of aerosols originated from different sources with distinctive physicochemical characteristics. Similar to the variation of AOD and $PM_{2.5}$, η also decreases with the increasing surface wind speed, indicating that the

contribution of surface $PM_{2.5}$ concentrations to AOD decreases with surface wind speed. ~~The vertical structure of aerosol exhibits a remarkable change with seasons, with most particles concentrated within about 500 m in summer and within 150 m in winter.~~ Compared to the AOD of the whole atmosphere, AOD below 500 m has a better correlation with $PM_{2.5}$, for which R^2 is 0.77. This study suggests that all the above influential factors should be considered when we investigate the AOD-$PM_{2.5}$ relationships.

Keywords: $PM_{2.5}$/AOD ratio, aerosol type, relative humidity (RH), atmospheric boundary layer height (PBLH), wind speed, aerosol vertical distribution.

1. Introduction

Atmospheric aerosols, also known as particulate matter, can influence the Earth's climate system by directly and indirectly modifying the incoming solar radiation and outgoing longwave radiation. The direct effect of aerosols on radiation refers to the absorption and scattering and absorption of the solar and longwave radiation by aerosols (Charlson et al., 1992; Koren et al., 2004; Lohmann and Feichter, 2005; Qian et al., 2007; Li et al., 2011; Huang et al., 2014; Yang et al., 2016). Aand the indirect effect of aerosols on radiation are associated with changes in the cloud macro- and micro-physical properties caused by aerosols which can serve as cloud condensation nuclei or ice nuclei (Twomey, 1977; Albrecht, 1989; Kaufman and Fraser, 1997; Feingold, 2003; Garrett et al., 2004; Garrett and Zhao, 2006; Zhao et al., 2012; Zhao and Garrett, 2015). The radiative effect of aerosols is relatively large due to increased emissions of pollution in East Asia (Wang et al., 2010a; Zhuang et al., 2013). Aerosols can also affect the precipitation intensity and patterns by changing cloud microphysical properties (Menon et al., 2002; Qian et al., 2009; Li et al., 2011; Guo et al., 2016a). Meanwhile, aerosols from anthropogenic pollution can cause serious impacts on atmospheric environment and human health by carrying hazardous materials (Pope et al., 2002; Zhang et al., 2007; Samoli et al., 2008; Xu et al., 2013). Thus, it is very important to get accurate information of aerosol properties, such as aerosol optical depth (AOD) and particle matter with size equal or smaller than 2.5 μm aerodynamic diameter ($PM_{2.5}$).

Aerosol properties are often obtained through satellite remote sensing, surface remote sensing, surface and aircraft in-situ observations. Remote sensing observation generally provides the aerosol optical properties such as ~~aerosol extinction coefficient and~~ AOD and aerosol extinction coefficient, but not the aerosol mass or number concentration. Differently, in-situ observations can provide direct measurements of aerosol number concentration and $PM_{2.5}$~~.~~ mass concentration. However, the limited samples for aircraft observation and limited sites for ground-based in-situ observation make it challenging to obtain the $PM_{2.5}$ over many locations, particularly the spatial distribution. Recent studies have proposed methods to estimate the surface $PM_{2.5}$ based on the AOD observations from satellites (van Donkel~~l~~aar et al., 2006, 2010, 2013; Drury et al., 2008; Wang et al., 2010b; Xin et al., 2016). Although $PM_{2.5}$ from AOD has not high temporal resolution and is not available when it is cloudy or very pollutant, these methods provide the spatial distribution of $PM_{2.5}$ globally or regionally (Paciorek et al., 2008; Li et al., 2017; Wang et al., 2017).

Many studies have focused on the building of statistical regression models to derive the surface $PM_{2.5}$ from AOD. For example, van Donkelaar et al. (2010) derived the global $PM_{2.5}$ concentration distribution from satellite-derived AOD using the $PM_{2.5}$/AOD ratios obtained from a global chemical transport model (CTM). Xin et al. (2015) investigated the relationships between $PM_{2.5}$ and AOD over China using the observations from the Campaign on atmospheric Aerosol Research-China network during the period from 2012 to 2013.

The relationships between $PM_{2.5}$ and AOD show significant differences over various locations (Corbin et al., 2002; Wang and Christopher, 2003; Hand et al., 2004; Ramachandran, 2005; Kumar et al., 2007; Zhang et al., 2009a; Ma et al., 2014). Some studies (e.g., Ma et al., 2014) have suggested that aerosol types and meteorological conditions can affect the relationship between $PM_{2.5}$ and AOD. However, systematic studies about the influential factors to the relationship between $PM_{2.5}$ and AOD have not been carried out, which are necessary for future derivation of accurate $PM_{2.5}$ from satellite AOD observations. Using both satellite and surface observation of aerosol properties and meteorology variables in Beijing from 2011 to 2015, this study analyzes the influential factors to AOD-$PM_{2.5}$ relationship, which includes aerosol type, relative humidity (RH), atmospheric planetary boundary layer height (PBLH), wind speed, and the vertical structure of aerosol distribution.

The paper is organized as follows. Section 2 describes the data and method. Section 3 analyzes the potential influential factors to AOD-$PM_{2.5}$ relationship, and section 4 summarizes the findings.

2. Data and Method

2.1 Data

The data used in this study are described as follows, including the data sources, their spatial and time resolutions, and the data period~~so on~~. These data includes surface $PM_{2.5}$ concentrations and AOD, satellite-based AOD from the

moderate-resolution imaging spectroradiometer (MODIS), satellite-based aerosol profiles from the Cloud-Aerosol Lidar and Infrared Pathfinder Satellite Observation (CALIPSO), and meteorology data from China Meteorological Administration (CMA) and European Centre for Medium Range Weather Forecast (ECMWF).

a. Ground $PM_{2.5}$ Measurements

The ground-based aerosol observation of $PM_{2.5}$ concentrations with hourly time resolution for the period of 2011 to 2015 is obtained from the U.S. Department of State at a single site (39.95 N, 116.47 E) in Beijing, as reported on the http://www.stateair.net/ website. The $PM_{2.5}$ mass concentration was measured using the U.S federal reference method. This method first uses a size selective inlet to remove particles larger than 10 μm, then takes use of another filter to remove the particles larger than 2.5 μm. The air parcels before entering the $PM_{2.5}$ instruments undergo a dry process (RH<35%), which ensure that all $PM_{2.5}$ observations are obtained at dry condition. While this dataset has not been officially evaluated, a comparison of $PM_{2.5}$ measurements from U.S Department of State and from Beijing Municipal Environmental Protection (MEP) Bureau at sites close to each other (1.6 km) in 2014 – 2016 shows great consistency with a correlation coefficient of 0.94 and root mean square difference of 14.3 μ~~u~~g/m^3. Considering that ~~T~~the~~is~~ data measured by U.S. Department of State have~~s relatively~~ longer time record, and have~~s~~ been widely used by many studies (Zheng et al., 2015; Jiang et al., 2015), they are adopted in this study.

b. Meteorological Data

Meteorological parameters with 3-hour temporal resolution at the MEP site which is about 1.6 km away from the U.S. Department of State site are provided by CMA, including cloud fraction (CF), 6-hour total precipitation (TP), relative humidity (RH), surface wind speed and wind direction. To eliminate the contamination of cloud and precipitation, data samples under cloudy (CF$\geqslant$0.1) or rainy conditions (TP>0) are removed. Same as Yang et al. (2016), we should note that even with this limitation, some days with few broken clouds (CF<0.1) still can introduce additional uncertainties to our study. Planetary boundary layer heights (PBLH) are extracted from the ~~European Centre for Medium-Range Weather Forecasts (~~ECMWF~~)~~ interim reanalysis (ERA-Interim; Dee et al. 2011), with a horizontal resolution of 0.125°× 0.125° and 3-hour temporal resolution. Guo et al. (2016b) have investigated the PBL in China from January 2011 to July 2015 using both the fine-resolution sounding observations and ECMWF reanalysis data. It was found that the seasonally averaged BLHs derived from reanalysis are generally in good agreement with those of observations in Beijing. Considering this and that there are only 2 times sounding observations every day, the seasonally averaged ERA-BLHs have been used in this study. We should admit that extra uncertainties could exist due to the distances between the MEP sit, U.S. Department of State site, and ECMWF grid, while they are close to each other.

c. AERONET measurements

The Aerosol Robotic Network (AERONET) program is a federation of ground-based remote sensing aerosol networks with more than 400 stations globally. At AERONET sites, the CE318 multiband sun-photometer is employed to measure spectral sun irradiance and sky radiances, from which AOD at 550 nm can be derived. The AOD data has been processed into three quality levels: Level 1.0 (unscreened), Level 1.5 (cloud-screened), and Level 2.0 (cloud screened and quality-assured) (Holben et al., 1998). A detailed description about AERONET retrievals is discussed in Holben et al. (1998). In this study, Level 2.0 AOD at 550 nm, SSA at 675 nm and Fine Mode Fraction (FMF) of Beijing (39ºN, 116ºE) are used. It's worth mentioning~~noting~~ that AOD retrieved from AERONET are accurate to within ±0.01 (Dubovik et al., 2000). Note that the AOD retrieved could have the impacts of relative humidity which has not been excluded yet.

d. CALIOPSO profile products

CALIPSO is one part of the National Aeronautics and Space Administration (NASA) A-Train, which is a constellation of satellites, tracking in a polar orbit and crossing the equator northbound at about 13:30 local time (LT) (Stephens et al. 2002). To investigate the characteristics of the aerosol vertical distribution, aerosol extinction profiles at 532 nm from Version 3.01 CALIOP Level 2 5 km Aerosol Profile for the period of 2011 to 2015 are used, which are provided by the CALIOP space borne lidar onboard the CALIPSO satellite (Winker et al., 2007, 2009; Hunt et al., 2009). The horizontal resolution is 5 km, and the vertical resolution varies with altitude. The

CALIPSO columnar AOD is the integration of aerosol extinction coefficient with the altitude, which has also been influenced by the relative humidity.

The extraction algorithm of the aerosol profile is shown in Figure. 1. First, the overpass time of CALIPSO satellite can be determined according to the geographical location of Beijing site (39.95ºN, 116.47ºE). Second, at each CALIPSO satellite pixel, AOD at each layer is derived as the integrationmultiplication of the extinction coefficient within thatand layer depth. Finally, the AOD profiles inside 100 km radius region surrounding the Beijing site is averaged as the final result. Note that when there are clouds or precipitation, the data are excluded in our analysis. Also, in this process, low-quality profiles in which *Extinction_Coefficient_Uncertainty_532* (*Sigma_Uncertainty* in Fig. 1) is greater than 99% and *COD* is greater than 0.1 have been excluded.

e. MODIS aerosol product

The MODIS instrument has a global coverage every one to two days with a viewing swath of 2330 km. It is operating on both the Terra and Aqua satellite, of which the overpass time are approximately 10:30 and 13:30 LT, respectively. To compare the AOD from MODIS and CALIPSO (only passes in the afternoon) observation, AOD from Terra (10:30 LT) are not used. Level 2 MODIS aerosol product data (Collection 5.1) for the period of 2011 to 2015 are obtained from the Level-1 and Atmosphere Archive and Distribution System (LAADS DAAC), of which the spatial resolution at nadir is 10 km×10 km (Levy et al., 2010). The AOD data

(MODIS parameter name: Deep_Blue_Aerosol_Optical_Depth_Land) at 550 nm are used in this study, which is only retrieved for daytime, cloud-free and snow/ice-free conditions with an uncertainty confidence level of ~20%.

2.2 Method

a. $PM_{2.5}$/AOD ratio

AOD represents the total attenuation that aerosols of the whole atmosphere exert on solar radiation, while $PM_{2.5}$ mass concentrations measured by the ground monitoring site can only reflect the near-surface air quality condition. Based on the assumption of linear relationship between AOD (unitless) and $PM_{2.5}$ (μg/m^3), van ~~Donkellar~~ Donkelaar et al. (2010) has introduced a conversion factor (η), which can be defined as:

$$\eta = \frac{PM_{2.5}}{AOD} \quad (1)$$

where η (μg/m^3) indicates the near surface aerosol $PM_{2.5}$ mass concentration per unit aerosol optical thickness ~~of aerosol particles per unit mass concentration~~. Its value depends on the aerosol type, aerosol size, RH, PBLH, and the vertical structure of aerosol distribution. At the same $PM_{2.5}$ mass concentration, the smaller the~~if~~ AOD ~~is smaller~~, the weaker the extinction capability ~~is weaker~~; and the larger the~~if~~ AOD ~~is larger~~, the stronger the extinction capability~~y is stronger~~. Note that the extinction capability here denotes the aerosol mass extinction coefficient. In other words, the larger the η, the weaker the aerosol extinction capability; the smaller the η, the

stronger the aerosol extinction capability. Using this factor, we can study the dependence of ~~$PM_{2.5}$~~-AOD-$PM_{2.5}$ relationship (represented by η) on different influential factors.

b. Aerosol Classification Method

Due to the difference of the sources, aerosols exhibit noticeable differences~~crepancies~~ in physical and optical properties with respect to the location and season. Fine-mode fraction (FMF) refers to the ~~AOD~~ fraction of AOD due to fine-mode aerosol particles with sizes smaller than 1 μm~~to the total~~. Angstrom exponent (AE) is exponent for the power law describing the wavelength dependence of the AOD~~an index reflecting the particulate size distribution of aerosols~~. Using FMF and AE, we can determine the dominant size mode of aerosols. We can also distinguish absorbing from non-absorbing aerosols based on measurements of single scattering albedo (SSA), which is defined as the ratio of the scatteringed coefficient to the extinction~~total attenuation~~ coefficient.

In this study, hourly averaged level 2 inversion products from AERONET at sites in Beijing are used, including FMF, AE and SSA data. Following Lee et al. (2010),~~.~~ ~~According to the radiation absorptivity and the size of aerosol particles (Lee, et al., 2010),~~ aerosols ~~is~~are classified into eight~~six~~ types as follows:

1) Coarse non-absorbing (SSA>0.95, FMF<=0.4 and AE<=0.6)
2) Coarse absorbing (SSA<=0.95, FMF<=0.4 and AE<=0.6)

3) Mixed non-absorbing (SSA>0.95, 0.4<=FMF<0.6 and 0.6<=AE<1.2)

4) Mixed absorbing (SSA<=0.95, 0.4<=FMF<0.6 and 0.6<=AE<1.2)

5) Fine non-absorbing (SSA>0.95, FMF>0.6 and AE>1.2)

6) Fine highly-absorbing (SSA<=0.85, FMF>0.6 and AE>1.2)

7) Fine moderately-absorbing (0.85<=SSA<0.9, FMF>0.6 and AE>1.2)

8) Fine slightly-absorbing (0.9<=SSA<0.95, FMF>0.6 and AE>1.2)

~~3) Fine non-absorbing (SSA>0.95, FMF>0.6 and AE>1.2)~~

~~4) Fine absorbing (SSA<=0.95, FMF>0.6 and AE>1.2)~~

~~5) Mixed non-absorbing (SSA>0.95, 0.4<=FMF<0.6 and 0.6<=AE<1.2)~~

~~6) Mixed absorbing (SSA<=0.95, 0.4<=FMF<0.6 and 0.6<=AE<1.2)~~

Coarse absorbing and fine absorbing aerosols can be~~are~~ considered as dust and black carbon (BC) respectively. ~~Since the high percentage of fine mode absorbing aerosol, it is further divided into heavily (SSA<=0.85), moderately (0.85<SSA<=0.9) and slightly (0.9<SSA<=0.95) absorbing aerosols.~~ Figure~~.~~ 2 shows the aerosol type classification performed using SSA, FMF and AE from AERONET at sites in Beijing using the classification method described above. Roughly, the aerosols are mainly fine mode slightly absorbing and non-absorbing particles in summer, and fine mode slightly and moderately absorbing particles in winter. The coarse mode dust aerosols mainly occurs in spring (MAM) and winter (DJF).

3. Analysis and Results

3.1 AOD

We first evaluate the uncertainties in the satellite observed AOD using the ground observations from AERONET at the satellite passing time, including both MODIS and CALIPSO at 13:30 LT. Based on the satellite overpass time, the corresponding AERONET AOD in time within 30-min are compared to MODIS AOD and CALIPSO AOD respectively, which is shown in Figure~~.~~ 3. The correlation between MODIS and AERONET AOD is significant (R^2 = 0.85, N = 415), with a slope of 1.32 and an RMS error of 0.23, indicating that MODIS AOD is biased high compared to AERONET AOD. In contrast, the correlation between CALIPSO and AERONET AOD is slightly lower than that between MODIS and AERONET (R^2 = 0.65, N = 70), with a slope of 0.78 and a RMS error of 0.31. In general, the CALIPSO AOD is biased low compared to AERONET AOD. The lower correlation of AOD between AERONET and CALIPSO than that between AERONET and MODIS is likely related to the limited data samples for AERONET-CALIPSO AOD comparison, which is also noted by Bibi et al. (2015).

Table 1 further shows the inter-comparison results of AOD between AERONET and MODIS in spring (MAM), summer (JJA), fall (SON) and winter (DJF), which include their seasonal averaged AOD, squared correlation, absolute bias, relative bias and sample number. The absolute bias is calculated as the difference of seasonally

averaged AOD from simultaneous AERONET and MODIS ~~at the same time~~measurements; and the relative bias is calculated as the ratio of the absolute bias to the seasonally averaged AERONET AOD. The seasonal averaged AOD are 0.49, 0.61, 0.30 and 0.19 respectively in four seasons for AERONET observations, and 0.66, 0.88, 0.39 and 0.21 for MODIS observations, which are highest in summer but lowest in winter. The corresponding sample numbers are 214, 103, 50 and 48 in four seasons. This seasonal variation pattern is also observed by Yu et al. (2009). MODIS has a substantial positive bias in spring, summer and fall (36.7, 44.7 and 32.9%), but a smaller positive bias in winter (10.2%). The squared correlation (R^2) between MODIS and~~correlates best with~~ AERONET in Beijing are 0.81, 0.87, 0.69 and 0.34 in four seasons, of which the corresponding RMSE are 0.23, 0.29, 0.15 and 0.08. Low correlation in winter may be caused by the shortage of data samples compared to other seasons~~spring and summer, of which R^2 is 0.81 and 0.87~~. When AOD becomes small, the relative errors in AOD from both MODIS and AERONET become large, which may cause the correlation of AOD between MODIS and AERONET also decrease as demonstrated in Table 1. ~~When the AOD becomes small, it seems that the correlation of AOD between MODIS and AERONET also decreases.~~

Same as Table 1, Table 2 shows the inter-comparison results of AOD between AERONET and CALIPSO in spring, summer, fall and winter. The bias shown in Table 2 is calculated in the same way as that in Table 1. The correlation (R^2) between CALIPSO and AERONET AOD are 0.52, 0.47~~8~~, 0.85 and 0.55 respectively in four

seasons. CALIPSO AOD has a positive bias in summer and winter (6.6 and 25.0%), but a negative bias in spring and fall (-5.2 and -14.2%). For all seasons, RMSE are less for MODIS than CALIPSO compared to AERONET. As indicated earlier, this is likely related to the limited data samples for AERONET-CALIPSO AOD comparison. The results shown in Fig. 2 and Tables 1 and 2 indicate that considerable uncertainties exist in the satellite observed AOD, introducing up to 45% errors (seasonal biases 5-45%) to the quantification of AOD-$PM_{2.5}$ relationships.

3.2 Effect of RH and PBLH

Relative humidity, by affecting the water uptake process of aerosols, can cause a pronounced change to the aerosol size distribution, chemical composition, and the extinction characteristics (Liu et al., 2008). The hygroscopic growth factor~~, defined as~~ f(RH), can be defined as~~denotes~~ the ratio of the aerosol scattering coefficients in ambient with a certain RH to that in dry air conditions (Li et al., 2014). In this ~~article~~study, f(RH) is expressed as follows in a simple function:

$$f(RH) = \frac{1}{(1 - RH/100)} \quad (2)$$

The hygroscopic growth process ~~causes the overestimation of the~~has a significant contribution to AOD~~, since the columnar AOD is derived under ambient conditions~~. Since $PM_{2.5}$ is often measured at a dry condition (<40% in relative humidity), we often need consider the impacts of relative humidity to AOD in order to get a more reliable $PM_{2.5}$-AOD relationship. A~~n adjusting~~ dehydration adjustment~~process~~ can be

applied to get the dry condition AOD, which is~~is needed, which can be described as~~:

$$AOD_{dry} = \frac{AOD}{f(RH)} \quad (3)$$

where AOD_{dry} represents the aerosol optical depth with dehydration adjustment.

PBLH influences the vertical profile of particulate matters. In general, the PBLH is dependent on many factors, including meteorological conditions, terrain, sensible heat flux, evaporation and ground roughness (Stull, 1988). Several aircraft observations studies (Liu et al., 2009; Zhang et al., 2009) have found that aerosol particles mainly concentrated within PBLH and that $PM_{2.5}$ mass concentration varies little with height within PBLH. ~~Based on the assumption that the air is uniformly mixed and aerosol particles are evenly distributed in the boundary layer~~Thus, the column integrated $PM_{2.5}$ mass concentration ($PM_{2.5\_column}$) within PBLH can be approximated as:

$$PM_{2.5\_column} = PM_{2.5} \times PBLH \quad (4)$$

In the atmosphere, the RH often increases with height within PBLH. This could definitely affect the dehydration adjustment of AOD in Eq. (3). Currently, we only use the surface RH to do the adjustment which could cause the dry condition AOD is actually somehow overestimated compared to its true value.

Previous studies have shown that aerosols are mainly concentrated within the PBL (Guinot et al., 2006; Zhang et al., 2009b). Here, we assume that the column integrated $PM_{2.5}$ within PBLH should be comparable to the whole column integrated $PM_{2.5}$. The calculation of column $PM_{2.5}$ mass concentration in Eq. (4) has implied that

there are no disconnected aerosol layers and could introduce errors in experimental conditions, which was not considered in this study. Eqs. (3) and (4) imply that for given $PM_{2.5}$, the increase of RH can result in the increase of AOD and the decrease of η, and that for given AOD, the increase of PBLH can cause the decrease of near-surface $PM_{2.5}$ concentrations and the decrease of η. Actually, PBLH often correlates with RH, making the separation of PBLH and RH effects challenging. Here, we simply show the effects of both PBLH and RH on the AOD-$PM_{2.5}$ relationship.

Figure~~.~~ 4(a) shows the time series of PBLH (km) and RH (%)**.** In Fig. 4a, the blue bands are for high PBLH and low RH, and the purple bands are for low PBLH and high PBLH, both of which indicate anti-correlated trends between PBLH and RH. Differently, the green (yellow) bands are for low (high) PBLH and low (high) RH, which indicates correlated trends of PBLH and RH. Clearly, there is generally an anti-correlated temporal trend between PBLH and RH.~~It's clear to see an opposite trend between PBLH and RH.~~ The averaged PBLH for 2011 to 2015 are 2.56 km, 1.97 km, 1.55 km and 1.32 km respectively in MAM, JJA, SON and DJF, of which the corresponding averaged RH are 27.58%, 48.73%, 42.78% and 33.05%. In May, PBLH has the highest value above 2.5 km, and in July, RH has the highest value above 50%. ~~The opposite trend between PBLH and RH shown in Fig. 6(a) implies that AOD-$PM_{2.5}$ relationship could be improved a lot while both of their effects are considered.~~ Without considering the variations of sources and sinks, PBLH is negatively correlated with $PM_{2.5}$, and RH is positively correlated with AOD. The

anti-correlated trend between PBLH and RH shown in Fig. 4a imply that the effects of PBLH and RH on the ~~$PM_{2.5}$~~-AOD-$PM_{2.5}$ relationship could be partially canceled out. However, it is still necessary to consider the effects of PBLH and RH for the study of $PM_{2.5}$-AOD relationship.

Figure~~.~~ 4(b) shows the temporal variation of monthly averaged AOD and $PM_{2.5}$ at 14:00 LT without any meteorology-based modification to the original observations. It shows a good positive relationship in the time variations of monthly averaged AOD and $PM_{2.5}$ with a high correlation (R^2 = 0.63). Although the temporal trend of AOD and $PM_{2.5}$ are basically consistent, AOD are considerably higher in MAM and JJA while $PM_{2.5}$ lower in JJA. That's because in MAM, PBLH is high and the vertical mixing of aerosols makes near-surface $PM_{2.5}$ concentrations low, while in JJA, RH is high and the hygroscopic growth of aerosols lead to the increase of AOD. Actually, PBLH and RH are influenced by the horizontal atmospheric circulation in different seasons, which contributes to the seasonal variations of $PM_{2.5}$ and AOD. Beijing is located in a mid-latitude East Asian monsoon region. In winter, heavy horizontal winds help the transportation of aerosols and result in a relatively low AOD, while low PBLH makes the surface $PM_{2.5}$ relatively high. By contrast, in summer, the high water vapor transported with the warm air from south makes both AOD and $PM_{2.5}$ relatively high, while high PBLH makes the surface $PM_{2.5}$ relatively low. These impacts from the horizontal atmospheric circulation make the seasonal variation of AOD is more significant than that for surface $PM_{2.5}$, as shown in Fig. 4b.

Figure. 4(c) further shows the temporal variation of monthly averaged AOD_{dry} and $PM_{2.5\_column}$ at 14:00 LT which have been adjusted based on Eqs. (3) and (4). Note that the AOD_{dry} is adjusted based on surface RH using Eqs. (2) and (3) and the vertical variation of RH has not been considered. As indicated earlier, the AOD_{dry} obtained here could be somehow overestimated compared to its true value. It shows much better positive relationship in the temporal variation of monthly averaged AOD_{dry} and $PM_{2.5\_column}$, with R^2 as 0.74. This promising result indicates that the PBLH and RH corrections are essential for the improvement of the retrieval accuracy of $PM_{2.5}$ from AOD.

Figure. 5 compares the diurnal variation of RH and PBLH over four seasons averaged from 2011 to 2015 in Beijing. In terms of seasonal difference, PBLH is the highest in MAM, followed by JJA and SON, the lowest in DJF, which is consistent with the results found by Guo et al. (2016b). In spring, high PBLH may be associated with the climatologically strongest near-surface wind speed, while in summer, high PBLH is contributed to the strong solar radiation (Guo et al., 2016b). RH is the highest in summer, followed by fall and winter, the lowest in spring. In terms of diurnal variation, it can be seen that from 8:00 to 14:00 LT, the solar radiation that surface receives increases, making PBLH rises and RH decreases gradually; PBLH at 14:00 LT is the highest and RH at 14:00 LT is the lowest within the whole day. However, from 14:00 to 20:00 LT, the solar radiation that surface receives reduces, thus PBLH goes down and RH increases gradually. PBLH is the lowest and RH is the

highest at 23:00 and 2:00 LT respectively within the whole day.

Figure. 6 shows the diurnal variation of multi-year (2011-2015) averaged RH and PBLH, AOD and $PM_{2.5}$, AOD_{dry} and $PM_{2.5\_cloumn}$ in four seasons when all four types of measurements are available. The columns represent four seasons of spring, summer, fall and winter and the rows represent different variables. Fig. 6(a1-d1) show that PBLH and RH demonstrate a steady increase and decrease trend from 6:00 to 17:00 LT, respectively, which is almost the same as their diurnal variation demonstrated in Fig. 5. As shown in Fig. 6(a2)-(d2), the AOD-$PM_{2.5}$ linear relationship shows that R^2 are 0.01, 0.24, 0.85 and 0.84 in four seasons respectively. After PBLH and RH corrections (Fig. 6(a3-d3)), it shows that R^2 between AOD_{dry} and $PM_{2.5\_cloumn}$ are 0.93, 0.84, 0.91, 0.93 in four seasons respectively. These results further indicate that RH and PBLH play essential roles for AOD-$PM_{2.5}$ relationship.

3.2 Aerosol type

To study the influence of aerosol type on η, we analyze the data from 11:00 to 17:00 LT in four seasons respectively. For this time period, the PBLH (RH) has high (low) values with weak variation, which make the impacts of PBLH and RH vary weakly with selected sample time in a season. By doing this, we try to keep a certain amount of data samples and limit the influence of diurnal and seasonal variation of RH and PBLH on η. The aerosol types can be classified based on the aerosol particle size and radiative absorptivity, and η is a good indicator to the extinction capability of

different aerosol types.

Figure. 7 depicts the seasonal frequency distribution of aerosol types in four seasons at Beijing for the period of 2011 to 2015. Dust accounts for 15.4%, 0.4%, 6.4% and 6.9% in spring (MAM), summer (JJA), fall (SON) and winter (DJF) respectively. Same as that indicated from Fig. 1, dust aerosols is heavy in spring and winter, particularly in spring. Higher proportion of dust in spring is mainly associated with the long-range transport from northwest arid areas (Yan et al., 2015, Tan et al., 2012). Fine mode absorbing aerosols account for 36.5%, 42.6%, 51.1% and 60.3% in four seasons respectively, of which moderately absorbing aerosols account for the highest. Owing to the biomass burning and soot emission generated from heating, the fine mode heavily-absorbing aerosol percentage is higher in winter than in other seasons, which is 7.7%. The content of ~~heavily~~ fine non-absorbing aerosol~~s~~ is significantly higher in summer and fall than in other two seasons, particularly in summer with a value of 48.4%. As a whole, the aerosol particles in Beijing are primarily fine-mode and absorbing aerosols in terms of particle size and optical property.

Figure. 8 presents the variation of η with the aerosol type by season in Beijing. Note that there are too few coarse-mode cases in summer and the corresponding η is a missing value. η generally decrease with particle size, with the smallest value for coarse-mode aerosols and largest value for fine-mode aerosols, and it seems that η of non-absorbing aerosols is smaller than absorbing aerosols. ~~This implies that the aerosol extinction capacity increases with particle size, and it is stronger for the~~

~~non-absorbing aerosols than absorbing aerosols.~~Theoretically, aerosol extinction capacity increases with particle size parameter ($x=2\pi r/\lambda$) and reaches a maximum value when size parameter is around 6. Therefore, for solar visible radiation (such as λ=500 nm), the extinction capacity for aerosol particles generally increases with size for particles with radius less than 0.5 μm, and then decreases when radius larger than 0.5 μm. Actually, for the wavelength of 550 nm, the extinction efficiency of fine-mode particles (peak radius ranging from ~0.11 to ~0.33 μm) is stronger than coarse-mode aerosols. Moreover, coarse particles, which may be not included in $PM_{2.5}$, can contribute a lot to the extinction at wavelengths in the visible, and thus to AOD. This is especially true for dust days dominated by coarse-mode aerosols, of which high AOD is more likely to be due to PM_{10} rather than $PM_{2.5}$. These make the lower η for coarse-mode than fine mode aerosol.

Table 3 further compares the AERONET hourly averaged AOD to $PM_{2.5}$ mass concentrations by aerosol type. Coarse Non-absorbing aerosols show the lowest correlation between AOD and $PM_{2.5}$, of which R^2 is 0.10. For all kinds of aerosols, the correlation between AOD and $PM_{2.5}$ is relatively lower than that for aerosols with a specific type other than coarse non-absorbing, of which R^2 is 0.51 and RMS error is 46.34 μg/m^3.

Figure~~.~~ 9 shows the difference in the relationship between~~of~~ $PM_{2.5}$ and AOD among five~~six~~ different aerosol types by season. The coarse non-absorbing aerosol is too few to be analyzed and shown here. We have also done the linear regression

analysis for~~For~~ all types of aerosols which is not shown here, and found that the slopes of the linear regression functions ($PM_{2.5}$=a×AOD+b) are 90.16, 56.9, 117.97 and 138.42 in four seasons respectively. The seasonal differences of the slopes are attributed to the effect of PBLH and RH. In summer, high RH brings about the hygroscopic growth of aerosol, thus increasing the extinction capacity~~efficiency~~ of aerosols and then reducing the slope. Moreover, the high PBLH in summer reduces the relative contribution of surface $PM_{2.5}$ to the columnar AOD and makes a smaller slope value. Differently, in winter, low PBLH value increases the relative contribution of surface $PM_{2.5}$ to the columnar AOD, thus increasing the slope. The slopes in spring and autumn fall in between. However, there are large differences in the slope of regression functions among different aerosol types~~, which varies from 13.75 to 111.09, 40.04 to 204.45, 70.79 to 130.56 and 43.58 to 157.93 μg/m^3 in four seasons respectively~~. For absorbing aerosols, the slope roughly decreases with increasing particle size from coarse, mixed to fine particles, with values of about 89, 111, 104 μg/m^3 in spring, 85, 122, 74 μg/m^3 in summer, 71, 163, 131 μg/m^3 in fall, and 44, 143, 158 μg/m^3 in winter. The slope is also generally larger for absorbing than non-absorbing aerosol. The slopes for mixed absorbing and non-absorbing aerosol are 111 and 65 μg/m^3 in spring, 122 and 40 μg/m^3 in summer, 163 and 109 μg/m^3 in fall, and 143 and 89 μg/m^3 in winter. And the slopes for fine absorbing and non-absorbing aerosol are 105 and 76 μg/m3 in spring, 74 and 65 μg/m^3 in summer, 131 and 96 μg/m^3 in fall, and 158 and 122 μg/m^3 in winter. Thus, s~~S~~ame as shown in Fig. 8~~4~~, the

slope roughly decreases with particle size, with smallest values for coarse-mode aerosols and largeest values for fine-mode aerosols in four seasons, and the slope of non-absorbing aerosols is generally smaller than absorbing aerosols.

The findings in this section implyies that AOD-$PM_{2.5}$ AOD relationship varies considerably with aerosol types. When we investigate the relationship between $PM_{2.5}$ and AOD, the aerosol types should be carefully considered for study regions.

3.4 Wind

This section discusses how wind affects the AOD-$PM_{2.5}$ relationship in two aspects: wind direction and surface wind speed. Surrounded by Hebei province with severe pollution, Beijing is affected by the long-range transport of aerosols and gas-phase pollutants. The seasonal variation of wind direction changes the transport and spatial-temporal distribution of aerosols and gas-phase pollutants originated from different sources with distinctive physicochemical characteristics, which has a direct influence on the AOD-$PM_{2.5}$ relationship.

Figure. 10 describes the wind rose of Beijing in four seasons for the period from 2011 to 2015. Surface wind speed is mainly distributed in the range of 0 to 9 m/s. Wind direction is mainly southwest in spring and summer, northeast in fall and northwest in winter. There are more windy days in spring and winter. The northwest wind in spring causes the transport of dust aerosols from gobi and desert regions of China to Beijing. The occurrence frequency of stable weather (v=0 m/s) are 4.2%,

5.8%, 9.2% and 8.3% in spring, summer, fall and winter, respectively. Different from the wind speed which will be analyzed in Figs. 12~~1~~ and 13~~2~~, the influence of wind direction to the AOD-$PM_{2.5}$ relationship is ~~not significant, at least in this study, which is worthy for further study in the future.~~often combined with the effect of wind speed. Beijing is surrounded by Hebei province and mountains in the northern areas. When the winds come from south, Beijing is in the downstream location to the pollution source from Hebei and the pollutants could be further accumulated in Beijing due to the mountain blocking effect. By contrast, when the winds come from north, Beijing is in the upstream region relative to the pollution source in Hebei, and the cold air from north can disperse the air pollutants. As shown in Figure 11, with similar wind speed, the occurrence rate of heavy air pollution is much higher for cases with winds from the south than from the north. Moreover, the aerosol pollution events also decrease with increasing wind speed for cases with winds both from the north and the south.

Figure~~.~~ 12~~1~~ illustrates the relationship between the severity extent of aerosol amount denoted by AOD and $PM_{2.5}$~~haze~~ and~~with~~ surface wind speed. For good air quality with ~~(~~$PM_{2.5}$<50 μg/m^3~~)~~, the occurrence rate increases with increasing wind speed, ranging from 39.3% (v<=1 m/s) to 92.9% (v>7 m/s). Differently, the occurrence of poor air quality with ~~(~~$PM_{2.5}$>150 μg/m^3~~)~~ ranges from 20.92% (v<=1 m/s) to 0 (v>7 m/s). The weakening of surface wind speed reduces the transport of near-surface aerosol~~haze~~ to the outside regions, leading to the build-up and

continuance of heavy aerosol pollution condition~~haze weather~~ in Beijing. On the contrary, the increase of surface wind speed, which may be due to the development of weather system like monsoon in Beijing, causes the disperse of aerosols, and then reduction of the heavy aerosol pollution~~haze~~ occurrence rate.

Figure~~.~~ 1~~3~~2 describes the variation of averaged AOD, $PM_{2.5}$ and η with surface wind speed. Although AOD and $PM_{2.5}$ are basically consistent in the decreasinge trend with the increasing surface wind speed, AOD variation is more complicated and less sensitive to surface wind speed. Compared with the $PM_{2.5}$ variation range of 10~110 $\mu g/m^3$, the variation range of AOD is between 0.2 and 0.6. Moreover, there are even cases that AOD increases with wind speed, such as when wind speed is less than 3 m/s. This is likely associated with the fact that the columnar AOD is affected by many factors, and the surface wind speed is just a disturbing term to surface $PM_{2.5}$. Similar to the variation of AOD and $PM_{2.5}$, η also decreases with the increasing surface wind speed, indicating that the contribution of surface $PM_{2.5}$ concentrations to AOD decreases with surface wind speed.

3.5 Vertical distribution of aerosols

It has indicated that the relationship between AOD and $PM_{2.5}$ varies with the surface wind speed and the surface aerosol amount. Considering that AOD is the vertical integration of aerosol optical properties, the AOD-$PM_{2.5}$ relationship should vary with the vertical distribution of aerosols. We examine this by using the extinction

profiles in 532 nm band from the Version 3.01 CALIOP Level 2 5 km Aerosol Profile product from 2011 to 2015.

~~Fig. 13 shows the CALIPSO aerosol optical depth vertical distribution profile and cumulative distribution with height in four seasons. Fig. 13(a) shows that there are different AOD vertical distribution patterns among four seasons. The maximum AOD occurs at different heights as described later in Fig. 14. These different vertical patterns could make the AOD-$PM_{2.5}$ relationship vary with season. Fig. 13(b) further shows that cumulative AOD is very different in summer from other seasons, with more concentrated at high heights.~~

~~Fig.14 shows the probability density distribution function (PDF) of AOD with altitude in four different seasons.~~ Within the atmospheric boundary layer, the main air movement form is the turbulent motion, promoting the vertical exchanges of heat, water vapor, momentum and various kinds of materials including aerosol pollutants. The turbulent energy is generally dependent on both the buoyancy and wind shear, particularly the buoyancy which is highly related to surface downwelling radiation. Obviously, compared to other seasons, the solar radiation received by the surface is more in summer, and the turbulence is stronger, making aerosol transfer to a higher altitude. The seasonal variation of PBLH shown earlier has illustrated this. Associated with the variation of PBLH, ~~As expected and that shown in Fig. 13 (a), the vertical distribution of AOD is highly different in four seasons, implying different AOD-$PM_{2.5}$ relationships. The height *h* with peak AOD is 516.8 m in summer, higher than that in~~

~~other seasons, indicating that the aerosols are mainly distributed in heights below ~500 m. The height *h* with peak AOD is about 337 and 277 m in spring and fall, respectively. In winter, the surface receives the least amount of solar radiation, leading to weak turbulence. Correspondingly, *h* with peak AOD is only 158 m in winter, indicating that the aerosols are mainly distributed near the surface layer, contributing to heavy haze events in this season.~~

~~The significant time variation of t~~the aerosol vertical distribution ~~makes it one of key factors to~~also varies and further influences the AOD-$PM_{2.5}$ relationship. We next examine the relationship between AOD from surface to different heights and $PM_{2.5}$ at surface. By defining AOD below a height as the integration of extinction coefficients vertically from surface to that height, the ratio of AOD below a specific height to the total AOD can be determined by CALIPSO vertical profile, which is

$$AOD_H = AOD_{AeronetTotal} \times \frac{AOD_{CalipsoBelowH}}{AOD_{CalipsoTotal}} \quad (5)$$

where $AOD_{AeronetTotal}$ is AOD derived by AERONET, $AOD_{CalipsoTotal}$ is the total AOD from CALIPSO. $AOD_{CalipsoBelowH}$ is AOD below H from CALIPSO. AOD_H is the AOD below H. As shown in Figure 3, the CALIPSO seems underestimate AOD compared to AEORNET. We here treat the AERONET AOD as more reliable or "ground truth" data, and use the CALIPSO vertical profile to scale the AERONET AOD for its vertical distribution.

We here examine four heights, which are 500 m, 1000 m, PBLH and ~~top of~~

~~atmosphere~~the whole columnar atmosphere that MODIS observes. Note that PBLH is not constant, but varies with time. Figure~~.~~ 1~~45~~ shows linear relationships between AOD below these four heights and $PM_{2.5}$ at surface. For ~~four~~ heights of 500 m, 1000 m, PBLH and the whole atmospheric column~~top of atmosphere~~, we can see that the correlation between AOD below and surface $PM_{2.5}$ decreases with selected heights, with R^2 of 0.77, 0.76, 0.66 and 0.64 respectively. More clearly, the slopes of linear regression lines vary a lot for heights 500 m, 1000 m and PBLH, but much smaller for *H* above PBLH. This further implies that most of aerosols concentrate within PBLH in the atmosphere, and the variation of aerosol vertical distribution could introduce large uncertainties to AOD-$PM_{2.5}$ relationship.~~–~~

4. Summary

This study analyzes the various factors that affect the AOD-$PM_{2.5}$ relationship qualitatively or quantitatively, including the satellite AOD observation, aerosol type, RH, PBLH, wind direction and speed, and the aerosol vertical distribution. It shows all of these factors can change the AOD-$PM_{2.5}$ relationship, with different contributions. AOD from MODIS and CALIPSO are evaluated against the AERONET data. The MODIS and AERONET AOD correlation is significant (R^2 = 0.85, N = 415), with a slope of 1.32 and a RMS error of 0.23, indicating that AOD is higher from MODIS than that from AERONET. In contrast, the correlation of AOD between CALIPSO and AERONET is slightly lower (R^2 = 0.65, N = 70), with a slope of 0.78 and a RMS error of 0.31.

There are large differences in the seasonal and diurnal variation of PBLH and RH. In Beijing, PBLH is the highest in spring, followed by summer and fall, the lowest in winter, and RH is the highest in summer, followed by fall and winter, the lowest in spring. For AOD and $PM_{2.5}$ data with the correction of RH and PBLH compared to those without, R^2 of monthly averaged $PM_{2.5}$ and AOD at 14:00 LT increases from 0.63 to 0.76, and R^2 of multi-year averaged $PM_{2.5}$ and AOD by time of day increases from 0.01 to 0.93, 0.24 to 0.84, 0.85 to 0.91 and 0.84 to 0.93 in four seasons respectively.

The aerosol particles in Beijing are primarily fine-mode and absorbing aerosols in terms of particle size and optical property. Due to the long-range transport of aerosols from northwest arid areas, dust aerosols is heavy in spring and winter, particularly in spring. It shows that η varies from 54.32 to 183.14, 87.32 to 104.79, 95.13 to 163.52 and 1.23 to 235.08 $\mu g/m^3$ with the aerosol type in spring, summer, fall and winter, respectively. η is generally smaller for scattering-dominant aerosols than for absorbing-dominant aerosols, and smaller for coarse mode aerosols than for fine mode aerosols.

The surface wind speed significantly affects the occurrence of haze events. For good air quality ($PM_{2.5}$<50 $\mu g/m^3$), the occurrence rate increases with increasing wind speed, ranging from 39.3% (v<=1 m/s) to 92.9% (v>7 m/s). Differently, the occurrence of poor air quality ($PM_{2.5}$>150 $\mu g/m^3$) ranges from 20.92% (v<=1 m/s) to 0 (v>7 m/s). It shows that η decreases with the increasing surface wind speed,

indicating that the contribution of surface $PM_{2.5}$ concentrations to AOD decreases with surface wind speed.

The vertical structure of aerosol distribution exhibits a remarkable change with seasons, which could also contribute a lot to the AOD-$PM_{2.5}$ relationship. This study shows that aerosols mainly concentrate within about 500 m height in summer, while concentrate within the surface layer of around 150 m height in winter in Beijing. Compared to the AOD of the whole atmosphere, AOD below 500 m has a better correlation with $PM_{2.5}$, of which R^2 is 0.77 and RMSE is 38.6 μg/m^3.

With these findings, we need consider at least the impacts of PBLH, RH, Wind speed and wind direction, and use the AOD within PBL heights to build up better $PM_{2.5}$-AOD relationship. The impacts of these influential factors have been investigated while an optimal empirical $PM_{2.5}$-AOD relationship scheme has not been reached, which definitely need further study in future.

Acknowledgements

This work was supported by the National Natural Science Foundation of China (NSFC: grant 41575143), the Ministry of Science and Technology of China (grants 20 13CB955802), the China "1000 Plan" young scholar program, and the Chinese Progra m for New Century Excellent Talents in University (NCET). Sincerest thanks to the AERONET, MODIS and CALIPSO teams for their datasets. The CALIPSO data were acquired~~obtained~~ from the NASA Langley Research Center Atmospheric Science Data Center. Special thanks to the U.S. Embassy and CMA providing the $PM_{2.5}$ data

and meteorological data respectively.

References

Alebrecht, B. A.: Aerosols, cloud microphysics, and fractional cloudiness, SCIENCE, 245, 1227-1230, 10.1126/science.245.4923.1227, 1989.

Bibi, H., Alam, K., Chishtie, F., et al.: Intercomparison of MODIS, MISR, OMI, and CALIPSO aerosol optical depth retrievals for four locations on the Indo-Gangetic plains and validation against AERONET data, Atmospheric Environment, 111, 113-126, 2015.

Charlson, R. J., Schwartz, S. E., Hales, J. M., Cess, R. D., Coakley, J. A., Hansen, J. E., and Hofmann, D. J.: Climate forcing by anthropogenic aerosols, SCIENCE, 255, 423-430, 10.1126/science.255.5043.423, 1992.

Corbin, K. C., Kreidenweis, S. M., and Vonder Haar, T. H.: Comparison of aerosol properties derived from Sun photometer data and ground-based chemical measurements, GEOPHYSICAL RESEARCH LETTERS, 29, 10.1029/2001gl014105, 2002.

Dee, D. P., Uppala, S. M., Simmons, A. J., Berrisford, P., Poli, P., Kobayashi, S., Andrae, U., Balmaseda, M. A., Balsamo, G., Bauer, P., Bechtold, P., Beljaars, A. C. M., van de Berg, L., Bidlot, J., Bormann, N., Delsol, C., Dragani, R., Fuentes, M., Geer, A. J., Haimberger, L., Healy, S. B., Hersbach, H., Holm, E. V., Isaksen, L., Kallberg, P., Koehler, M., Matricardi, M., McNally, A. P., Monge-Sanz, B. M., Morcrette, J. J., Park, B. K., Peubey, C., de Rosnay, P., Tavolato, C., Thepaut, J. N., and Vitart, F.: The ERA-Interim reanalysis: configuration and performance of

the data assimilation system, QUARTERLY JOURNAL OF THE ROYAL METEOROLOGICAL SOCIETY, 137, 553-597, 10.1002/qj.828, 2011.

Drury, E., Jacob, D. J., Wang, J., Spurr, R. J. D., and Chance, K.: Improved algorithm for MODIS satellite retrievals of aerosol optical depths over western North America, JOURNAL OF GEOPHYSICAL RESEARCH-ATMOSPHERES, 113, 10.1029/2007jd009573, 2008.

Dubovik, O., Smirnov, A., Holben, B. N., King, M. D., Kaufman, Y. J., Eck, T. F., and Slutsker, I.: Accuracy assessments of aerosol optical properties retrieved from Aerosol Robotic Network (AERONET) Sun and sky radiance measurements, JOURNAL OF GEOPHYSICAL RESEARCH-ATMOSPHERES, 105, 9791-9806, 10.1029/2000jd900040, 2000.

Feingold, G.: Modeling of the first indirect effect: Analysis of measurement requirements, GEOPHYSICAL RESEARCH LETTERS, 30, 10.1029/2003gl017967, 2003.

Garrett, T. J., Zhao, C., Dong, X., Mace, G. G., and Hobbs, P. V.: Effects of varying aerosol regimes on low-level Arctic stratus, GEOPHYSICAL RESEARCH LETTERS, 31, 10.1029/2004gl019928, 2004.

Garrett, T. J., and Zhao, C. F.: Increased Arctic cloud longwave emissivity associated with pollution from mid-latitudes, NATURE, 440, 787-789, 10.1038/nature04636, 2006.

Green, M., Kondragunta, S., Ciren, P., and Xu, C.: Comparison of GOES and MODIS

Aerosol Optical Depth (AOD) to Aerosol Robotic Network (AERONET) AOD and IMPROVE $PM_{2.5}$ Mass at Bondville, Illinois, JOURNAL OF THE AIR & WASTE MANAGEMENT ASSOCIATION, 59, 1082-1091, 10.3155/1047-3289.59.9.1082, 2009.

Guinot, B., Roger, J.-C., Cachier, H., Wang, P., Bai, J., and Tong, Y.: Impact of vertical atmospheric structure on Beijing aerosol distribution, ATMOSPHERIC ENVIRONMENT, 40, 5167-5180, 10.1016/j.atmosenv.2006.03.051, 2006.

Guo, J., Deng, M., Lee, S. S., Wang, F., Li, Z., Zhai, P., Liu, H., Lv, W., Yao, W., and Li, X.: Delaying precipitation and lightning by air pollution over the Pearl River Delta. Part I: Observational analyses, JOURNAL OF GEOPHYSICAL RESEARCH-ATMOSPHERES, 121, 6472-6488, 10.1002/2015jd023257, 2016a.

Guo, J., Miao, Y., Zhang, Y., Liu, H., Li, Z., Zhang, W., He, J., Lou, M., Yan, Y., Bian, L., and Zhai, P.: The climatology of planetary boundary layer height in China derived from radiosonde and reanalysis data, ATMOSPHERIC CHEMISTRY AND PHYSICS, 16, 13309-13319, 10.5194/acp-16-13309-2016, 2016b.

Hand, J. L., Kreidenweis, S. M., Slusser, J., and Scott, G.: Comparisons of aerosol optical properties derived from Sun photometry to estimates inferred from surface measurements in Big Bend National Park, Texas, ATMOSPHERIC ENVIRONMENT, 38, 6813-6821, 10.1016/j.atmosenv.2004.09.004, 2004.

Holben, B. N., Eck, T. F., Slutsker, I., Tanre, D., Buis, J. P., Setzer, A., Vermote, E., Reagan, J. A., Kaufman, Y. J., Nakajima, T., Lavenu, F., Jankowiak, I., and

Smirnov, A.: AERONET - A federated instrument network and data archive for aerosol characterization, REMOTE SENSING OF ENVIRONMENT, 66, 1-16, 10.1016/s0034-4257(98)00031-5, 1998.

Huang, J., Wang, T., Wang, W., Li, Z., and Yan, H.: Climate effects of dust aerosols over East Asian arid and semiarid regions, JOURNAL OF GEOPHYSICAL RESEARCH-ATMOSPHERES, 119, 11398-11416, 10.1002/2014jd021796, 2014.

Hunt, W. H., Winker, D. M., Vaughan, M. A., Powell, K. A., Lucker, P. L., and Weimer, C.: CALIPSO Lidar Description and Performance Assessment, JOURNAL OF ATMOSPHERIC AND OCEANIC TECHNOLOGY, 26, 1214-1228, 10.1175/2009jtecha1223.1, 2009.

Jiang, J., Zhou, W., Cheng, Z., Wang, S., He, K., and Hao, J.: Particulate Matter Distributions in China during a Winter Period with Frequent Pollution Episodes (January 2013), AEROSOL AND AIR QUALITY RESEARCH, 15, 494-U157, 10.4209/aaqr.2014.04.0070, 2015.

Kaufman, Y. J., and Fraser, R. S.: The effect of smoke particles on clouds and climate forcing, 5332, 1636-1639 pp., 1997.

Koren, I., Kaufman, Y. J., Remer, L. A., and Martins, J. V.: Measurement of the effect of Amazon smoke on inhibition of cloud formation, SCIENCE, 303, 1342-1345, 10.1126/science.1089424, 2004.

Kumar, N., Chu, A., and Foster, A.: An empirical relationship between $PM_{2.5}$ and

aerosol optical depth in Delhi Metropolitan, ATMOSPHERIC ENVIRONMENT, 41, 4492-4503, 10.1016/j.atmosenv.2007.01.046, 2007.

Lee, J., Kim, J., Song, C. H., Kim, S. B., Chun, Y., Sohn, B. J., and Holben, B. N.: Characteristics of aerosol types from AERONET sunphotometer measurements, ATMOSPHERIC ENVIRONMENT, 44, 3110-3117, 10.1016/j.atmosenv.2010.05.035, 2010.

Levy, R. C., Remer, L. A., Kleidman, R. G., Mattoo, S., Ichoku, C., Kahn, R., and Eck, T. F.: Global evaluation of the Collection 5 MODIS dark-target aerosol products over land, ATMOSPHERIC CHEMISTRY AND PHYSICS, 10, 10399-10420, 10.5194/acp-10-10399-2010, 2010.

Li, J., Han, Z., and Zhang, R.: Influence of aerosol hygroscopic growth parameterization on aerosol optical depth and direct radiative forcing over East Asia, ATMOSPHERIC RESEARCH, 140, 14-27, 10.1016/j.atmosres.2014.01.013, 2014.

Li, S., Joseph, E., Min, Q., Yin, B., Sakai, R., and Payne, M. K.: Remote sensing of $PM_{2.5}$ during cloudy and nighttime periods using ceilometer backscatter, ATMOSPHERIC MEASUREMENT TECHNIQUES, 10, 2093-2104, 10.5194/amt-10-2093-2017, 2017.

Li, Z., Niu, F., Fan, J., Liu, Y., Rosenfeld, D., and Ding, Y.: Long-term impacts of aerosols on the vertical development of clouds and precipitation, NATURE GEOSCIENCE, 4, 888-894, 10.1038/ngeo1313, 2011.

Liu, P., Zhao, C.,Zhang, Q., Deng, Z., Huang, M., Ma, X., and Tie, X.: Aircraft study of aerosol vertical distributions over Beijing and their optical properties. *Tellus B.*, **61**, 756–767, doi: 10.1111/j.1600-0889.2009.00440.x, 2009.

Liu, X., Cheng, Y., Zhang, Y., Jung, J., Sugimoto, N., Chang, S.-Y., Kim, Y. J., Fan, S., and Zeng, L.: Influences of relative humidity and particle chemical composition on aerosol scattering properties during the 2006 PRD campaign, ATMOSPHERIC ENVIRONMENT, 42, 1525-1536, 10.1016/j.atmosenv.2007.10.077, 2008.

Lohmann, U., and Feichter, J.: Global indirect aerosol effects: a review, ATMOSPHERIC CHEMISTRY AND PHYSICS, 5, 715-737, 2005.

Ma, Z., Hu, X., Huang, L., Bi, J., and Liu, Y.: Estimating ground-Level $PM_{2.5}$ in China using satellite remote sensing, ENVIRONMENTAL SCIENCE & TECHNOLOGY, 48, 7436-7444, 10.1021/es5009399, 2014.

Menon, S., Hansen, J., Nazarenko, L., and Luo, Y. F.: Climate effects of black carbon aerosols in China and India, SCIENCE, 297, 2250-2253, 10.1126/science.1075159, 2002.

Paciorek, C. J., Liu, Y., Moreno-Macias, H., and Kondragunta, S.: Spatiotemporal associations between GOES aerosol optical depth retrievals and ground-level $PM_{2.5}$, ENVIRONMENTAL SCIENCE & TECHNOLOGY, 42, 5800-5806, 10.1021/es703181j, 2008.

Pope, C. A., Burnett, R. T., Thun, M. J., Calle, E. E., Krewski, D., Ito, K., and

Thurston, G. D.: Lung cancer, cardiopulmonary mortality, and long-term exposure to fine particulate air pollution, JAMA-JOURNAL OF THE AMERICAN MEDICAL ASSOCIATION, 287, 1132-1141, 10.1001/jama.287.9.1132, 2002.

Qian, Y., Wang, W., Leung, L. R., and Kaiser, D. P.: Variability of solar radiation under cloud-free skies in China: The role of aerosols, GEOPHYSICAL RESEARCH LETTERS, 34, 10.1029/2006gl028800, 2007.

Qian, Y., Gong, D., Fan, J., Leung, L. R., Bennartz, R., Chen, D., and Wang, W.: Heavy pollution suppresses light rain in China: Observations and modeling, JOURNAL OF GEOPHYSICAL RESEARCH-ATMOSPHERES, 114, 10.1029/2008jd011575, 2009.

Ramachandran, S.: $PM_{2.5}$ mass concentrations in comparison with aerosol optical depths over the Arabian Sea and Indian Ocean during winter monsoon, ATMOSPHERIC ENVIRONMENT, 39, 1879-1890, 10.1016/j.atmosenv.2004.12.003, 2005.

Samoli, E., Peng, R., Ramsay, T., Pipikou, M., Touloumi, G., Dominici, F., Burnett, R., Cohen, A., Krewski, D., Samet, J., and Katsouyanni, K.: Acute Effects of Ambient Particulate Matter on Mortality in Europe and North America: Results from the APHENA Study, ENVIRONMENTAL HEALTH PERSPECTIVES, 116, 1480-1486, 10.1289/ehp.11345, 2008.

Stephens, G. L., Vane, D. G., Boain, R. J., Mace, G. G., Sassen, K., Wang, Z. E.,

Illingworth, A. J., O'Connor, E. J., Rossow, W. B., Durden, S. L., Miller, S. D., Austin, R. T., Benedetti, A., and Mitrescu, C.: The cloudsat mission and the a-train - A new dimension of space-based observations of clouds and precipitation, BULLETIN OF THE AMERICAN METEOROLOGICAL SOCIETY, 83, 1771-1790, 10.1175/bams-83-12-1771, 2002.

Stull, R. B.: An introduction to boundary layer meteorology, Kluwer Academic Publishers, Dordrecht, 670 pp., 1988.

Tan, S.-C., Shi, G.-Y., and Wang, H.: Long-range transport of spring dust storms in Inner Mongolia and impact on the China seas, ATMOSPHERIC ENVIRONMENT, 46, 299-308, 10.1016/j.atmosenv.2011.09.058, 2012.

Twomey, S.: Influence of pollution on shortwave albedo of clouds, JOURNAL OF THE ATMOSPHERIC SCIENCES, 34, 1149-1152, 10.1175/1520-0469(1977)034<1149:tiopot>2.0.co;2, 1977.

van Donkelaar, A., Martin, R. V., and Park, R. J.: Estimating ground-level $PM_{2.5}$ using aerosol optical depth determined from satellite remote sensing, JOURNAL OF GEOPHYSICAL RESEARCH-ATMOSPHERES, 111, 10.1029/2005jd006996, 2006.

van Donkelaar, A., Martin, R. V., Brauer, M., Kahn, R., Levy, R., Verduzco, C., and Villeneuve, P. J.: Global Estimates of Ambient Fine Particulate Matter Concentrations from Satellite-Based Aerosol Optical Depth: Development and Application, ENVIRONMENTAL HEALTH PERSPECTIVES, 118, 847-855,

10.1289/ehp.0901623, 2010.

van Donkelaar, A., Martin, R. V., Spurr, R. J. D., Drury, E., Remer, L. A., Levy, R. C., and Wang, J.: Optimal estimation for global ground-level fine particulate matter concentrations, JOURNAL OF GEOPHYSICAL RESEARCH-ATMOSPHERES, 118, 5621-5636, 10.1002/jgrd.50479, 2013.

Wang, J., and Christopher, S. A.: Intercomparison between satellite-derived aerosol optical thickness and $PM_{2.5}$ mass: Implications for air quality studies, GEOPHYSICAL RESEARCH LETTERS, 30, 10.1029/2003gl018174, 2003.

Wang, T., Li, S., Shen, Y., Deng, J., and Xie, M.: Investigations on direct and indirect effect of nitrate on temperature and precipitation in China using a regional climate chemistry modeling system, JOURNAL OF GEOPHYSICAL RESEARCH-ATMOSPHERES, 115, 10.1029/2009jd013264, 2010a.

Wang, J., Xu, X., Spurr, R., Wang, Y., and Drury, E.: Improved algorithm for MODIS satellite retrievals of aerosol optical thickness over land in dusty atmosphere: Implications for air quality monitoring in China, REMOTE SENSING OF ENVIRONMENT, 114, 2575-2583, 10.1016/j.rse.2010.05.034, 2010b.

Wang, Y., Chen, L., Li, S., Wang, X., Yu, C., Si, Y., and Zhang, Z.: Interference of Heavy Aerosol Loading on the VIIRS Aerosol Optical Depth (AOD) Retrieval Algorithm, REMOTE SENSING, 9, 10.3390/rs9040397, 2017.

Winker, D. M., Hunt, W. H., and McGill, M. J.: Initial performance assessment of CALIOP, GEOPHYSICAL RESEARCH LETTERS, 34, 10.1029/2007gl030135,

2007.

Winker, D. M., Vaughan, M. A., Omar, A., Hu, Y., Powell, K. A., Liu, Z., Hunt, W. H., and Young, S. A.: Overview of the CALIPSO Mission and CALIOP Data Processing Algorithms, JOURNAL OF ATMOSPHERIC AND OCEANIC TECHNOLOGY, 26, 2310-2323, 10.1175/2009jtecha1281.1, 2009.

Xin, J., Gong, C., Liu, Z., Cong, Z., Gao, W., Song, T., Pan, Y., Sun, Y., Ji, D., Wang, L., Tang, G., and Wang, Y.: The observation-based relationships between $PM_{2.5}$ and AOD over China, JOURNAL OF GEOPHYSICAL RESEARCH-ATMOSPHERES, 121, 10701-10716, 10.1002/2015jd024655, 2016.

Xing, J., Mathur, R., Pleim, J., Hogrefe, C., Gan, C.-M., Wong, D. C., Wei, C., and Wang, J.: Air pollution and climate response to aerosol direct radiative effects: A modeling study of decadal trends across the northern hemisphere, JOURNAL OF GEOPHYSICAL RESEARCH-ATMOSPHERES, 120, 10.1002/2015jd023933, 2015.

Xu, P., Chen, Y., and Ye, X.: Haze, air pollution, and health in China, LANCET, 382, 2067-2067, 2013.

Yan, Y., Sun, Y. B., Weiss, D., Liang, L. J., and Chen, H. Y.: Polluted dust derived from long-range transport as a major end member of urban aerosols and its implication of non-point pollution in northern China, SCIENCE OF THE TOTAL ENVIRONMENT, 506, 538-545, 10.1016/j.scitotenv.2014.11.071, 2015.

Yang, X., Zhao, C., Zhou, L., Wang, Y., and Liu, X.: Distinct impact of different types of aerosols on surface solar radiation in China, JOURNAL OF GEOPHYSICAL RESEARCH-ATMOSPHERES, 121, 6459-6471, 10.1002/2016jd024938, 2016.

Yu, X., Zhu, B., and Zhang, M.: Seasonal variability of aerosol optical properties over Beijing, ATMOSPHERIC ENVIRONMENT, 43, 4095-4101, 10.1016/j.atmosenv.2009.03.061, 2009.

Zhang, H., Hoff, R. M., and Engel-Cox, J. A.: The Relation between Moderate Resolution Imaging Spectroradiometer (MODIS) Aerosol Optical Depth and $PM_{2.5}$ over the United States: A Geographical Comparison by US Environmental Protection Agency Regions, JOURNAL OF THE AIR & WASTE MANAGEMENT ASSOCIATION, 59, 1358-1369, 10.3155/1047-3289.59.11.1358, 2009a.

Zhang, M., Song, Y., Cai, X., Lin, W. S., Sui, C. H., Yang, L. M., Wang, X. M., Deng, R. R., Fani, S. J., Wu, C. S., Wang, A. Y., Fong, S. K., and Lin, H.: A health-based assessment of particulate air pollution in urban areas of Beijing in 2000-2004.

Zhang, Q., Ma, X., Tie, X., Huang, M., and Zhao, C.: Vertical distributions of aerosols under different weather conditions: Analysis of in-situ aircraft measurements in Beijing, China, ATMOSPHERIC ENVIRONMENT, 43, 5526-5535, 10.1016/j.atmosenv.2009.05.037, 2009b.

Zhao, C., Klein, S. A., Xie, S., Liu, X., Boyle, J. S., and Zhang, Y.: Aerosol first

indirect effects on non-precipitating low-level liquid cloud properties as simulated by CAM5 at ARM sites, GEOPHYSICAL RESEARCH LETTERS, 39, 10.1029/2012gl051213, 2012.

Zhao, C., and Garrett, T. J.: Effects of Arctic haze on surface cloud radiative forcing, GEOPHYSICAL RESEARCH LETTERS, 42, 557-564, 10.1002/2014gl062015, 2015.

Zheng, S., Pozzer, A., Cao, C. X., and Lelieveld, J.: Long-term (2001-2012) concentrations of fine particulate matter ($PM_{2.5}$) and the impact on human health in Beijing, China, ATMOSPHERIC CHEMISTRY AND PHYSICS, 15, 5715-5725, 10.5194/acp-15-5715-2015, 2015.

Zhuang, B. L., Li, S., Wang, T. J., Deng, J. J., Xie, M., Yin, C. Q., and Zhu, J. L.: Direct radiative forcing and climate effects of anthropogenic aerosols with different mixing states over China, ATMOSPHERIC ENVIRONMENT, 79, 349-361, 10.1016/j.atmosenv.2013.07.004, 2013.

Table 1. Comparison of AERONET and MODIS AOD by season and over all seasons.

Season	AERONET mean AOD	MODIS mean AOD	R^2	Bias	Bias%	RMSE	*N*
Spring	0.49	0.66	0.81	0.18	36.7	0.23	214
Summer	0.61	0.88	0.87	0.27	44.7	0.29	103
Fall	0.30	0.39	0.69	0.10	32.9	0.15	50
Winter	0.19	0.21	0.34	0.02	10.2	0.08	48
All	0.46	0.63	0.85	0.17	37.8	0.23	415

Note: Bias% is defined as 100 × (MODIS AOD-AERONET AOD)/AERONET AOD (Green et al., 2009). RMSE is the root mean squared prediction error (μg/m^3).Period for comparison is 2011–2015.

Table 2. Comparison of AERONET and CALIPSO AOD by season and over all seasons

Season	AERONET mean AOD	CALIPSO mean AOD	R^2	Bias	Bias%	RMSE	*N*
Spring	0.44	0.42	0.52	-0.02	-5.2	0.33	21
Summer	0.53	0.57	0.47	0.04	6.6	0.32	16
Fall	0.95	0.81	0.85	-0.14	-14.2	0.34	12
Winter	0.42	0.53	0.55	0.11	25.0	0.27	21
All	0.54	0.55	0.65	0.01	1.7	0.31	70

Table 3. Correlations between AOD and $PM_{2.5}$ mass by dominant aerosol specie

Dominant Aerosol Specie	**R^2**	**RMSE ($\mu g/m^3$)**	***N***
Coarse Absorbing	0.56	27.07	480
Mixed Absorbing	0.67	36.44	1383
Fine Absorbing	0.53	48.06	2143
Coarse Non-absorbing	0.10	44.51	56
Mixed Non-absorbing	0.61	44.05	234
Fine Non-absorbing	0.58	40.19	434
All	0.51	46.34	4728

Figure Captions

Figure 1. Flow chart of deriving aerosol vertical profile from CALIPSO data.

Figure 2. The aerosol classification scheme in four seasons from 2011 to 2015 using AE, SSA and FMF data from AERONET at sites in Beijing. The scatter plots of different colors is the distribution of aerosol types with different physic-optics characteristics in four seasons.

Figure 3. Scatter plots of AERONET AOD vs. MODIS AOD (a), and AERONET AOD vs. CALIPSO AOD (b) for the period of 2011 to 2015 in Beijing.

Figure 4. Comparison of monthly averaged RH and PBLH (a), AOD and $PM_{2.5}$ (b), AOD_{dry} and $PM_{2.5\_column}$ (c) at 14:00 LT for the period of 2011 to 2015 in Beijing. The blue, purple, green and yellow bands in (a) are for high PBLH and low RH, low PBLH and high PBLH, low PBLH and low RH, high PBLH and high RH, respectively.

Figure 5. Diurnal variations of multi-year (2011-2015) averaged RH and PBLH over four seasons in Beijing.

Figure 6. Comparison of multi-year (2011-2015) averaged RH and PBLH (a1~d1), AOD and $PM_{2.5}$ (a2~d2), AOD_{dry} and $PM_{2.5\_column}$ (a3~d3) by time of day in different seasons. The columns represent four seasons and the rows represent three different variables.

Figure 7. The frequency distribution of aerosol types over four seasons for the period of 2011 to 2015 in Beijing.

Figure 8. The variation of η with the aerosol type in four seasons for the period of 2011 to 2015.

Figure 9. Scatter plots between AERONET AOD and $PM_{2.5}$ concentrations in four different seasons for five ~~six~~ different types of aerosols. The first to 5~~6~~th columns represent the aerosol types of coarse absorbing, mixed absorbing, fine absorbing, ~~coarse non-absorbing,~~ mixed non-absorbing, and fine non-absorbing, respectively. The colors also represent different aerosol types. The rows represent four seasons.

Figure 10. Wind rose of Beijing in four seasons for the period of 2011 to 2015.

Figure 11. The relative distribution of $PM_{2.5}$ within different value ranges at Beijing for different surface wind speed in different wind direction.

Figure 12~~1~~. The relative distribution of AOD (upper panel) and $PM_{2.5}$ (lower panel)

within different value ranges at Beijing for different surface wind speed ranges from 2011 to 2015. v and N represent the wind speed and samples respectively. The colors represent the value ranges of AOD (upper panel) and $PM_{2.5}$ (lower panel).

Figure 13~~2~~. Variation of averaged AOD, $PM_{2.5}$ (left panel) and η (right panel) with the surface wind speed.

~~**Figure 13.** Aerosol vertical distribution profile (a), and aerosol cumulative distribution from high to low with altitude (b) in four seasons. The colors represent different seasons.~~

~~**Figure 14.** The normalized vertical distribution of AOD in four seasons. *h* values shown in each panels are the heights with the highest AOD contribution (percentage). The colors represent different seasons.~~

Figure 14~~5~~. Scatter plots of stratified AOD vs. PM2.5 concentrations. The red solid line is the linear fitting regression lines. It shows the relationship between (a) AOD below 500m, (b) AOD below 1000m, (c) AOD below PBL and (d) AOD of the whole atmosphere and PM2.5 concentrations.

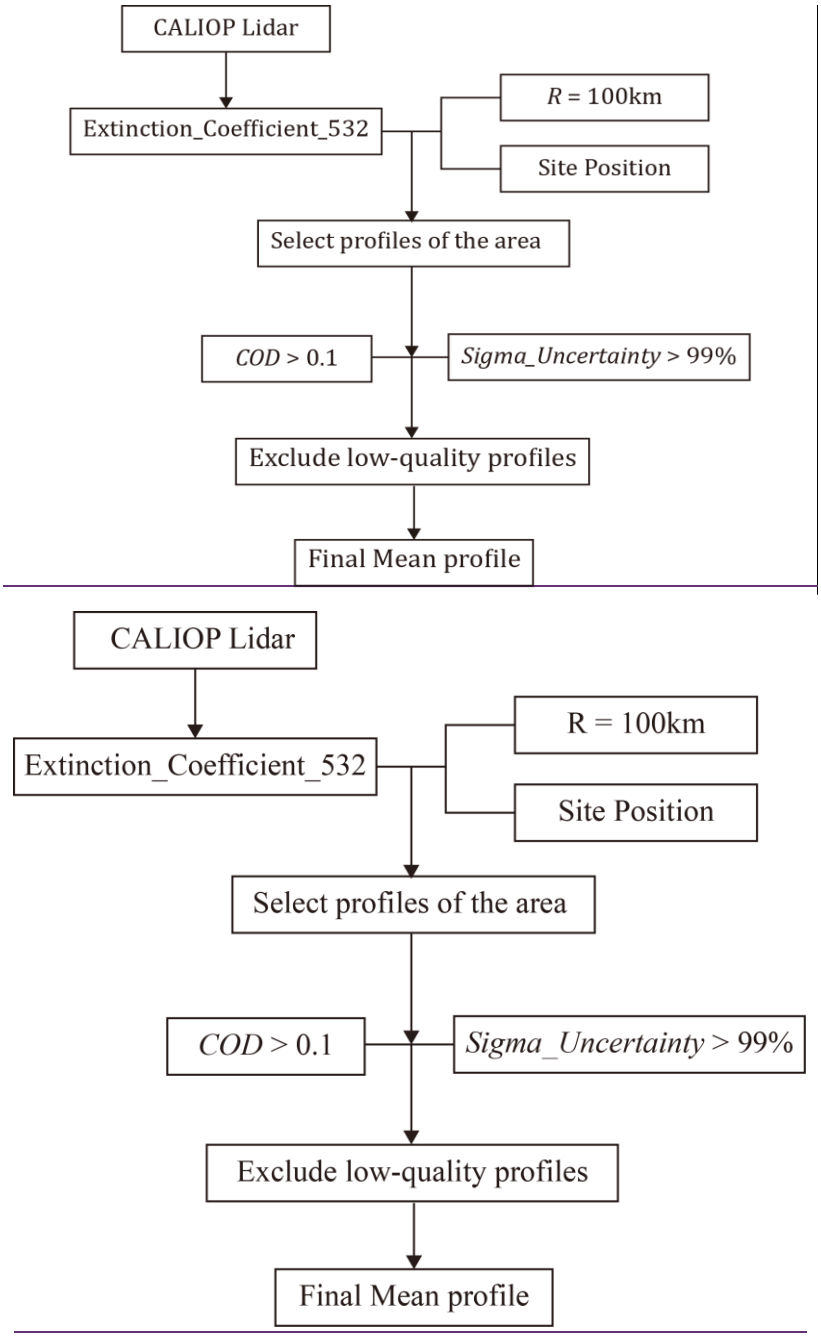

Figure 1. Flow chart of deriving aerosol vertical profile from CALIPSO data.

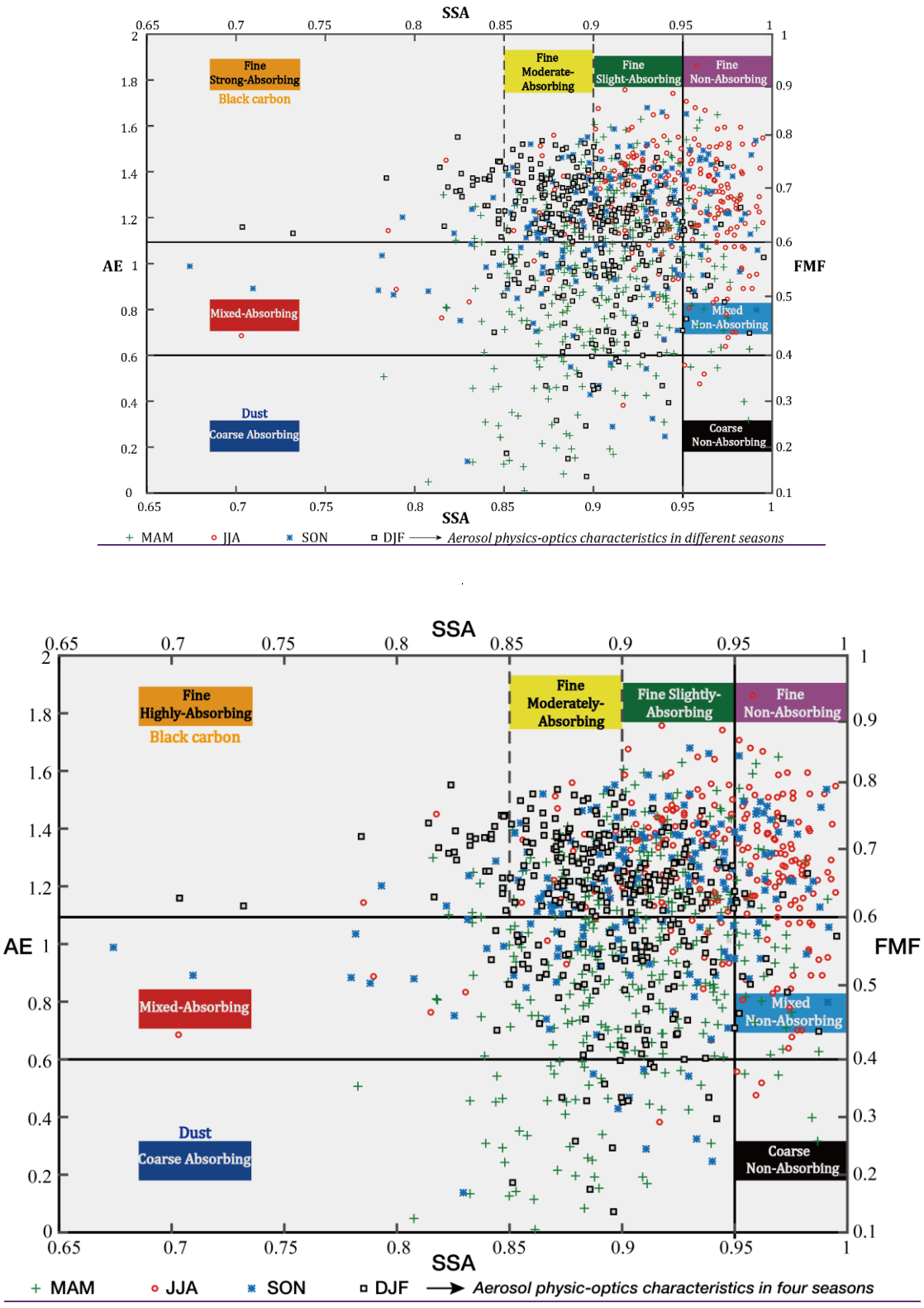

Figure 2. The aerosol classification scheme in four seasons from 2011 to 2015 using AE, SSA and FMF data from AERONET at sites in Beijing. The scatter plots of different colors is the distribution of aerosol types with different physic-optics characteristics in four seasons.

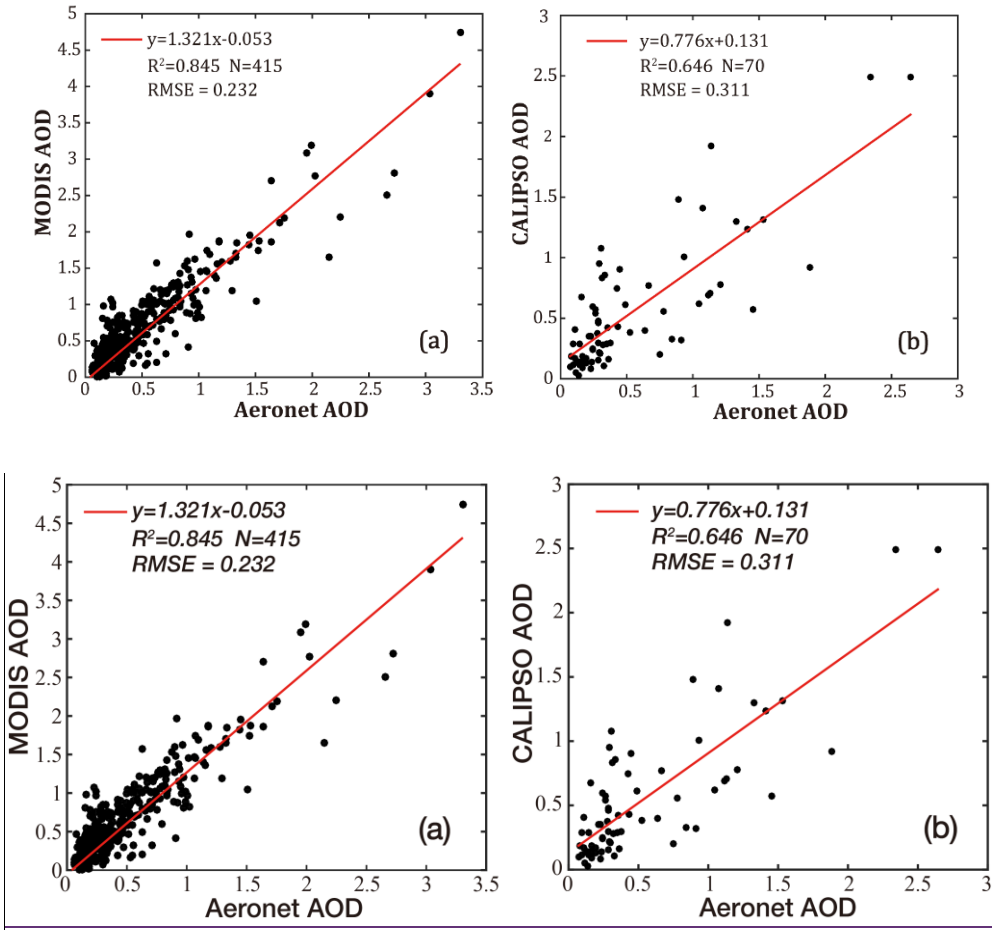

Figure 3. Scatter plots of AERONET AOD vs. MODIS AOD (a), and AERONET AOD vs. CALIPSO AOD (b) for the period of 2011 to 2015 in Beijing.

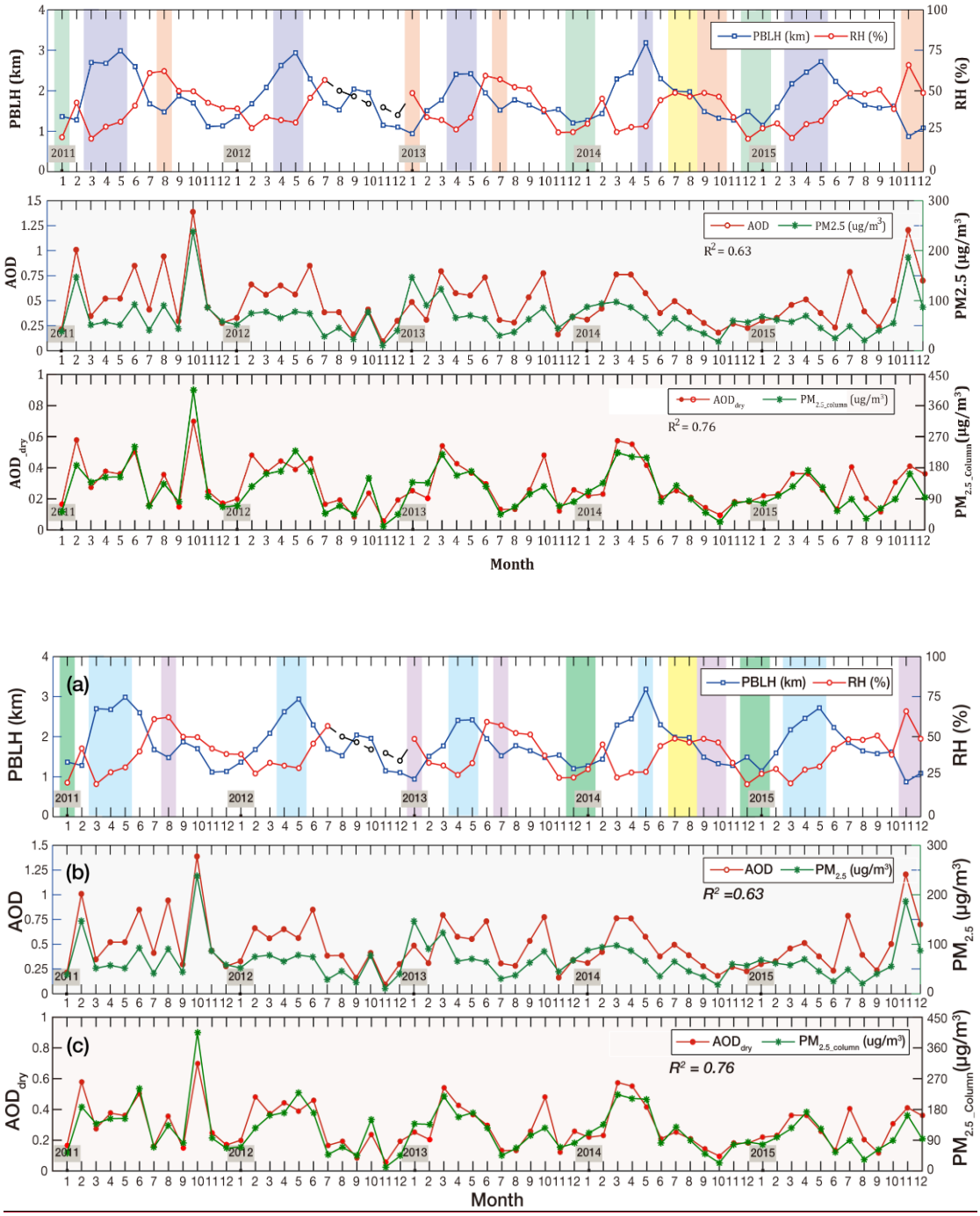

Figure 4. Comparison of monthly averaged RH and PBLH (a), AOD and $PM_{2.5}$ (b), AOD_{dry} and $PM_{2.5\_column}$ (c) at 14:00 LT for the period of 2011 to 2015 in Beijing. The blue, purple, green and yellow bands in (a) are for high PBLH and low RH, low PBLH and high PBLH, low PBLH and low RH, high PBLH and high RH, respectively.

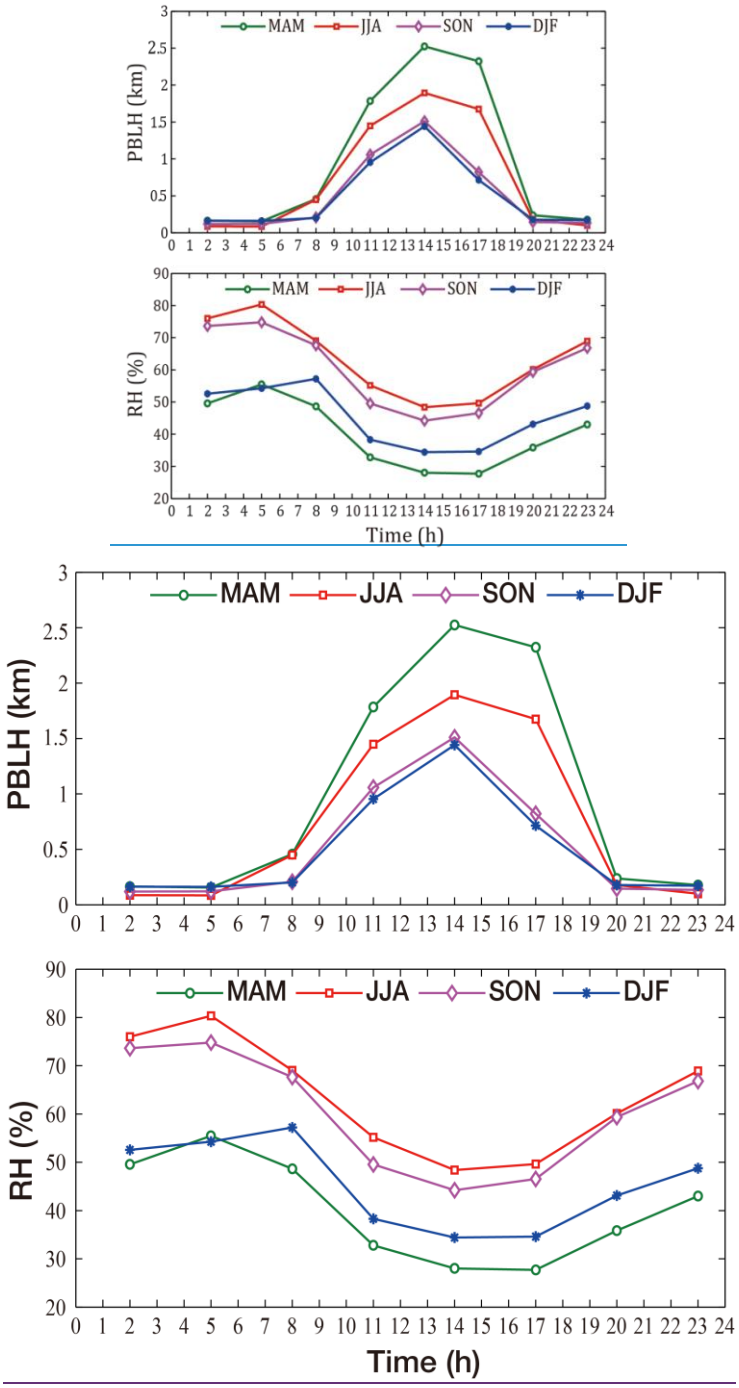

Figure 5. Diurnal variations of multi-year (2011-2015) averaged RH and PBLH over four seasons in Beijing.

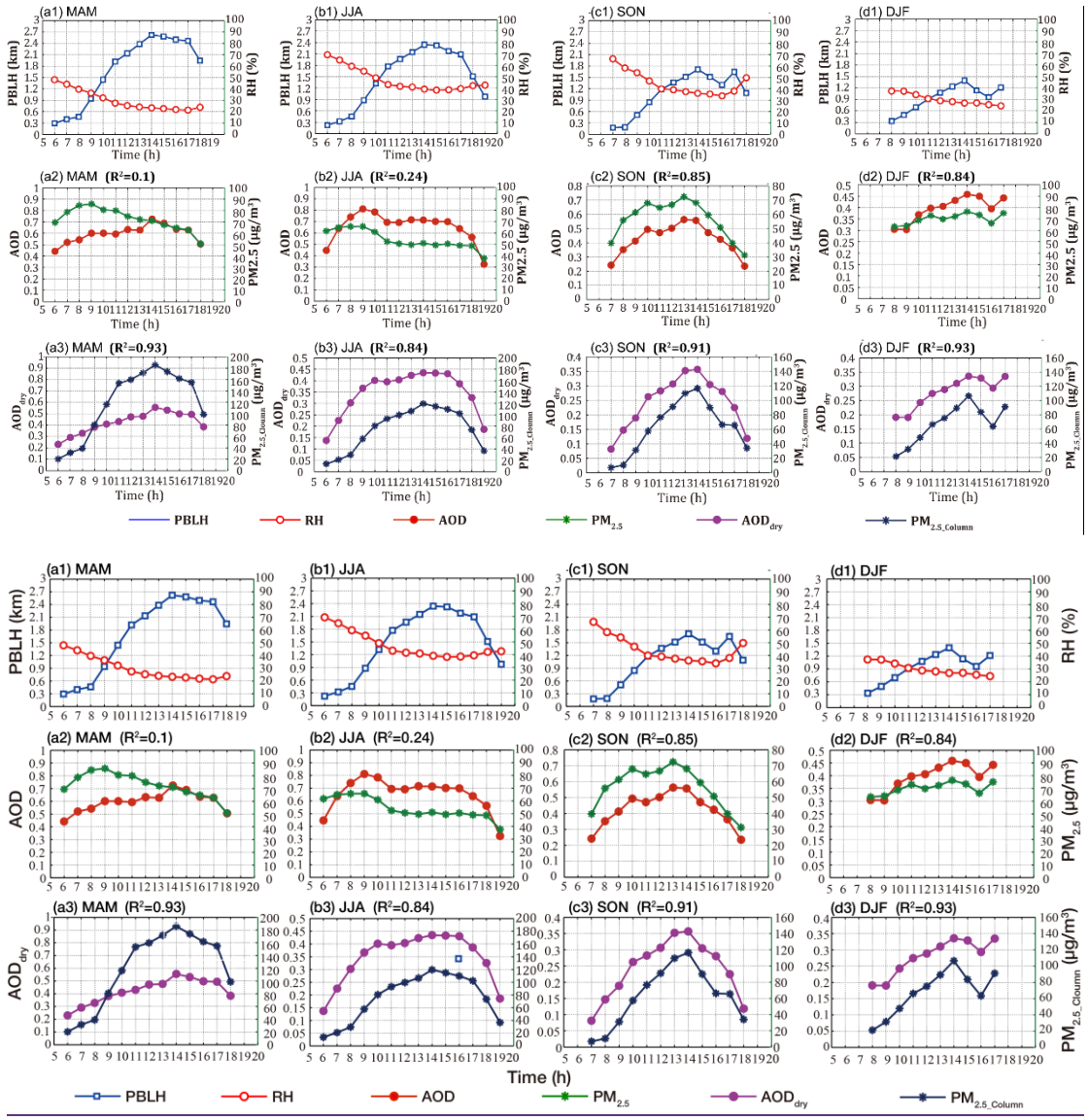

Figure 6. Comparison of multi-year (2011-2015) averaged RH and PBLH (a1~d1), AOD and $PM_{2.5}$ (a2~d2), AOD_{dry} and $PM_{2.5\_column}$ (a3~d3) by time of day in different seasons. The columns represent four seasons and the rows represent three different variables.

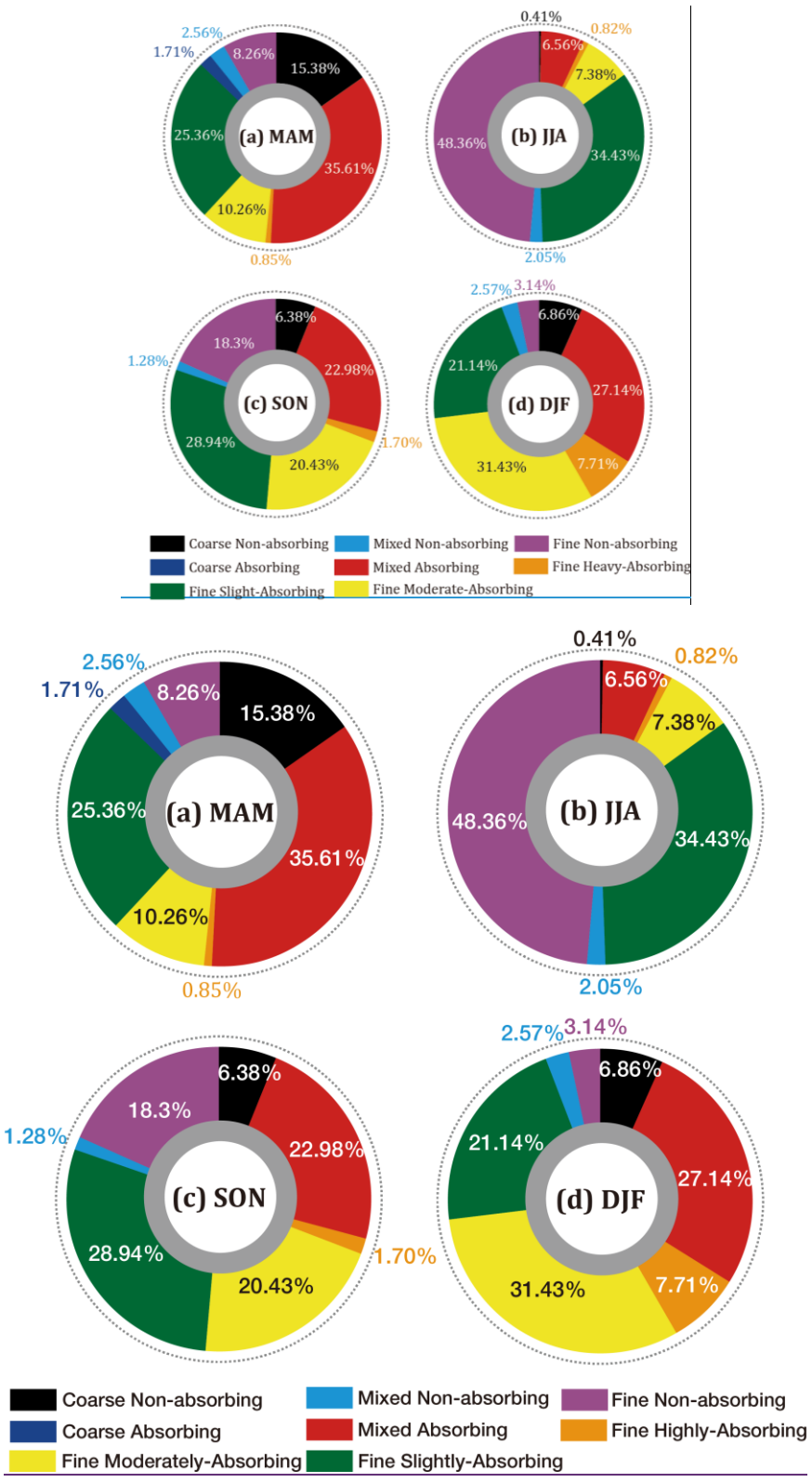

Figure 7. The frequency distribution of aerosol types over four seasons for the period of 2011 to 2015 in Beijing.

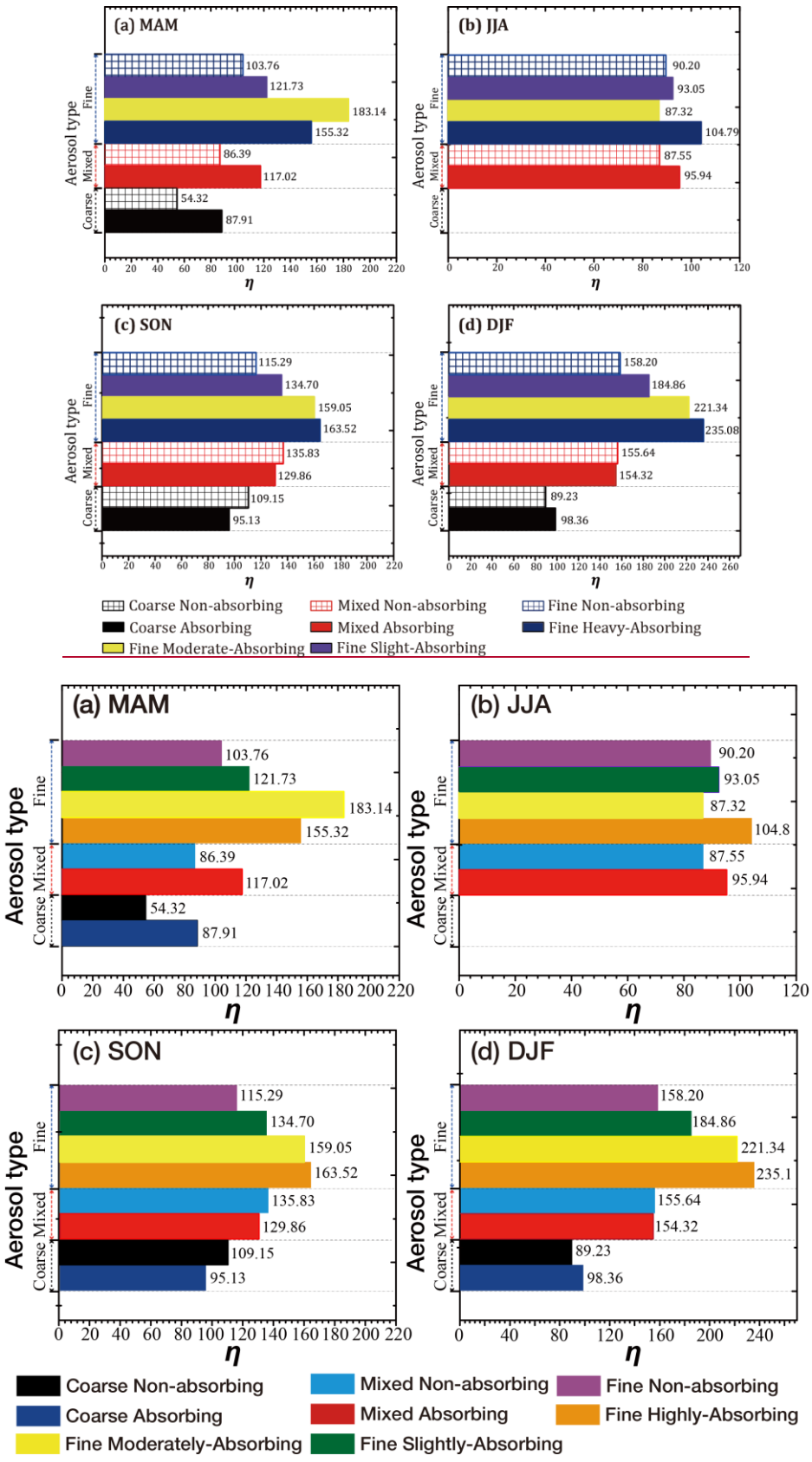

Figure 8. The variation of η with the aerosol type in four seasons for the period of 2011 to 2015.

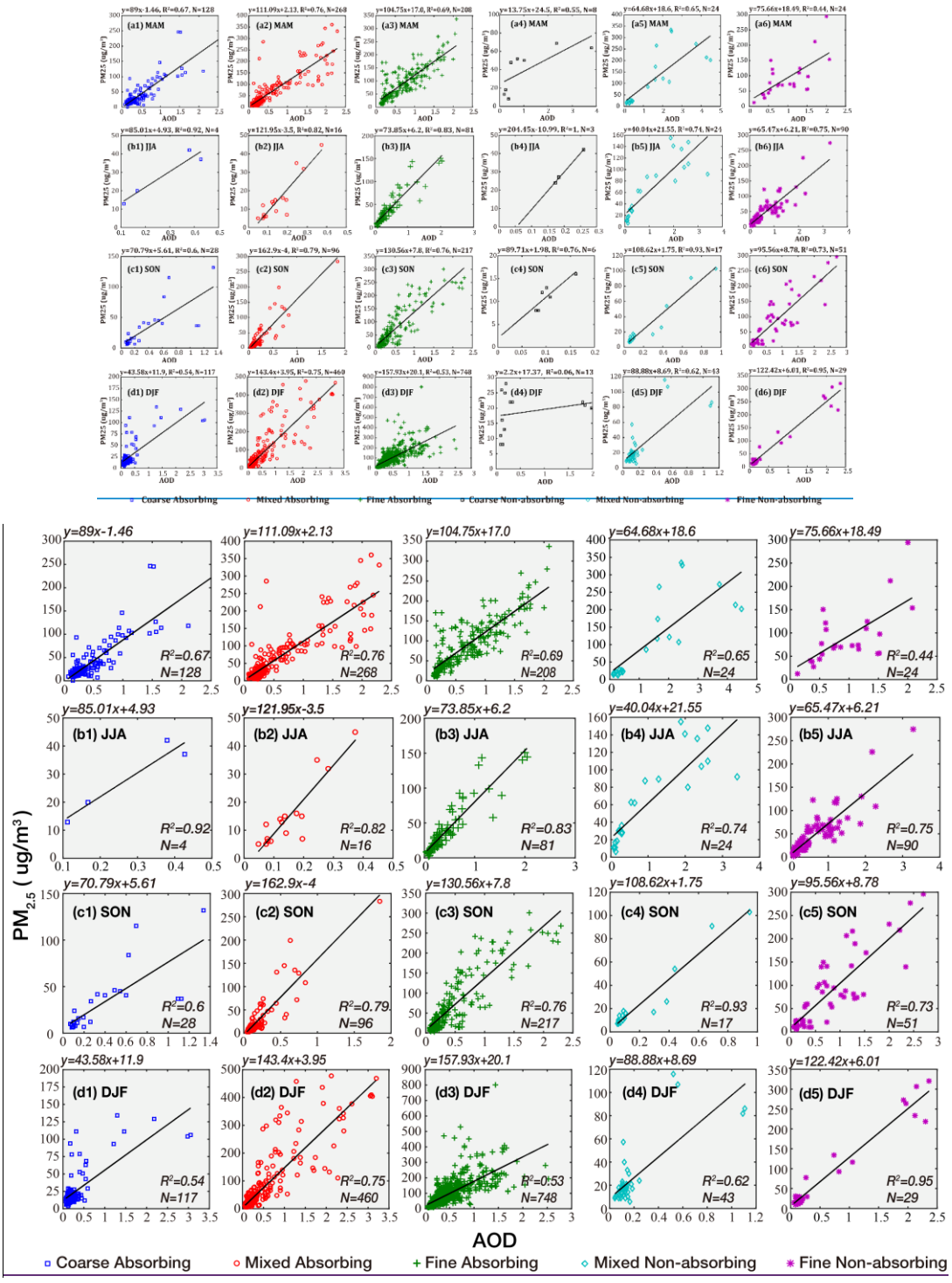

Figure 9. Scatter plots between AERONET AOD and $PM_{2.5}$ concentrations in four different seasons for fivesix different types of aerosols. The first to 56th columns represent the aerosol types of coarse absorbing, mixed absorbing, fine absorbing, coarse non-absorbing, mixed non-absorbing, and fine non-absorbing, respectively. The colors also represent different aerosol types. The rows represent four seasons.

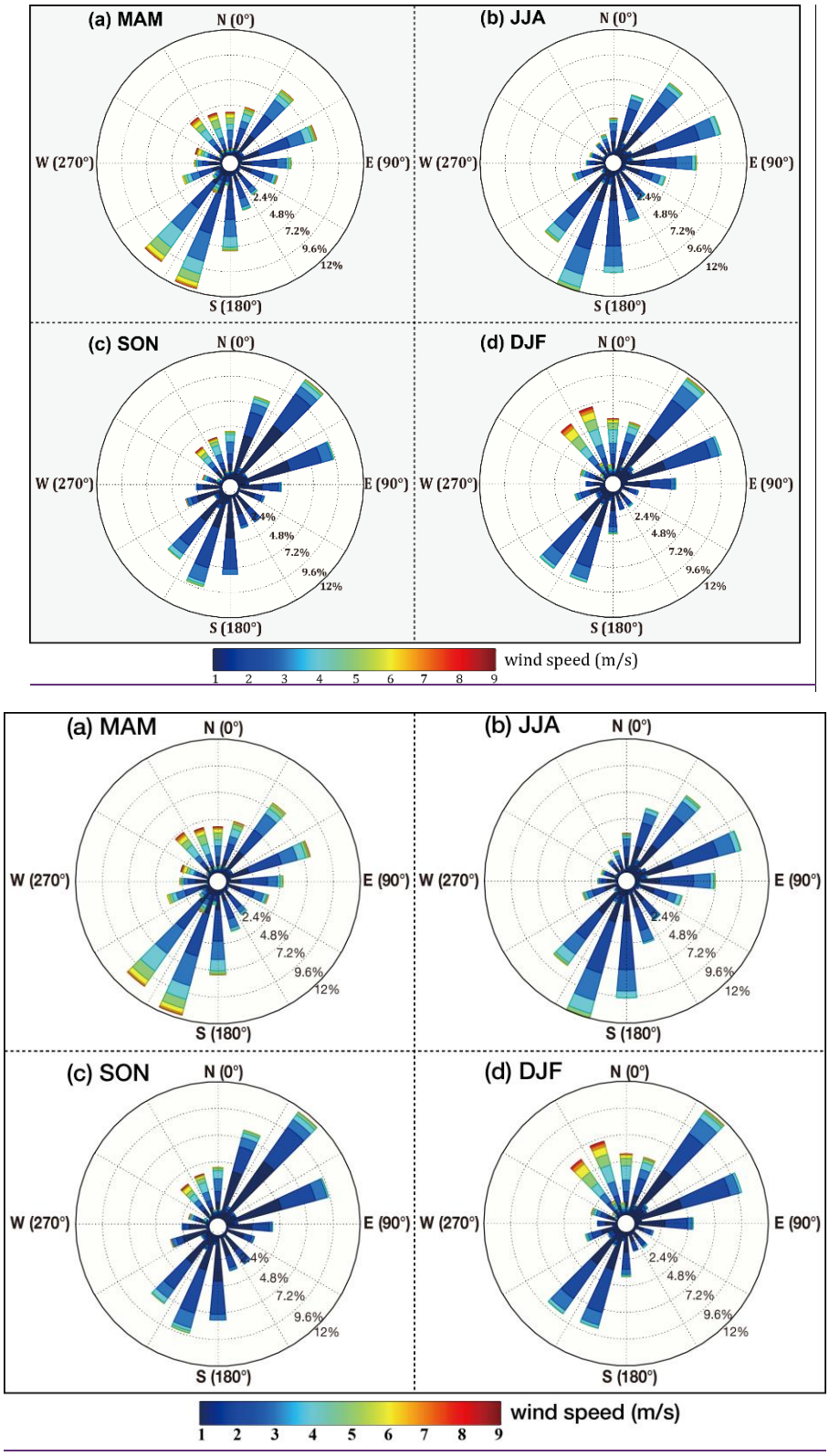

Figure 10. Wind rose of Beijing in four seasons for the period of 2011 to 2015

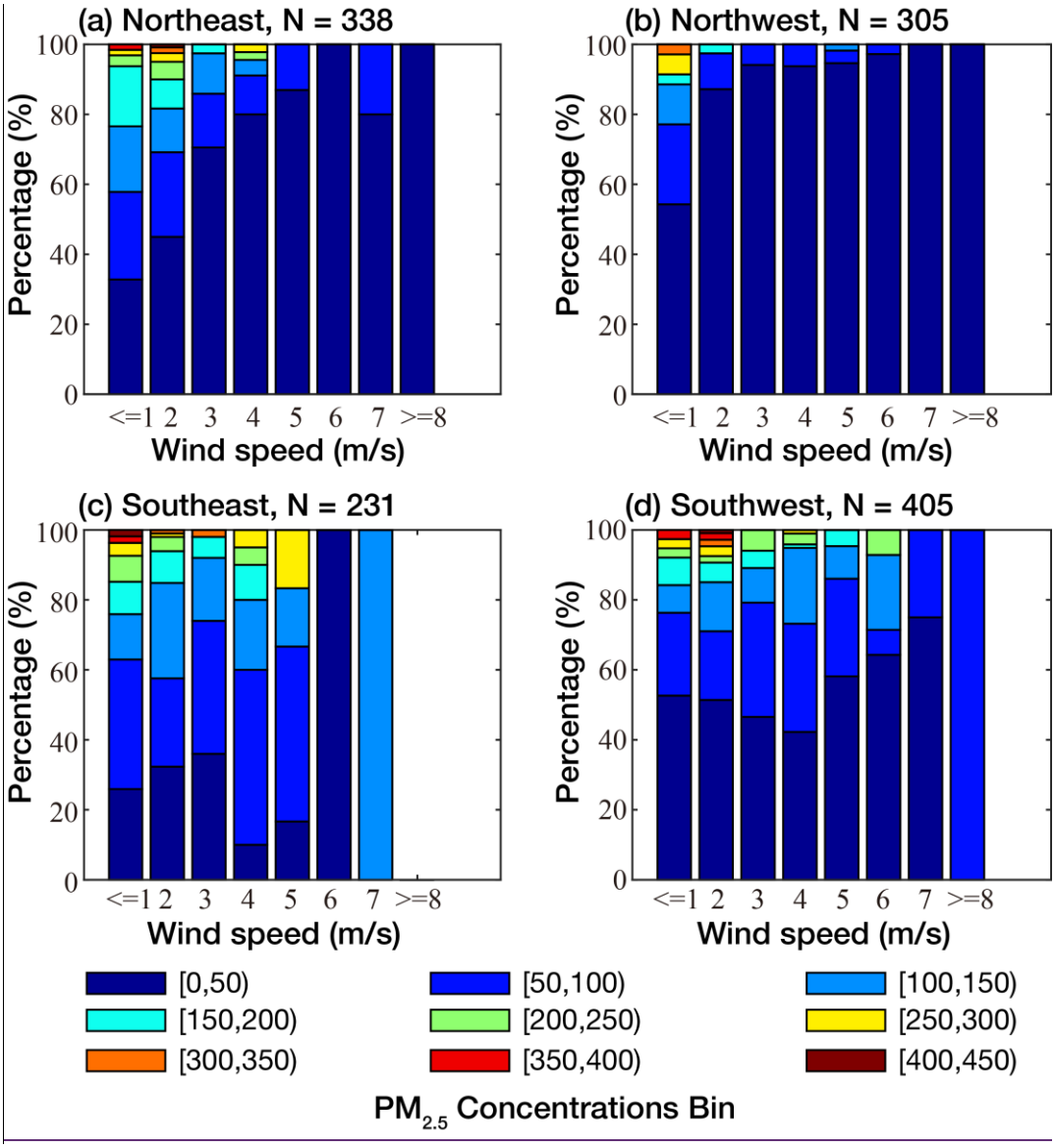

Figure 11. The relative distribution of $PM_{2.5}$ within different value ranges at Beijing for different surface wind speed in different wind direction.

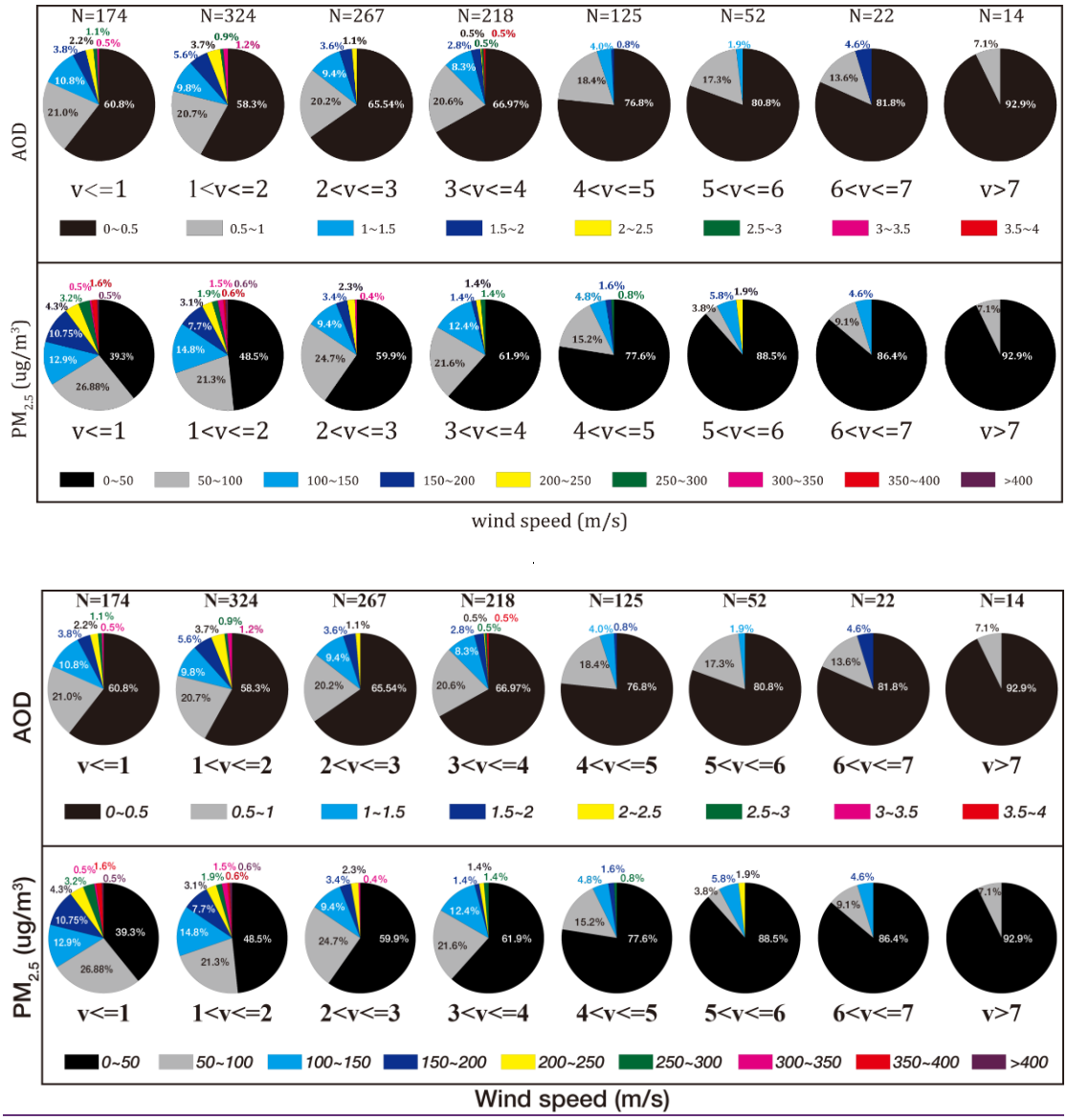

Figure 12~~1~~. The relative distribution of AOD (upper panel) and $PM_{2.5}$ (lower panel) within different value ranges at Beijing for different surface wind speed ranges from 2011 to 2015. v and N represent the wind speed and samples respectively. The colors represent the value ranges of AOD (upper panel) and $PM_{2.5}$ (lower panel).

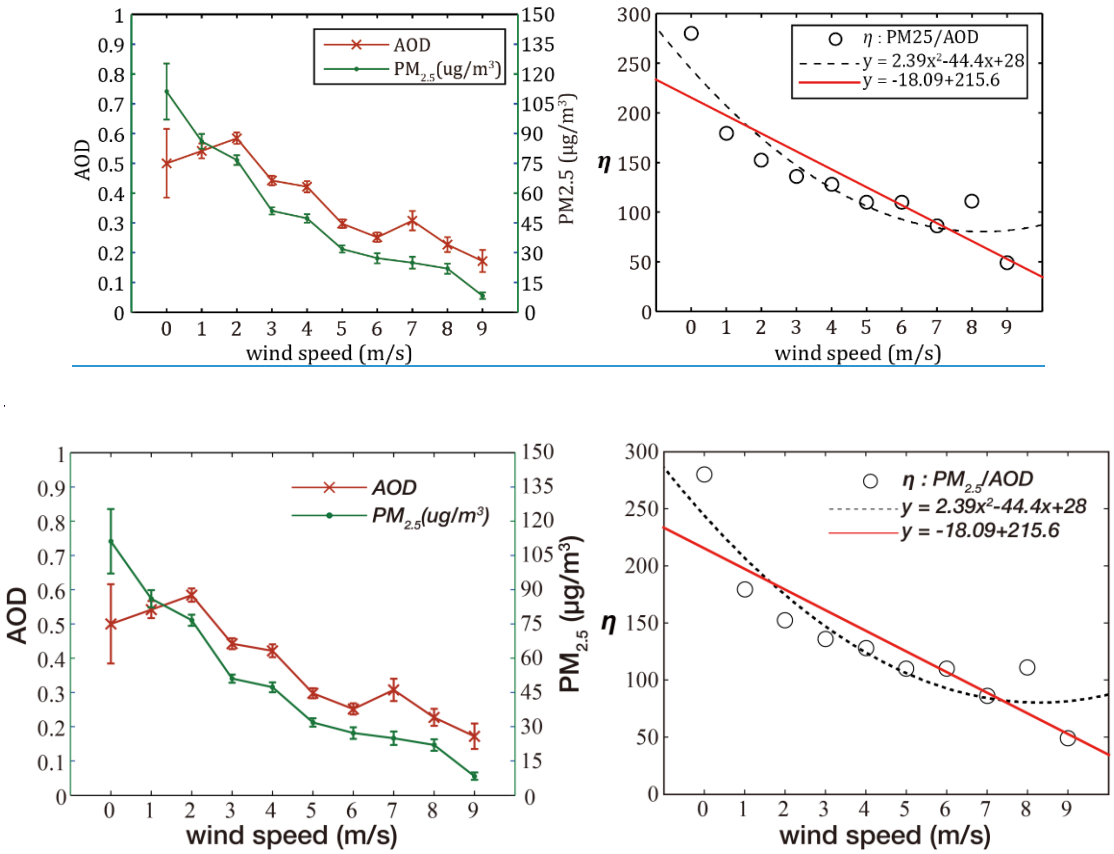

Figure 132. Variation of averaged AOD, $PM_{2.5}$ (left panel) and η (right panel) with the surface wind speed.

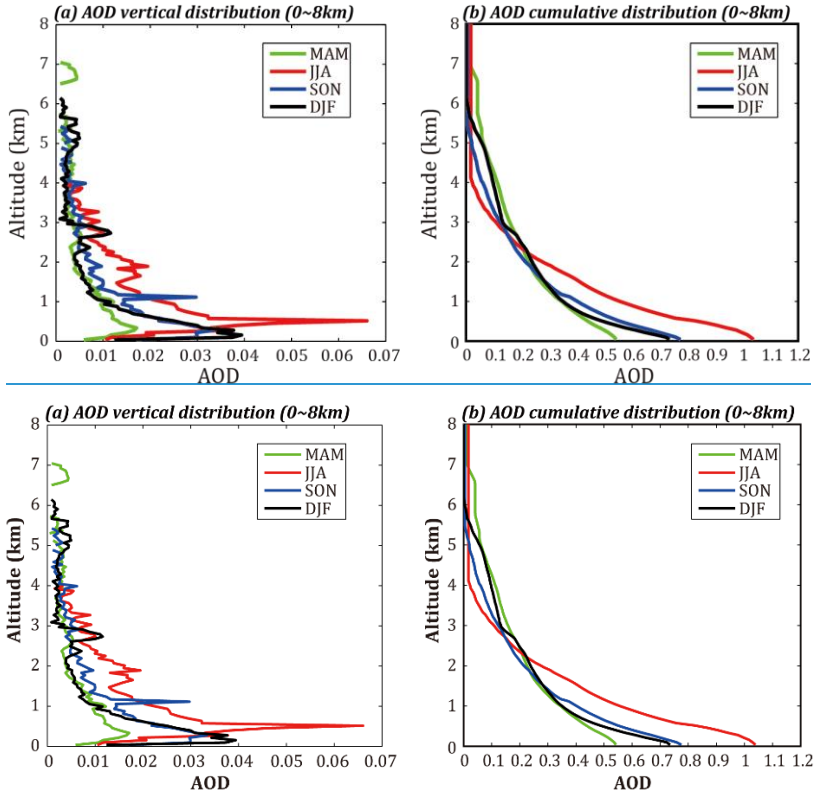

Figure 13. Aerosol vertical distribution profile (a), and aerosol cumulative distribution from high to low with altitude (b) in four seasons. The colors represent different seasons.

5

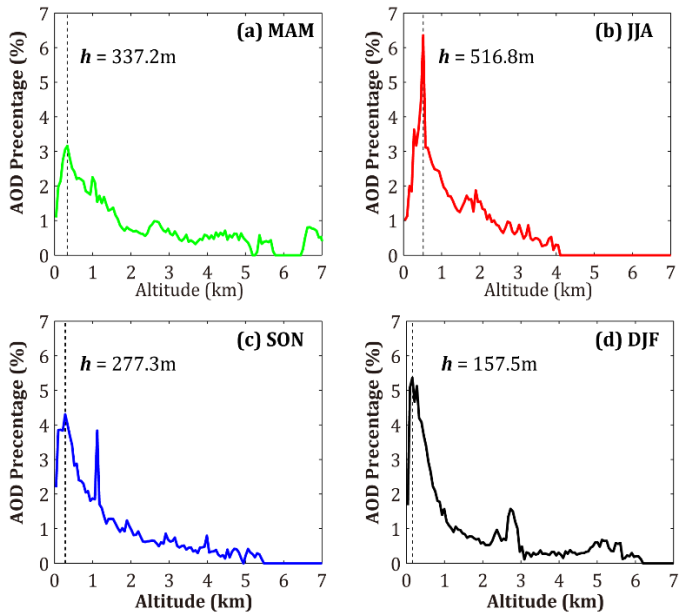

Figure 14. The normalized vertical distribution of AOD in four seasons. *h* values shown in each panels are the heights with the highest AOD contribution (percentage). The colors represent different seasons.

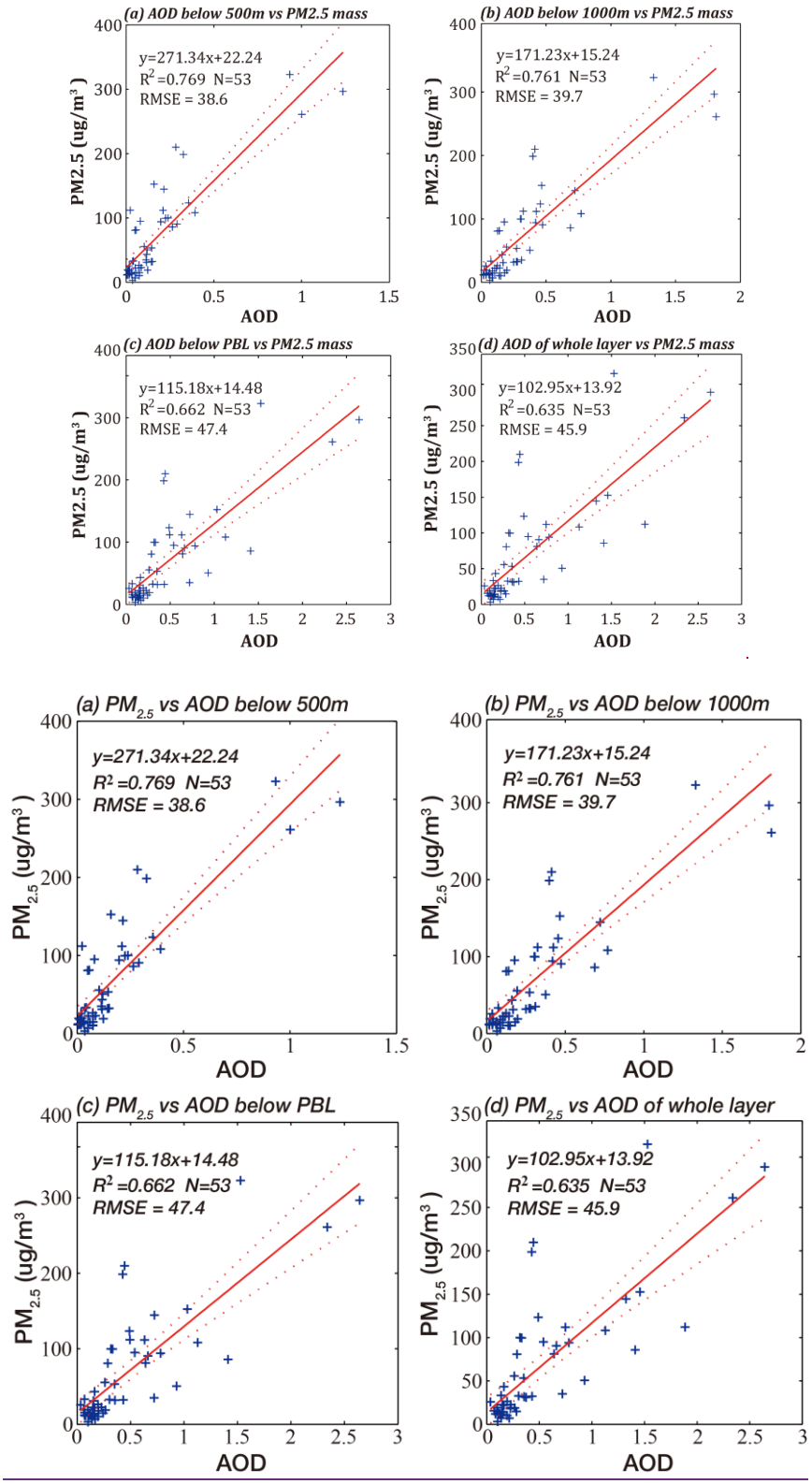

Figure 145. Scatter plots of stratified AOD vs. $PM_{2.5}$ concentrations. The red solid line is the linear fitting regression lines. It shows the relationship between (a) AOD below 500m, (b) AOD below 1000m, (c) AOD below PBL and (d) AOD of the whole atmosphere and $PM_{2.5}$ concentrations.

Analysis of Influential Factors for the Relationship between $PM_{2.5}$ and AOD in Beijing

Caiwang Zheng[1,2], Chuanfeng Zhao[1,2,3]*, Yannian Zhu[1,2,4]*, Yang Wang[1,2], Xiaoqin Shi[1,2], Xiaolin Wu[1,2], Tianmeng Chen[1,2], Fang Wu[1,2], Yanmei Qiu[1,2]

1. State Key Laboratory of Earth Surface Processes and Resource Ecology, and College of Global Change and Earth System Science, Beijing Normal University, Beijing 100875, China

2. Joint Center for Global Change Studies, Beijing, 100875, China

3. Division of Geological and Planetary Sciences, California Institute of Technology, Pasadena, CA 91125, USA.

4. Meteorological Institute of Shaanxi Province, Xi' an, China

Correspondence to: Chuanfeng Zhao, czhao@bnu.edu.cn
Yannian Zhu, yannianzhu@gmail.com

Abstract: Relationship between aerosol optical depth (AOD) and $PM_{2.5}$ is often investigated in order to obtain surface $PM_{2.5}$ from satellite observation of AOD with a broad area coverage. However, various factors could affect the AOD-$PM_{2.5}$ regressions. Using both ground and satellite observations in Beijing from 2011 to 2015, this study analyzes the influential factors including the aerosol type, relative humidity (RH), atmospheric boundary layer height (PBLH), wind speed and direction, and the vertical structure of aerosol distribution. The ratio of $PM_{2.5}$ to AOD, which is defined as η, and the square of their correlation coefficient (R^2) have been examined. It shows that η varies from 54.32 to 183.14, 87.32 to 104.79, 95.13 to 163.52 and 1.23 to 235.08 $\mu g/m^3$ with aerosol type in four seasons respectively. η is smaller for scattering-dominant aerosols than for absorbing-dominant aerosols, and smaller for coarse mode aerosols than for fine mode aerosols. Both RH and PBLH affect the η value significantly. The higher the RH or the higher the PBLH, the smaller the η. For AOD and $PM_{2.5}$ data with the correction of RH and PBLH compared to those without, R^2 of monthly averaged $PM_{2.5}$ and AOD at 14:00 LT increases from 0.63 to 0.76, and R^2 of multi-year averaged $PM_{2.5}$ and AOD by time of day increases from 0.01 to 0.93, 0.24 to 0.84, 0.85 to 0.91 and 0.84 to 0.93 in four seasons respectively. Wind direction is a key factor to the transport and spatial-temporal distribution of aerosols originated from different sources with distinctive physicochemical characteristics. Similar to the variation of AOD and $PM_{2.5}$, η also decreases with the increasing surface wind speed, indicating that the contribution of surface $PM_{2.5}$ concentrations to AOD decreases with surface wind speed.

Compared to the AOD of the whole atmosphere, AOD below 500 m has a better correlation with $PM_{2.5}$, for which R^2 is 0.77. This study suggests that all the above influential factors should be considered when we investigate the AOD-$PM_{2.5}$ relationships.

Keywords: $PM_{2.5}$/AOD ratio, aerosol type, relative humidity (RH), atmospheric boundary layer height (PBLH), wind speed, aerosol vertical distribution.

1. Introduction

Atmospheric aerosols, also known as particulate matter, can influence the Earth's climate system by directly and indirectly modifying the incoming solar radiation and outgoing longwave radiation. The direct effect of aerosols on radiation refers to the scattering and absorption of the solar and longwave radiation by aerosols (Charlson et al., 1992; Koren et al., 2004; Lohmann and Feichter, 2005; Qian et al., 2007; Li et al., 2011; Huang et al., 2014; Yang et al., 2016). And the indirect effect of aerosols on radiation are associated with changes in the cloud macro- and micro-physical properties caused by aerosols which can serve as cloud condensation nuclei or ice nuclei (Twomey, 1977; Albrecht, 1989; Kaufman and Fraser, 1997; Feingold, 2003; Garrett et al., 2004; Garrett and Zhao, 2006; Zhao et al., 2012; Zhao and Garrett, 2015). The radiative effect of aerosols is relatively large due to increased emissions of pollution in East Asia (Wang et al., 2010a; Zhuang et al., 2013). Aerosols can also affect the precipitation intensity and patterns by changing cloud microphysical properties (Menon et al., 2002; Qian et al., 2009; Li et al., 2011; Guo et al., 2016a). Meanwhile, aerosols from anthropogenic pollution can cause serious impacts on atmospheric environment and human health by carrying hazardous materials (Pope et al., 2002; Zhang et al., 2007; Samoli et al., 2008; Xu et al., 2013). Thus, it is very important to get accurate information of aerosol properties, such as aerosol optical depth (AOD) and particle matter with size equal or smaller than 2.5 μm aerodynamic diameter ($PM_{2.5}$).

Aerosol properties are often obtained through satellite remote sensing, surface

remote sensing, surface and aircraft in-situ observations. Remote sensing observation generally provides the aerosol optical properties such as AOD and aerosol extinction coefficient, but not the aerosol mass or number concentration. Differently, in-situ observations can provide direct measurements of aerosol number concentration and $PM_{2.5}$ mass concentration. However, the limited samples for aircraft observation and limited sites for ground-based in-situ observation make it challenging to obtain the $PM_{2.5}$ over many locations, particularly the spatial distribution. Recent studies have proposed methods to estimate the surface $PM_{2.5}$ based on the AOD observations from satellites (van Donkelaar et al., 2006, 2010, 2013; Drury et al., 2008; Wang et al., 2010b; Xin et al., 2016). Although $PM_{2.5}$ from AOD has not high temporal resolution and is not available when it is cloudy or very pollutant, these methods provide the spatial distribution of $PM_{2.5}$ globally or regionally (Paciorek et al., 2008; Li et al., 2017; Wang et al., 2017).

Many studies have focused on the building of statistical regression models to derive the surface $PM_{2.5}$ from AOD. For example, van Donkelaar et al. (2010) derived the global $PM_{2.5}$ concentration distribution from satellite-derived AOD using the $PM_{2.5}$/AOD ratios obtained from a global chemical transport model (CTM). Xin et al. (2015) investigated the relationships between $PM_{2.5}$ and AOD over China using the observations from the Campaign on atmospheric Aerosol Research-China network during the period from 2012 to 2013.

The relationships between $PM_{2.5}$ and AOD show significant differences over

various locations (Corbin et al., 2002; Wang and Christopher, 2003; Hand et al., 2004; Ramachandran, 2005; Kumar et al., 2007; Zhang et al., 2009a; Ma et al., 2014). Some studies (e.g., Ma et al., 2014) have suggested that aerosol types and meteorological conditions can affect the relationship between $PM_{2.5}$ and AOD. However, systematic studies about the influential factors to the relationship between $PM_{2.5}$ and AOD have not been carried out, which are necessary for future derivation of accurate $PM_{2.5}$ from satellite AOD observations. Using both satellite and surface observation of aerosol properties and meteorology variables in Beijing from 2011 to 2015, this study analyzes the influential factors to AOD-$PM_{2.5}$ relationship, which includes aerosol type, relative humidity (RH), atmospheric planetary boundary layer height (PBLH), wind speed, and the vertical structure of aerosol distribution.

The paper is organized as follows. Section 2 describes the data and method. Section 3 analyzes the potential influential factors to AOD-$PM_{2.5}$ relationship, and section 4 summarizes the findings.

2. Data and Method

2.1 Data

The data used in this study are described as follows, including the data sources, their spatial and time resolutions, and the data period. These data includes surface $PM_{2.5}$ concentrations and AOD, satellite-based AOD from the moderate-resolution imaging spectroradiometer (MODIS), satellite-based aerosol profiles from the Cloud-Aerosol

Lidar and Infrared Pathfinder Satellite Observation (CALIPSO), and meteorology data from China Meteorological Administration (CMA) and European Centre for Medium Range Weather Forecast (ECMWF).

a. Ground $PM_{2.5}$ Measurements

The ground-based aerosol observation of $PM_{2.5}$ concentrations with hourly time resolution for the period of 2011 to 2015 is obtained from the U.S. Department of State at a single site (39.95 N, 116.47 E) in Beijing, as reported on the http://www.stateair.net/ website. The $PM_{2.5}$ mass concentration was measured using the U.S federal reference method. This method first uses a size selective inlet to remove particles larger than 10 μm, then takes use of another filter to remove the particles larger than 2.5 μm. The air parcels before entering the $PM_{2.5}$ instruments undergo a dry process (RH<35%), which ensure that all $PM_{2.5}$ observations are obtained at dry condition. While this dataset has not been officially evaluated, a comparison of $PM_{2.5}$ measurements from U.S Department of State and from Beijing Municipal Environmental Protection (MEP) Bureau at sites close to each other (1.6 km) in 2014 – 2016 shows great consistency with a correlation coefficient of 0.94 and root mean square difference of 14.3 $\mu g/m^3$. Considering that the data measured by U.S. Department of State have longer time record, and have been widely used by many studies (Zheng et al., 2015; Jiang et al., 2015), they are adopted in this study.

b. Meteorological Data

Meteorological parameters with 3-hour temporal resolution at the MEP site which

is about 1.6 km away from the U.S. Department of State site are provided by CMA, including cloud fraction (CF), 6-hour total precipitation (TP), relative humidity (RH), surface wind speed and wind direction. To eliminate the contamination of cloud and precipitation, data samples under cloudy ($CF \geqslant 0.1$) or rainy conditions ($TP>0$) are removed. Same as Yang et al. (2016), we should note that even with this limitation, some days with few broken clouds ($CF<0.1$) still can introduce additional uncertainties to our study. Planetary boundary layer heights (PBLH) are extracted from the ECMWF interim reanalysis (ERA-Interim; Dee et al. 2011), with a horizontal resolution of $0.125° \times 0.125°$ and 3-hour temporal resolution. Guo et al. (2016b) have investigated the PBL in China from January 2011 to July 2015 using both the fine-resolution sounding observations and ECMWF reanalysis data. It was found that the seasonally averaged BLHs derived from reanalysis are generally in good agreement with those of observations in Beijing. Considering this and that there are only 2 times sounding observations every day, the seasonally averaged ERA-BLHs have been used in this study. We should admit that extra uncertainties could exist due to the distances between the MEP sit, U.S. Department of State site, and ECMWF grid, while they are close to each other.

c. AERONET measurements

The Aerosol Robotic Network (AERONET) program is a federation of ground-based remote sensing aerosol networks with more than 400 stations globally. At AERONET sites, the CE318 multiband sun-photometer is employed to measure

spectral sun irradiance and sky radiances, from which AOD at 550 nm can be derived. The AOD data has been processed into three quality levels: Level 1.0 (unscreened), Level 1.5 (cloud-screened), and Level 2.0 (cloud screened and quality-assured) (Holben et al., 1998). A detailed description about AERONET retrievals is discussed in Holben et al. (1998). In this study, Level 2.0 AOD at 550 nm, SSA at 675 nm and Fine Mode Fraction (FMF) of Beijing (39ºN, 116ºE) are used. It's worth mentioning that AOD retrieved from AERONET are accurate to within ±0.01 (Dubovik et al., 2000). Note that the AOD retrieved could have the impacts of relative humidity which has not been excluded yet.

d. CALIOPSO profile products

CALIPSO is one part of the National Aeronautics and Space Administration (NASA) A-Train, which is a constellation of satellites, tracking in a polar orbit and crossing the equator northbound at about 13:30 local time (LT) (Stephens et al. 2002). To investigate the characteristics of the aerosol vertical distribution, aerosol extinction profiles at 532 nm from Version 3.01 CALIOP Level 2 5 km Aerosol Profile for the period of 2011 to 2015 are used, which are provided by the CALIOP space borne lidar onboard the CALIPSO satellite (Winker et al., 2007, 2009; Hunt et al., 2009). The horizontal resolution is 5 km, and the vertical resolution varies with altitude. The CALIPSO columnar AOD is the integration of aerosol extinction coefficient with the altitude, which has also been influenced by the relative humidity.

The extraction algorithm of the aerosol profile is shown in Figure 1. First, the

overpass time of CALIPSO satellite can be determined according to the geographical location of Beijing site (39.95ºN, 116.47ºE). Second, at each CALIPSO satellite pixel, AOD at each layer is derived as the integration of the extinction coefficient within that layer. Finally, the AOD profiles inside 100 km radius region surrounding the Beijing site is averaged as the final result. Note that when there are clouds or precipitation, the data are excluded in our analysis. Also, in this process, low-quality profiles in which *Extinction_Coefficient_Uncertainty_532* (*Sigma_Uncertainty* in Fig. 1) is greater than 99% and *COD* is greater than 0.1 have been excluded.

e. MODIS aerosol product

The MODIS instrument has a global coverage every one to two days with a viewing swath of 2330 km. It is operating on both the Terra and Aqua satellite, of which the overpass time are approximately 10:30 and 13:30 LT, respectively. To compare the AOD from MODIS and CALIPSO (only passes in the afternoon) observation, AOD from Terra (10:30 LT) are not used. Level 2 MODIS aerosol product data (Collection 5.1) for the period of 2011 to 2015 are obtained from the Level-1 and Atmosphere Archive and Distribution System (LAADS DAAC), of which the spatial resolution at nadir is 10 km×10 km (Levy et al., 2010). The AOD data (MODIS parameter name: Deep_Blue_Aerosol_Optical_Depth_Land) at 550 nm are used in this study, which is only retrieved for daytime, cloud-free and snow/ice-free conditions with an uncertainty confidence level of ~20%.

2.2 Method

a. $PM_{2.5}$/AOD ratio

AOD represents the total attenuation that aerosols of the whole atmosphere exert on solar radiation, while $PM_{2.5}$ mass concentrations measured by the ground monitoring site can only reflect the near-surface air quality condition. Based on the assumption of linear relationship between AOD (unitless) and $PM_{2.5}$ (μg/m^3), van Donkelaar et al. (2010) has introduced a conversion factor (η), which can be defined as:

$$\eta = \frac{PM_{2.5}}{AOD} \quad (1)$$

where η (μg/m^3) indicates the near surface aerosol $PM_{2.5}$ mass concentration per unit aerosol optical thickness. Its value depends on the aerosol type, aerosol size, RH, PBLH, and the vertical structure of aerosol distribution. At the same $PM_{2.5}$ mass concentration, the smaller the AOD, the weaker the extinction capability; and the larger the AOD, the stronger the extinction capability. Note that the extinction capability here denotes the aerosol mass extinction coefficient. In other words, the larger the η, the weaker the aerosol extinction capability; the smaller the η, the stronger the aerosol extinction capability. Using this factor, we can study the dependence of AOD-$PM_{2.5}$ relationship (represented by η) on different influential factors.

b. Aerosol Classification Method

Due to the difference of the sources, aerosols exhibit noticeable differences in physical and optical properties with respect to the location and season. Fine-mode

fraction (FMF) refers to the fraction of AOD due to fine-mode aerosol particles with sizes smaller than 1 μm. Angstrom exponent (AE) is exponent for the power law describing the wavelength dependence of the AOD. Using FMF and AE, we can determine the dominant size mode of aerosols. We can also distinguish absorbing from non-absorbing aerosols based on measurements of single scattering albedo (SSA), which is defined as the ratio of the scattering coefficient to the extinction coefficient.

In this study, hourly averaged level 2 inversion products from AERONET at sites in Beijing are used, including FMF, AE and SSA data. Following Lee et al. (2010), aerosol is classified into eight types as follows:

1) Coarse non-absorbing (SSA>0.95, FMF<=0.4 and AE<=0.6)
2) Coarse absorbing (SSA<=0.95, FMF<=0.4 and AE<=0.6)
3) Mixed non-absorbing (SSA>0.95, 0.4<=FMF<0.6 and 0.6<=AE<1.2)
4) Mixed absorbing (SSA<=0.95, 0.4<=FMF<0.6 and 0.6<=AE<1.2)
5) Fine non-absorbing (SSA>0.95, FMF>0.6 and AE>1.2)
6) Fine highly-absorbing (SSA<=0.85, FMF>0.6 and AE>1.2)
7) Fine moderately-absorbing (0.85<=SSA<0.9, FMF>0.6 and AE>1.2)
8) Fine slightly-absorbing (0.9<=SSA<0.95, FMF>0.6 and AE>1.2)

Coarse absorbing and fine absorbing aerosols can be considered as dust and black carbon (BC) respectively. Figure 2 shows the aerosol type classification performed using SSA, FMF and AE from AERONET at sites in Beijing using the classification method described above. Roughly, the aerosols are mainly fine mode slightly absorbing

and non-absorbing particles in summer, and fine mode slightly and moderately absorbing particles in winter. The coarse mode dust aerosols mainly occurs in spring (MAM) and winter (DJF).

3. Analysis and Results

3.1 AOD

We first evaluate the uncertainties in the satellite observed AOD using the ground observations from AERONET at the satellite passing time, including both MODIS and CALIPSO at 13:30 LT. Based on the satellite overpass time, the corresponding AERONET AOD in time within 30-min are compared to MODIS AOD and CALIPSO AOD respectively, which is shown in Figure 3. The correlation between MODIS and AERONET AOD is significant (R^2 = 0.85, N = 415), with a slope of 1.32 and an RMS error of 0.23, indicating that MODIS AOD is biased high compared to AERONET AOD. In contrast, the correlation between CALIPSO and AERONET AOD is slightly lower than that between MODIS and AERONET (R^2 = 0.65, N = 70), with a slope of 0.78 and a RMS error of 0.31. In general, the CALIPSO AOD is biased low compared to AERONET AOD. The lower correlation of AOD between AERONET and CALIPSO than that between AERONET and MODIS is likely related to the limited data samples for AERONET-CALIPSO AOD comparison, which is also noted by Bibi et al. (2015).

Table 1 further shows the inter-comparison results of AOD between AERONET and MODIS in spring (MAM), summer (JJA), fall (SON) and winter (DJF), which

include their seasonal averaged AOD, squared correlation, absolute bias, relative bias and sample number. The absolute bias is calculated as the difference of seasonally averaged AOD from simultaneous AERONET and MODIS measurements; and the relative bias is calculated as the ratio of the absolute bias to the seasonally averaged AERONET AOD. The seasonal averaged AOD are 0.49, 0.61, 0.30 and 0.19 respectively in four seasons for AERONET observations, and 0.66, 0.88, 0.39 and 0.21 for MODIS observations, which are highest in summer but lowest in winter. The corresponding sample numbers are 214, 103, 50 and 48 in four seasons. This seasonal variation pattern is also observed by Yu et al. (2009). MODIS has a substantial positive bias in spring, summer and fall (36.7, 44.7 and 32.9%), but a smaller positive bias in winter (10.2%). The squared correlation (R^2) between MODIS and AERONET in Beijing are 0.81, 0.87, 0.69 and 0.34 in four seasons, of which the corresponding RMSE are 0.23, 0.29, 0.15 and 0.08. Low correlation in winter may be caused by the shortage of data samples compared to other seasons. When AOD becomes small, the relative errors in AOD from both MODIS and AERONET become large, which may cause the correlation of AOD between MODIS and AERONET also decrease as demonstrated in Table 1.

Same as Table 1, Table 2 shows the inter-comparison results of AOD between AERONET and CALIPSO in spring, summer, fall and winter. The bias shown in Table 2 is calculated in the same way as that in Table 1. The correlation (R^2) between CALIPSO and AERONET AOD are 0.52, 0.47, 0.85 and 0.55 respectively in four

seasons. CALIPSO AOD has a positive bias in summer and winter (6.6 and 25.0%), but a negative bias in spring and fall (-5.2 and -14.2%). For all seasons, RMSE are less for MODIS than CALIPSO compared to AERONET. As indicated earlier, this is likely related to the limited data samples for AERONET-CALIPSO AOD comparison. The results shown in Fig. 2 and Tables 1 and 2 indicate that considerable uncertainties exist in the satellite observed AOD, introducing up to 45% errors (seasonal biases 5-45%) to the quantification of AOD-$PM_{2.5}$ relationships.

3.2 Effect of RH and PBLH

Relative humidity, by affecting the water uptake process of aerosols, can cause a pronounced change to the aerosol size distribution, chemical composition, and the extinction characteristics (Liu et al., 2008). The hygroscopic growth factor f(RH), can be defined as the ratio of the aerosol scattering coefficients in ambient with a certain RH to that in dry air conditions (Li et al., 2014). In this study, f(RH) is expressed as follows in a simple function:

$$f(RH) = \frac{1}{(1 - RH/100)} \quad (2)$$

The hygroscopic growth process has a significant contribution to AOD. Since $PM_{2.5}$ is often measured at a dry condition (<40% in relative humidity), we often need consider the impacts of relative humidity to AOD in order to get a more reliable $PM_{2.5}$-AOD relationship. A dehydration adjustment can be applied to get the dry condition AOD, which is:

$$AOD_{dry} = \frac{AOD}{f(RH)} \quad (3)$$

where AOD_{dry} represents the aerosol optical depth with dehydration adjustment.

PBLH influences the vertical profile of particulate matters. In general, the PBLH is dependent on many factors, including meteorological conditions, terrain, sensible heat flux, evaporation and ground roughness (Stull, 1988). Several aircraft observations studies (Liu et al., 2009; Zhang et al., 2009) have found that aerosol particles mainly concentrated within PBLH and that $PM_{2.5}$ mass concentration varies little with height within PBLH. Thus, the column integrated $PM_{2.5}$ mass concentration ($PM_{2.5\_column}$) within PBLH can be approximated as:

$$PM_{2.5\_column} = PM_{2.5} \times PBLH \quad (4)$$

In the atmosphere, the RH often increases with height within PBLH. This could definitely affect the dehydration adjustment of AOD in Eq. (3). Currently, we only use the surface RH to do the adjustment which could cause the dry condition AOD is actually somehow overestimated compared to its true value.

Previous studies have shown that aerosols are mainly concentrated within the PBL (Guinot et al., 2006; Zhang et al., 2009b). Here, we assume that the column integrated $PM_{2.5}$ within PBLH should be comparable to the whole column integrated $PM_{2.5}$. The calculation of column $PM_{2.5}$ mass concentration in Eq. (4) has implied that there are no disconnected aerosol layers and could introduce errors in experimental conditions, which was not considered in this study. Eqs. (3) and (4) imply that for given $PM_{2.5}$, the increase of RH can result in the increase of AOD and the decrease of η, and that for

given AOD, the increase of PBLH can cause the decrease of near-surface $PM_{2.5}$ concentrations and the decrease of η. Actually, PBLH often correlates with RH, making the separation of PBLH and RH effects challenging. Here, we simply show the effects of both PBLH and RH on the AOD-$PM_{2.5}$ relationship.

Figure 4(a) shows the time series of PBLH (km) and RH (%)**.** In Fig. 4a, the blue bands are for high PBLH and low RH, and the purple bands are for low PBLH and high PBLH, both of which indicate anti-correlated trends between PBLH and RH. Differently, the green (yellow) bands are for low (high) PBLH and low (high) RH, which indicates correlated trends of PBLH and RH. Clearly, there is generally an anti-correlated temporal trend between PBLH and RH. The averaged PBLH for 2011 to 2015 are 2.56 km, 1.97 km, 1.55 km and 1.32 km respectively in MAM, JJA, SON and DJF, of which the corresponding averaged RH are 27.58%, 48.73%, 42.78% and 33.05%. In May, PBLH has the highest value above 2.5 km, and in July, RH has the highest value above 50%. Without considering the variations of sources and sinks, PBLH is negatively correlated with $PM_{2.5}$, and RH is positively correlated with AOD. The anti-correlated trend between PBLH and RH shown in Fig. 4a imply that the effects of PBLH and RH on the AOD-$PM_{2.5}$ relationship could be partially canceled out. However, it is still necessary to consider the effects of PBLH and RH for the study of $PM_{2.5}$-AOD relationship.

Figure 4(b) shows the temporal variation of monthly averaged AOD and $PM_{2.5}$ at 14:00 LT without any meteorology-based modification to the original observations. It

shows a good positive relationship in the time variations of monthly averaged AOD and $PM_{2.5}$ with a high correlation (R^2 = 0.63). Although the temporal trend of AOD and $PM_{2.5}$ are basically consistent, AOD are considerably higher in MAM and JJA while $PM_{2.5}$ lower in JJA. That's because in MAM, PBLH is high and the vertical mixing of aerosols makes near-surface $PM_{2.5}$ concentrations low, while in JJA, RH is high and the hygroscopic growth of aerosols lead to the increase of AOD. Actually, PBLH and RH are influenced by the horizontal atmospheric circulation in different seasons, which contributes to the seasonal variations of $PM_{2.5}$ and AOD. Beijing is located in a mid-latitude East Asian monsoon region. In winter, heavy horizontal winds help the transportation of aerosols and result in a relatively low AOD, while low PBLH makes the surface $PM_{2.5}$ relatively high. By contrast, in summer, the high water vapor transported with the warm air from south makes both AOD and $PM_{2.5}$ relatively high, while high PBLH makes the surface $PM_{2.5}$ relatively low. These impacts from the horizontal atmospheric circulation make the seasonal variation of AOD is more significant than that for surface $PM_{2.5}$, as shown in Fig. 4b.

Figure 4(c) further shows the temporal variation of monthly averaged AOD_{dry} and $PM_{2.5\_column}$ at 14:00 LT which have been adjusted based on Eqs. (3) and (4). Note that the AOD_{dry} is adjusted based on surface RH using Eqs. (2) and (3) and the vertical variation of RH has not been considered. As indicated earlier, the AOD_{dry} obtained here could be somehow overestimated compared to its true value. It shows much better positive relationship in the temporal variation of monthly average AOD_{dry} and

$PM_{2.5\_column}$, with R^2 as 0.74. This promising result indicates that the PBLH and RH corrections are essential for the improvement of the retrieval accuracy of $PM_{2.5}$ from AOD.

Figure 5 compares the diurnal variation of RH and PBLH over four seasons averaged from 2011 to 2015 in Beijing. In terms of seasonal difference, PBLH is the highest in MAM, followed by JJA and SON, the lowest in DJF, which is consistent with the results found by Guo et al. (2016b). In spring, high PBLH may be associated with the climatologically strongest near-surface wind speed, while in summer, high PBLH is contributed to the strong solar radiation (Guo et al., 2016b). RH is the highest in summer, followed by fall and winter, the lowest in spring. In terms of diurnal variation, it can be seen that from 8:00 to 14:00 LT, the solar radiation that surface receives increases, making PBLH rises and RH decreases gradually; PBLH at 14:00 LT is the highest and RH at 14:00 LT is the lowest within the whole day. However, from 14:00 to 20:00 LT, the solar radiation that surface receives reduces, thus PBLH goes down and RH increases gradually. PBLH is the lowest and RH is the highest at 23:00 and 2:00 LT respectively within the whole day.

Figure 6 shows the diurnal variation of multi-year (2011-2015) averaged RH and PBLH, AOD and $PM_{2.5}$, AOD_{dry} and $PM_{2.5\_cloumn}$ in four seasons when all four types of measurements are available. The columns represent four seasons of spring, summer, fall and winter and the rows represent different variables. Fig. 6(a1-d1) show that PBLH and RH demonstrate a steady increase and decrease trend from 6:00 to 17:00 LT,

respectively, which is almost the same as their diurnal variation demonstrated in Fig. 5. As shown in Fig. 6(a2)-(d2), the AOD-$PM_{2.5}$ linear relationship shows that R^2 are 0.1, 0.24, 0.85 and 0.84 in four seasons respectively. After PBLH and RH corrections (Fig. 6(a3-d3)), it shows that R^2 between AOD_{dry} and $PM_{2.5\_cloumn}$ are 0.93, 0.84, 0.91, 0.93 in four seasons respectively. These results further indicate that RH and PBLH play essential roles for AOD-$PM_{2.5}$ relationship.

3.2 Aerosol type

To study the influence of aerosol type on η, we analyze the data from 11:00 to 17:00 LT in four seasons respectively. For this time period, the PBLH (RH) has high (low) values with weak variation, which make the impacts of PBLH and RH vary weakly with selected sample time in a season. By doing this, we try to keep a certain amount of data samples and limit the influence of diurnal variation of RH and PBLH on η. The aerosol types can be classified based on the aerosol particle size and radiative absorptivity, and η is a good indicator to the extinction capability of different aerosol types.

Figure 7 depicts the seasonal frequency distribution of aerosol types in four seasons at Beijing for the period of 2011 to 2015. Dust accounts for 15.4%, 0.4%, 6.4% and 6.9% in spring (MAM), summer (JJA), fall (SON) and winter (DJF) respectively. Same as that indicated from Fig. 1, dust aerosols is heavy in spring and winter, particularly in spring. Higher proportion of dust in spring is mainly associated with the

long-range transport from northwest arid areas (Yan et al., 2015, Tan et al., 2012). Fine mode absorbing aerosols account for 36.5%, 42.6%, 51.1% and 60.3% in four seasons respectively, of which moderately absorbing aerosols account for the highest. Owing to the biomass burning and soot emission generated from heating, the fine mode heavily-absorbing aerosol percentage is higher in winter than in other seasons, which is 7.7%. The content of fine non-absorbing aerosol is significantly higher in summer and fall than in other two seasons, particularly in summer with a value of 48.4%. As a whole, the aerosol particles in Beijing are primarily fine-mode and absorbing aerosols in terms of particle size and optical property.

Figure 8 presents the variation of η with the aerosol type by season in Beijing. Note that there are too few coarse-mode cases in summer and the corresponding η is a missing value. η generally decrease with particle size, with the smallest value for coarse-mode aerosols and largest value for fine-mode aerosols, and it seems that η of non-absorbing aerosols is smaller than absorbing aerosols. Theoretically, aerosol extinction capacity increases with particle size parameter ($x=2\pi r/\lambda$) and reaches a maximum value when size parameter is around 6. Therefore, for solar visible radiation (such as λ=500 nm), the extinction capacity for aerosol particles generally increases with size for particles with radius less than 0.5 μm, and then decreases when radius larger than 0.5 μm. Actually, for the wavelength of 550 nm, the extinction efficiency of fine-mode particles (peak radius ranging from ~0.11 to ~0.33 μm) is stronger than coarse-mode aerosols. Moreover, coarse particles, which may be not included in $PM_{2.5}$,

can contribute a lot to the extinction at wavelengths in the visible, and thus to AOD. This is especially true for dust days dominated by coarse-mode aerosols, of which high AOD is more likely to be due to PM_{10} rather than $PM_{2.5}$. These make the lower η for coarse-mode than fine mode aerosol.

Table 3 further compares the AERONET hourly averaged AOD to $PM_{2.5}$ mass concentrations by aerosol type. Coarse Non-absorbing aerosols show the lowest correlation between AOD and $PM_{2.5}$, of which R^2 is 0.10. For all kinds of aerosols, the correlation between AOD and $PM_{2.5}$ is relatively lower than that for aerosols with a specific type other than coarse non-absorbing, of which R^2 is 0.51 and RMS error is 46.34 $\mu g/m^3$.

Figure 9 shows the difference in the relationship between $PM_{2.5}$ and AOD among five different aerosol types by season. The coarse non-absorbing aerosol is too few to be analyzed and shown here. We have also done the linear regression analysis for all types of aerosols which is not shown here, and found that the slopes of the linear regression functions ($PM_{2.5}=a\times AOD+b$) are 90.16, 56.9, 117.97 and 138.42 in four seasons respectively. The seasonal differences of the slopes are attributed to the effect of PBLH and RH. In summer, high RH brings about the hygroscopic growth of aerosol, thus increasing the extinction capacity of aerosols and then reducing the slope. Moreover, the high PBLH in summer reduces the relative contribution of surface $PM_{2.5}$ to the columnar AOD and makes a smaller slope value. Differently, in winter, low PBLH value increases the relative contribution of surface $PM_{2.5}$ to the columnar AOD,

thus increasing the slope. The slopes in spring and autumn fall in between. However, there are large differences in the slope of regression functions among different aerosol types. For absorbing aerosols, the slope roughly decreases with increasing particle size from coarse, mixed to fine particles, with values of about 89, 111, 104 μg/m^3 in spring, 85, 122, 74 μg/m^3 in summer, 71, 163, 131 μg/m^3 in fall, and 44, 143, 158 μg/m^3 in winter. The slope is also generally larger for absorbing than non-absorbing aerosol. The slopes for mixed absorbing and non-absorbing aerosol are 111 and 65 μg/m^3 in spring, 122 and 40 μg/m^3 in summer, 163 and 109 μg/m^3 in fall, and 143 and 89 μg/m^3 in winter. And the slopes for fine absorbing and non-absorbing aerosol are 105 and 76 μg/m3 in spring, 74 and 65 μg/m^3 in summer, 131 and 96 μg/m^3 in fall, and 158 and 122 μg/m^3 in winter. Thus, same as shown in Fig. 8, the slope roughly decreases with particle size, with small values for coarse-mode aerosols and large values for fine-mode aerosols in four seasons, and the slope of non-absorbing aerosols is generally smaller than absorbing aerosols.

The findings in this section imply that AOD-$PM_{2.5}$ relationship varies considerably with aerosol types. When we investigate the relationship between $PM_{2.5}$ and AOD, the aerosol types should be carefully considered for study regions.

3.4 Wind

This section discusses how wind affects the AOD-$PM_{2.5}$ relationship in two aspects: wind direction and surface wind speed. Surrounded by Hebei province with severe

pollution, Beijing is affected by the long-range transport of aerosols and gas-phase pollutants. The seasonal variation of wind direction changes the transport and spatial-temporal distribution of aerosols and gas-phase pollutants originated from different sources with distinctive physicochemical characteristics, which has a direct influence on the AOD-$PM_{2.5}$ relationship.

Figure 10 describes the wind rose of Beijing in four seasons for the period from 2011 to 2015. Surface wind speed is mainly distributed in the range of 0 to 9 m/s. Wind direction is mainly southwest in spring and summer, northeast in fall and northwest in winter. There are more windy days in spring and winter. The northwest wind in spring causes the transport of dust aerosols from gobi and desert regions of China to Beijing. The occurrence frequency of stable weather (v=0 m/s) are 4.2%, 5.8%, 9.2% and 8.3% in spring, summer, fall and winter, respectively. Different from the wind speed which will be analyzed in Figs. 12 and 13, the influence of wind direction to the AOD-$PM_{2.5}$ relationship is often combined with the effect of wind speed. Beijing is surrounded by Hebei province and mountains in the northern areas. When the winds come from south, Beijing is in the downstream location to the pollution source from Hebei and the pollutants could be further accumulated in Beijing due to the mountain blocking effect. By contrast, when the winds come from north, Beijing is in the upstream region relative to the pollution source in Hebei, and the cold air from north can disperse the air pollutants. As shown in Figure 11, with similar wind speed, the occurrence rate of heavy air pollution is much higher for cases with winds from the south than from the north.

Moreover, the aerosol pollution events also decrease with increasing wind speed for cases with winds both from the north and the south.

Figure 12 illustrates the relationship between the severity extent of aerosol amount denoted by AOD and $PM_{2.5}$ and surface wind speed. For good air quality with $PM_{2.5}$<50 μg/m^3, the occurrence rate increases with increasing wind speed, ranging from 39.3% (v<=1 m/s) to 92.9% (v>7 m/s). Differently, the occurrence of poor air quality with $PM_{2.5}$>150 μg/m^3 ranges from 20.92% (v<=1 m/s) to 0 (v>7 m/s). The weakening of surface wind speed reduces the transport of near-surface aerosol to the outside regions, leading to the build-up and continuance of heavy aerosol pollution condition in Beijing. On the contrary, the increase of surface wind speed, which may be due to the development of weather system like monsoon in Beijing, causes the disperse of aerosols, and then reduction of the heavy aerosol pollution occurrence rate.

Figure 13 describes the variation of averaged AOD, $PM_{2.5}$ and η with surface wind speed. Although AOD and $PM_{2.5}$ are basically consistent in the decreasing trend with the increasing surface wind speed, AOD variation is more complicated and less sensitive to surface wind speed. Compared with the $PM_{2.5}$ variation range of 10~110 μg/m^3, the variation range of AOD is between 0.2 and 0.6. Moreover, there are even cases that AOD increases with wind speed, such as when wind speed is less than 3 m/s. This is likely associated with the fact that the columnar AOD is affected by many factors, and the surface wind speed is just a disturbing term to surface $PM_{2.5}$. Similar to the

variation of AOD and $PM_{2.5}$, η also decreases with the increasing surface wind speed, indicating that the contribution of surface $PM_{2.5}$ concentrations to AOD decreases with surface wind speed.

3.5 Vertical distribution of aerosols

It has indicated that the relationship between AOD and $PM_{2.5}$ varies with the surface wind speed and the surface aerosol amount. Considering that AOD is the vertical integration of aerosol optical properties, the AOD-$PM_{2.5}$ relationship should vary with the vertical distribution of aerosols. We examine this by using the extinction profiles in 532 nm band from the Version 3.01 CALIOP Level 2 5 km Aerosol Profile product from 2011 to 2015.

Within the atmospheric boundary layer, the main air movement form is the turbulent motion, promoting the vertical exchanges of heat, water vapor, momentum and various kinds of materials including aerosol pollutants. The turbulent energy is generally dependent on both the buoyancy and wind shear, particularly the buoyancy which is highly related to surface downwelling radiation. Obviously, compared to other seasons, the solar radiation received by the surface is more in summer, and the turbulence is stronger, making aerosol transfer to a higher altitude. The seasonal variation of PBLH shown earlier has illustrated this. Associated with the variation of PBLH, the aerosol vertical distributionalso varies and further influences the AOD-$PM_{2.5}$ relationship. We next examine the relationship between AOD from surface to different

heights and $PM_{2.5}$ at surface. By defining AOD below a height as the integration of extinction coefficients vertically from surface to that height, the ratio of AOD below a specific height to the total AOD can be determined by CALIPSO vertical profile, which is

$$AOD_H = AOD_{AeronetTotal} \times \frac{AOD_{CalipsoBelowH}}{AOD_{CalipsoTotal}} \quad (5)$$

where $AOD_{AeronetTotal}$ is AOD derived by AERONET, $AOD_{CalipsoTotal}$ is the total AOD from CALIPSO. $AOD_{CalipsoBelowH}$ is AOD below H from CALIPSO. AOD_H is the AOD below H. As shown in Figure 3, the CALIPSO seems underestimate AOD compared to AEORNET. We here treat the AERONET AOD as more reliable or "ground truth" data, and use the CALIPSO vertical profile to scale the AERONET AOD for its vertical distribution.

We here examine four heights, which are 500 m, 1000 m, PBLH and the whole columnar atmosphere that MODIS observes. Note that PBLH is not constant, but varies with time. Figure 14 shows linear relationships between AOD below these four heights and $PM_{2.5}$ at surface. For heights of 500 m, 1000 m, PBLH and the whole atmospheric column, we can see that the correlation between AOD below and surface $PM_{2.5}$ decreases with selected heights, with R^2 of 0.77, 0.76, 0.66 and 0.64 respectively. More clearly, the slopes of linear regression lines vary a lot for heights 500 m, 1000 m and PBLH, but much smaller for H above PBLH. This further implies that most of aerosols concentrate within PBLH in the atmosphere, and the variation of aerosol vertical

distribution could introduce large uncertainties to AOD-$PM_{2.5}$ relationship.

4. Summary

This study analyzes the various factors that affect the AOD-$PM_{2.5}$ relationship qualitatively or quantitatively, including the satellite AOD observation, aerosol type, RH, PBLH, wind direction and speed, and the aerosol vertical distribution. It shows all of these factors can change the AOD-$PM_{2.5}$ relationship, with different contributions. AOD from MODIS and CALIPSO are evaluated against the AERONET data. The MODIS and AERONET AOD correlation is significant (R^2 = 0.85, N = 415), with a slope of 1.32 and a RMS error of 0.23, indicating that AOD is higher from MODIS than that from AERONET. In contrast, the correlation of AOD between CALIPSO and AERONET is slightly lower (R^2 = 0.65, N = 70), with a slope of 0.78 and a RMS error of 0.31.

There are large differences in the seasonal and diurnal variation of PBLH and RH. In Beijing, PBLH is the highest in spring, followed by summer and fall, the lowest in winter, and RH is the highest in summer, followed by fall and winter, the lowest in spring. For AOD and $PM_{2.5}$ data with the correction of RH and PBLH compared to those without, R^2 of monthly averaged $PM_{2.5}$ and AOD at 14:00 LT increases from 0.63 to 0.76, and R^2 of multi-year averaged $PM_{2.5}$ and AOD by time of day increases from 0.01 to 0.93, 0.24 to 0.84, 0.85 to 0.91 and 0.84 to 0.93 in four seasons respectively.

The aerosol particles in Beijing are primarily fine-mode and absorbing aerosols in terms of particle size and optical property. Due to the long-range transport of aerosols

from northwest arid areas, dust aerosols is heavy in spring and winter, particularly in spring. It shows that η varies from 54.32 to 183.14, 87.32 to 104.79, 95.13 to 163.52 and 1.23 to 235.08 μg/m^3 with the aerosol type in spring, summer, fall and winter, respectively. η is generally smaller for scattering-dominant aerosols than for absorbing-dominant aerosols, and smaller for coarse mode aerosols than for fine mode aerosols.

The surface wind speed significantly affects the occurrence of haze events. For good air quality ($PM_{2.5}$<50 μg/m^3), the occurrence rate increases with increasing wind speed, ranging from 39.3% (v<=1 m/s) to 92.9% (v>7 m/s). Differently, the occurrence of poor air quality ($PM_{2.5}$>150 μg/m^3) ranges from 20.92% (v<=1 m/s) to 0 (v>7 m/s). It shows that η decreases with the increasing surface wind speed, indicating that the contribution of surface $PM_{2.5}$ concentrations to AOD decreases with surface wind speed.

The vertical structure of aerosol distribution exhibits a remarkable change with seasons, which could also contribute a lot to the AOD-$PM_{2.5}$ relationship. This study shows that aerosols mainly concentrate within about 500 m height in summer, while concentrate within the surface layer of around 150 m height in winter in Beijing. Compared to the AOD of the whole atmosphere, AOD below 500 m has a better correlation with $PM_{2.5}$, of which R^2 is 0.77 and RMSE is 38.6 μg/m^3.

With these findings, we need consider at least the impacts of PBLH, RH, Wind speed and wind direction, and use the AOD within PBL heights to build up better $PM_{2.5}$-AOD relationship. The impacts of these influential factors have been investigated while an optimal empirical $PM_{2.5}$-AOD relationship scheme has not been reached, which

definitely need further study in future.

Acknowledgements

This work was supported by the National Natural Science Foundation of China (NSFC: grant 41575143), the Ministry of Science and Technology of China (grants 20 13CB955802), the China "1000 Plan" young scholar program, and the Chinese Progra m for New Century Excellent Talents in University (NCET). Sincerest thanks to the AERONET, MODIS and CALIPSO teams for their datasets. The CALIPSO data were acquired from the NASA Langley Research Center Atmospheric Science Data Center. Special thanks to the U.S. Embassy and CMA providing the $PM_{2.5}$ data and meteorological data respectively.

References

Alebrecht, B. A.: Aerosols, cloud microphysics, and fractional cloudiness, SCIENCE, 245, 1227-1230, 10.1126/science.245.4923.1227, 1989.

Bibi, H., Alam, K., Chishtie, F., et al.: Intercomparison of MODIS, MISR, OMI, and CALIPSO aerosol optical depth retrievals for four locations on the Indo-Gangetic plains and validation against AERONET data, Atmospheric Environment, 111, 113-126, 2015.

Charlson, R. J., Schwartz, S. E., Hales, J. M., Cess, R. D., Coakley, J. A., Hansen, J. E., and Hofmann, D. J.: Climate forcing by anthropogenic aerosols, SCIENCE, 255, 423-430, 10.1126/science.255.5043.423, 1992.

Corbin, K. C., Kreidenweis, S. M., and Vonder Haar, T. H.: Comparison of aerosol properties derived from Sun photometer data and ground-based chemical measurements, GEOPHYSICAL RESEARCH LETTERS, 29, 10.1029/2001gl014105, 2002.

Dee, D. P., Uppala, S. M., Simmons, A. J., Berrisford, P., Poli, P., Kobayashi, S., Andrae, U., Balmaseda, M. A., Balsamo, G., Bauer, P., Bechtold, P., Beljaars, A. C. M., van de Berg, L., Bidlot, J., Bormann, N., Delsol, C., Dragani, R., Fuentes, M., Geer, A. J., Haimberger, L., Healy, S. B., Hersbach, H., Holm, E. V., Isaksen, L., Kallberg, P., Koehler, M., Matricardi, M., McNally, A. P., Monge-Sanz, B. M., Morcrette, J. J., Park, B. K., Peubey, C., de Rosnay, P., Tavolato, C., Thepaut, J. N., and Vitart, F.: The ERA-Interim reanalysis: configuration and performance of the data

assimilation system, QUARTERLY JOURNAL OF THE ROYAL METEOROLOGICAL SOCIETY, 137, 553-597, 10.1002/qj.828, 2011.

Drury, E., Jacob, D. J., Wang, J., Spurr, R. J. D., and Chance, K.: Improved algorithm for MODIS satellite retrievals of aerosol optical depths over western North America, JOURNAL OF GEOPHYSICAL RESEARCH-ATMOSPHERES, 113, 10.1029/2007jd009573, 2008.

Dubovik, O., Smirnov, A., Holben, B. N., King, M. D., Kaufman, Y. J., Eck, T. F., and Slutsker, I.: Accuracy assessments of aerosol optical properties retrieved from Aerosol Robotic Network (AERONET) Sun and sky radiance measurements, JOURNAL OF GEOPHYSICAL RESEARCH-ATMOSPHERES, 105, 9791-9806, 10.1029/2000jd900040, 2000.

Feingold, G.: Modeling of the first indirect effect: Analysis of measurement requirements, GEOPHYSICAL RESEARCH LETTERS, 30, 10.1029/2003gl017967, 2003.

Garrett, T. J., Zhao, C., Dong, X., Mace, G. G., and Hobbs, P. V.: Effects of varying aerosol regimes on low-level Arctic stratus, GEOPHYSICAL RESEARCH LETTERS, 31, 10.1029/2004gl019928, 2004.

Garrett, T. J., and Zhao, C. F.: Increased Arctic cloud longwave emissivity associated with pollution from mid-latitudes, NATURE, 440, 787-789, 10.1038/nature04636, 2006.

Green, M., Kondragunta, S., Ciren, P., and Xu, C.: Comparison of GOES and MODIS

Aerosol Optical Depth (AOD) to Aerosol Robotic Network (AERONET) AOD and IMPROVE $PM_{2.5}$ Mass at Bondville, Illinois, JOURNAL OF THE AIR & WASTE MANAGEMENT ASSOCIATION, 59, 1082-1091, 10.3155/1047-3289.59.9.1082, 2009.

Guinot, B., Roger, J.-C., Cachier, H., Wang, P., Bai, J., and Tong, Y.: Impact of vertical atmospheric structure on Beijing aerosol distribution, ATMOSPHERIC ENVIRONMENT, 40, 5167-5180, 10.1016/j.atmosenv.2006.03.051, 2006.

Guo, J., Deng, M., Lee, S. S., Wang, F., Li, Z., Zhai, P., Liu, H., Lv, W., Yao, W., and Li, X.: Delaying precipitation and lightning by air pollution over the Pearl River Delta. Part I: Observational analyses, JOURNAL OF GEOPHYSICAL RESEARCH-ATMOSPHERES, 121, 6472-6488, 10.1002/2015jd023257, 2016a.

Guo, J., Miao, Y., Zhang, Y., Liu, H., Li, Z., Zhang, W., He, J., Lou, M., Yan, Y., Bian, L., and Zhai, P.: The climatology of planetary boundary layer height in China derived from radiosonde and reanalysis data, ATMOSPHERIC CHEMISTRY AND PHYSICS, 16, 13309-13319, 10.5194/acp-16-13309-2016, 2016b.

Hand, J. L., Kreidenweis, S. M., Slusser, J., and Scott, G.: Comparisons of aerosol optical properties derived from Sun photometry to estimates inferred from surface measurements in Big Bend National Park, Texas, ATMOSPHERIC ENVIRONMENT, 38, 6813-6821, 10.1016/j.atmosenv.2004.09.004, 2004.

Holben, B. N., Eck, T. F., Slutsker, I., Tanre, D., Buis, J. P., Setzer, A., Vermote, E., Reagan, J. A., Kaufman, Y. J., Nakajima, T., Lavenu, F., Jankowiak, I., and

Smirnov, A.: AERONET - A federated instrument network and data archive for aerosol characterization, REMOTE SENSING OF ENVIRONMENT, 66, 1-16, 10.1016/s0034-4257(98)00031-5, 1998.

Huang, J., Wang, T., Wang, W., Li, Z., and Yan, H.: Climate effects of dust aerosols over East Asian arid and semiarid regions, JOURNAL OF GEOPHYSICAL RESEARCH-ATMOSPHERES, 119, 11398-11416, 10.1002/2014jd021796, 2014.

Hunt, W. H., Winker, D. M., Vaughan, M. A., Powell, K. A., Lucker, P. L., and Weimer, C.: CALIPSO Lidar Description and Performance Assessment, JOURNAL OF ATMOSPHERIC AND OCEANIC TECHNOLOGY, 26, 1214-1228, 10.1175/2009jtecha1223.1, 2009.

Jiang, J., Zhou, W., Cheng, Z., Wang, S., He, K., and Hao, J.: Particulate Matter Distributions in China during a Winter Period with Frequent Pollution Episodes (January 2013), AEROSOL AND AIR QUALITY RESEARCH, 15, 494-U157, 10.4209/aaqr.2014.04.0070, 2015.

Kaufman, Y. J., and Fraser, R. S.: The effect of smoke particles on clouds and climate forcing, 5332, 1636-1639 pp., 1997.

Koren, I., Kaufman, Y. J., Remer, L. A., and Martins, J. V.: Measurement of the effect of Amazon smoke on inhibition of cloud formation, SCIENCE, 303, 1342-1345, 10.1126/science.1089424, 2004.

Kumar, N., Chu, A., and Foster, A.: An empirical relationship between $PM_{2.5}$ and aerosol optical depth in Delhi Metropolitan, ATMOSPHERIC ENVIRONMENT,

41, 4492-4503, 10.1016/j.atmosenv.2007.01.046, 2007.

Lee, J., Kim, J., Song, C. H., Kim, S. B., Chun, Y., Sohn, B. J., and Holben, B. N.: Characteristics of aerosol types from AERONET sunphotometer measurements, ATMOSPHERIC ENVIRONMENT, 44, 3110-3117, 10.1016/j.atmosenv.2010.05.035, 2010.

Levy, R. C., Remer, L. A., Kleidman, R. G., Mattoo, S., Ichoku, C., Kahn, R., and Eck, T. F.: Global evaluation of the Collection 5 MODIS dark-target aerosol products over land, ATMOSPHERIC CHEMISTRY AND PHYSICS, 10, 10399-10420, 10.5194/acp-10-10399-2010, 2010.

Li, J., Han, Z., and Zhang, R.: Influence of aerosol hygroscopic growth parameterization on aerosol optical depth and direct radiative forcing over East Asia, ATMOSPHERIC RESEARCH, 140, 14-27, 10.1016/j.atmosres.2014.01.013, 2014.

Li, S., Joseph, E., Min, Q., Yin, B., Sakai, R., and Payne, M. K.: Remote sensing of $PM_{2.5}$ during cloudy and nighttime periods using ceilometer backscatter, ATMOSPHERIC MEASUREMENT TECHNIQUES, 10, 2093-2104, 10.5194/amt-10-2093-2017, 2017.

Li, Z., Niu, F., Fan, J., Liu, Y., Rosenfeld, D., and Ding, Y.: Long-term impacts of aerosols on the vertical development of clouds and precipitation, NATURE GEOSCIENCE, 4, 888-894, 10.1038/ngeo1313, 2011.

Liu, P., Zhao, C.,Zhang, Q., Deng, Z., Huang, M., Ma, X., and Tie, X.: Aircraft study

of aerosol vertical distributions over Beijing and their optical properties. *Tellus B.*, **61**, 756–767, doi: 10.1111/j.1600-0889.2009.00440.x, 2009.

Liu, X., Cheng, Y., Zhang, Y., Jung, J., Sugimoto, N., Chang, S.-Y., Kim, Y. J., Fan, S., and Zeng, L.: Influences of relative humidity and particle chemical composition on aerosol scattering properties during the 2006 PRD campaign, ATMOSPHERIC ENVIRONMENT, 42, 1525-1536, 10.1016/j.atmosenv.2007.10.077, 2008.

Lohmann, U., and Feichter, J.: Global indirect aerosol effects: a review, ATMOSPHERIC CHEMISTRY AND PHYSICS, 5, 715-737, 2005.

Ma, Z., Hu, X., Huang, L., Bi, J., and Liu, Y.: Estimating ground-Level $PM_{2.5}$ in China using satellite remote sensing, ENVIRONMENTAL SCIENCE & TECHNOLOGY, 48, 7436-7444, 10.1021/es5009399, 2014.

Menon, S., Hansen, J., Nazarenko, L., and Luo, Y. F.: Climate effects of black carbon aerosols in China and India, SCIENCE, 297, 2250-2253, 10.1126/science.1075159, 2002.

Paciorek, C. J., Liu, Y., Moreno-Macias, H., and Kondragunta, S.: Spatiotemporal associations between GOES aerosol optical depth retrievals and ground-level $PM_{2.5}$, ENVIRONMENTAL SCIENCE & TECHNOLOGY, 42, 5800-5806, 10.1021/es703181j, 2008.

Pope, C. A., Burnett, R. T., Thun, M. J., Calle, E. E., Krewski, D., Ito, K., and Thurston, G. D.: Lung cancer, cardiopulmonary mortality, and long-term exposure to fine particulate air pollution, JAMA-JOURNAL OF THE AMERICAN MEDICAL

ASSOCIATION, 287, 1132-1141, 10.1001/jama.287.9.1132, 2002.

Qian, Y., Wang, W., Leung, L. R., and Kaiser, D. P.: Variability of solar radiation under cloud-free skies in China: The role of aerosols, GEOPHYSICAL RESEARCH LETTERS, 34, 10.1029/2006gl028800, 2007.

Qian, Y., Gong, D., Fan, J., Leung, L. R., Bennartz, R., Chen, D., and Wang, W.: Heavy pollution suppresses light rain in China: Observations and modeling, JOURNAL OF GEOPHYSICAL RESEARCH-ATMOSPHERES, 114, 10.1029/2008jd011575, 2009.

Ramachandran, S.: $PM_{2.5}$ mass concentrations in comparison with aerosol optical depths over the Arabian Sea and Indian Ocean during winter monsoon, ATMOSPHERIC ENVIRONMENT, 39, 1879-1890, 10.1016/j.atmosenv.2004.12.003, 2005.

Samoli, E., Peng, R., Ramsay, T., Pipikou, M., Touloumi, G., Dominici, F., Burnett, R., Cohen, A., Krewski, D., Samet, J., and Katsouyanni, K.: Acute Effects of Ambient Particulate Matter on Mortality in Europe and North America: Results from the APHENA Study, ENVIRONMENTAL HEALTH PERSPECTIVES, 116, 1480-1486, 10.1289/ehp.11345, 2008.

Stephens, G. L., Vane, D. G., Boain, R. J., Mace, G. G., Sassen, K., Wang, Z. E., Illingworth, A. J., O'Connor, E. J., Rossow, W. B., Durden, S. L., Miller, S. D., Austin, R. T., Benedetti, A., and Mitrescu, C.: The cloudsat mission and the a-train - A new dimension of space-based observations of clouds and precipitation,

BULLETIN OF THE AMERICAN METEOROLOGICAL SOCIETY, 83, 1771-1790, 10.1175/bams-83-12-1771, 2002.

Stull, R. B.: An introduction to boundary layer meteorology, Kluwer Academic Publishers, Dordrecht, 670 pp., 1988.

Tan, S.-C., Shi, G.-Y., and Wang, H.: Long-range transport of spring dust storms in Inner Mongolia and impact on the China seas, ATMOSPHERIC ENVIRONMENT, 46, 299-308, 10.1016/j.atmosenv.2011.09.058, 2012.

Twomey, S.: Influence of pollution on shortwave albedo of clouds, JOURNAL OF THE ATMOSPHERIC SCIENCES, 34, 1149-1152, 10.1175/1520-0469(1977)034<1149:tiopot>2.0.co;2, 1977.

van Donkelaar, A., Martin, R. V., and Park, R. J.: Estimating ground-level $PM_{2.5}$ using aerosol optical depth determined from satellite remote sensing, JOURNAL OF GEOPHYSICAL RESEARCH-ATMOSPHERES, 111, 10.1029/2005jd006996, 2006.

van Donkelaar, A., Martin, R. V., Brauer, M., Kahn, R., Levy, R., Verduzco, C., and Villeneuve, P. J.: Global Estimates of Ambient Fine Particulate Matter Concentrations from Satellite-Based Aerosol Optical Depth: Development and Application, ENVIRONMENTAL HEALTH PERSPECTIVES, 118, 847-855, 10.1289/ehp.0901623, 2010.

van Donkelaar, A., Martin, R. V., Spurr, R. J. D., Drury, E., Remer, L. A., Levy, R. C., and Wang, J.: Optimal estimation for global ground-level fine particulate matter

concentrations, JOURNAL OF GEOPHYSICAL RESEARCH-ATMOSPHERES, 118, 5621-5636, 10.1002/jgrd.50479, 2013.

Wang, J., and Christopher, S. A.: Intercomparison between satellite-derived aerosol optical thickness and $PM_{2.5}$ mass: Implications for air quality studies, GEOPHYSICAL RESEARCH LETTERS, 30, 10.1029/2003gl018174, 2003.

Wang, T., Li, S., Shen, Y., Deng, J., and Xie, M.: Investigations on direct and indirect effect of nitrate on temperature and precipitation in China using a regional climate chemistry modeling system, JOURNAL OF GEOPHYSICAL RESEARCH-ATMOSPHERES, 115, 10.1029/2009jd013264, 2010a.

Wang, J., Xu, X., Spurr, R., Wang, Y., and Drury, E.: Improved algorithm for MODIS satellite retrievals of aerosol optical thickness over land in dusty atmosphere: Implications for air quality monitoring in China, REMOTE SENSING OF ENVIRONMENT, 114, 2575-2583, 10.1016/j.rse.2010.05.034, 2010b.

Wang, Y., Chen, L., Li, S., Wang, X., Yu, C., Si, Y., and Zhang, Z.: Interference of Heavy Aerosol Loading on the VIIRS Aerosol Optical Depth (AOD) Retrieval Algorithm, REMOTE SENSING, 9, 10.3390/rs9040397, 2017.

Winker, D. M., Hunt, W. H., and McGill, M. J.: Initial performance assessment of CALIOP, GEOPHYSICAL RESEARCH LETTERS, 34, 10.1029/2007gl030135, 2007.

Winker, D. M., Vaughan, M. A., Omar, A., Hu, Y., Powell, K. A., Liu, Z., Hunt, W. H., and Young, S. A.: Overview of the CALIPSO Mission and CALIOP Data

Processing Algorithms, JOURNAL OF ATMOSPHERIC AND OCEANIC TECHNOLOGY, 26, 2310-2323, 10.1175/2009jtecha1281.1, 2009.

Xin, J., Gong, C., Liu, Z., Cong, Z., Gao, W., Song, T., Pan, Y., Sun, Y., Ji, D., Wang, L., Tang, G., and Wang, Y.: The observation-based relationships between $PM_{2.5}$ and AOD over China, JOURNAL OF GEOPHYSICAL RESEARCH-ATMOSPHERES, 121, 10701-10716, 10.1002/2015jd024655, 2016.

Xing, J., Mathur, R., Pleim, J., Hogrefe, C., Gan, C.-M., Wong, D. C., Wei, C., and Wang, J.: Air pollution and climate response to aerosol direct radiative effects: A modeling study of decadal trends across the northern hemisphere, JOURNAL OF GEOPHYSICAL RESEARCH-ATMOSPHERES, 120, 10.1002/2015jd023933, 2015.

Xu, P., Chen, Y., and Ye, X.: Haze, air pollution, and health in China, LANCET, 382, 2067-2067, 2013.

Yan, Y., Sun, Y. B., Weiss, D., Liang, L. J., and Chen, H. Y.: Polluted dust derived from long-range transport as a major end member of urban aerosols and its implication of non-point pollution in northern China, SCIENCE OF THE TOTAL ENVIRONMENT, 506, 538-545, 10.1016/j.scitotenv.2014.11.071, 2015.

Yang, X., Zhao, C., Zhou, L., Wang, Y., and Liu, X.: Distinct impact of different types of aerosols on surface solar radiation in China, JOURNAL OF GEOPHYSICAL RESEARCH-ATMOSPHERES, 121, 6459-6471, 10.1002/2016jd024938, 2016.

Yu, X., Zhu, B., and Zhang, M.: Seasonal variability of aerosol optical properties over

Beijing, ATMOSPHERIC ENVIRONMENT, 43, 4095-4101, 10.1016/j.atmosenv.2009.03.061, 2009.

Zhang, H., Hoff, R. M., and Engel-Cox, J. A.: The Relation between Moderate Resolution Imaging Spectroradiometer (MODIS) Aerosol Optical Depth and $PM_{2.5}$ over the United States: A Geographical Comparison by US Environmental Protection Agency Regions, JOURNAL OF THE AIR & WASTE MANAGEMENT ASSOCIATION, 59, 1358-1369, 10.3155/1047-3289.59.11.1358, 2009a.

Zhang, M., Song, Y., Cai, X., Lin, W. S., Sui, C. H., Yang, L. M., Wang, X. M., Deng, R. R., Fani, S. J., Wu, C. S., Wang, A. Y., Fong, S. K., and Lin, H.: A health-based assessment of particulate air pollution in urban areas of Beijing in 2000-2004.

Zhang, Q., Ma, X., Tie, X., Huang, M., and Zhao, C.: Vertical distributions of aerosols under different weather conditions: Analysis of in-situ aircraft measurements in Beijing, China, ATMOSPHERIC ENVIRONMENT, 43, 5526-5535, 10.1016/j.atmosenv.2009.05.037, 2009b.

Zhao, C., Klein, S. A., Xie, S., Liu, X., Boyle, J. S., and Zhang, Y.: Aerosol first indirect effects on non-precipitating low-level liquid cloud properties as simulated by CAM5 at ARM sites, GEOPHYSICAL RESEARCH LETTERS, 39, 10.1029/2012gl051213, 2012.

Zhao, C., and Garrett, T. J.: Effects of Arctic haze on surface cloud radiative forcing, GEOPHYSICAL RESEARCH LETTERS, 42, 557-564, 10.1002/2014gl062015,

2015.

Zheng, S., Pozzer, A., Cao, C. X., and Lelieveld, J.: Long-term (2001-2012) concentrations of fine particulate matter ($PM_{2.5}$) and the impact on human health in Beijing, China, ATMOSPHERIC CHEMISTRY AND PHYSICS, 15, 5715-5725, 10.5194/acp-15-5715-2015, 2015.

Zhuang, B. L., Li, S., Wang, T. J., Deng, J. J., Xie, M., Yin, C. Q., and Zhu, J. L.: Direct radiative forcing and climate effects of anthropogenic aerosols with different mixing states over China, ATMOSPHERIC ENVIRONMENT, 79, 349-361, 10.1016/j.atmosenv.2013.07.004, 2013.

Table 1. Comparison of AERONET and MODIS AOD by season and over all seasons.

Season	**AERONET mean AOD**	**MODIS mean AOD**	**R^2**	**Bias**	**Bias%**	**RMSE**	***N***
Spring	0.49	0.66	0.81	0.18	36.7	0.23	214
Summer	0.61	0.88	0.87	0.27	44.7	0.29	103
Fall	0.30	0.39	0.69	0.10	32.9	0.15	50
Winter	0.19	0.21	0.34	0.02	10.2	0.08	48
All	0.46	0.63	0.85	0.17	37.8	0.23	415

Note: Bias% is defined as 100 × (MODIS AOD-AERONET AOD)/AERONET AOD (Green et al., 2009). RMSE is the root mean squared prediction error ($\mu g/m^3$).Period for comparison is 2011–2015.

Table 2. Comparison of AERONET and CALIPSO AOD by season and over all seasons

Season	**AERONET mean AOD**	**CALIPSO mean AOD**	**R^2**	**Bias**	**Bias%**	**RMSE**	***N***
Spring	0.44	0.42	0.52	-0.02	-5.2	0.33	21
Summer	0.53	0.57	0.47	0.04	6.6	0.32	16
Fall	0.95	0.81	0.85	-0.14	-14.2	0.34	12
Winter	0.42	0.53	0.55	0.11	25.0	0.27	21
All	0.54	0.55	0.65	0.01	1.7	0.31	70

Table 3. Correlations between AOD and $PM_{2.5}$ mass by dominant aerosol specie

Dominant Aerosol Specie	**R^2**	**RMSE (μg/m^3)**	***N***
Coarse Absorbing	0.56	27.07	480
Mixed Absorbing	0.67	36.44	1383
Fine Absorbing	0.53	48.06	2143
Coarse Non-absorbing	0.10	44.51	56
Mixed Non-absorbing	0.61	44.05	234
Fine Non-absorbing	0.58	40.19	434
All	0.51	46.34	4728

Figure Captions

Figure 1. Flow chart of deriving aerosol vertical profile from CALIPSO data.

Figure 2. The aerosol classification scheme in four seasons from 2011 to 2015 using AE, SSA and FMF data from AERONET at sites in Beijing. The scatter plots of different colors is the distribution of aerosol types with different physic-optics characteristics in four seasons.

Figure 3. Scatter plots of AERONET AOD vs. MODIS AOD (a), and AERONET AOD vs. CALIPSO AOD (b) for the period of 2011 to 2015 in Beijing.

Figure 4. Comparison of monthly averaged RH and PBLH (a), AOD and $PM_{2.5}$ (b), AOD_{dry} and $PM_{2.5\_column}$ (c) at 14:00 LT for the period of 2011 to 2015 in Beijing. The blue, purple, green and yellow bands in (a) are for high PBLH and low RH, low PBLH and high PBLH, low PBLH and low RH, high PBLH and high RH, respectively.

Figure 5. Diurnal variations of multi-year (2011-2015) averaged RH and PBLH over four seasons in Beijing.

Figure 6. Comparison of multi-year (2011-2015) averaged RH and PBLH (a1~d1), AOD and $PM_{2.5}$ (a2~d2), AOD_{dry} and $PM_{2.5\_column}$ (a3~d3) by time of day in different seasons. The columns represent four seasons and the rows represent three different variables.

Figure 7. The frequency distribution of aerosol types over four seasons for the period of 2011 to 2015 in Beijing.

Figure 8. The variation of η with the aerosol type in four seasons for the period of 2011 to 2015.

Figure 9. Scatter plots between AERONET AOD and $PM_{2.5}$ concentrations in four different seasons for five different types of aerosols. The first to 5^{th} columns represent the aerosol types of coarse absorbing, mixed absorbing, fine absorbing, mixed non-absorbing, and fine non-absorbing, respectively. The colors also represent different aerosol types. The rows represent four seasons.

Figure 10. Wind rose of Beijing in four seasons for the period of 2011 to 2015.

Figure 11. The relative distribution of $PM_{2.5}$ within different value ranges at Beijing for different surface wind speed in different wind direction.

Figure 12. The relative distribution of AOD (upper panel) and $PM_{2.5}$ (lower panel) within different value ranges at Beijing for different surface wind speed ranges

from 2011 to 2015. v and N represent the wind speed and samples respectively. The colors represent the value ranges of AOD (upper panel) and $PM_{2.5}$ (lower panel).

Figure 13. Variation of averaged AOD, $PM_{2.5}$ (left panel) and η (right panel) with the surface wind speed.

Figure 14. Scatter plots of stratified AOD vs. PM2.5 concentrations. The red solid line is the linear fitting regression lines. It shows the relationship between (a) AOD below 500m, (b) AOD below 1000m, (c) AOD below PBL and (d) AOD of the whole atmosphere and PM2.5 concentrations.

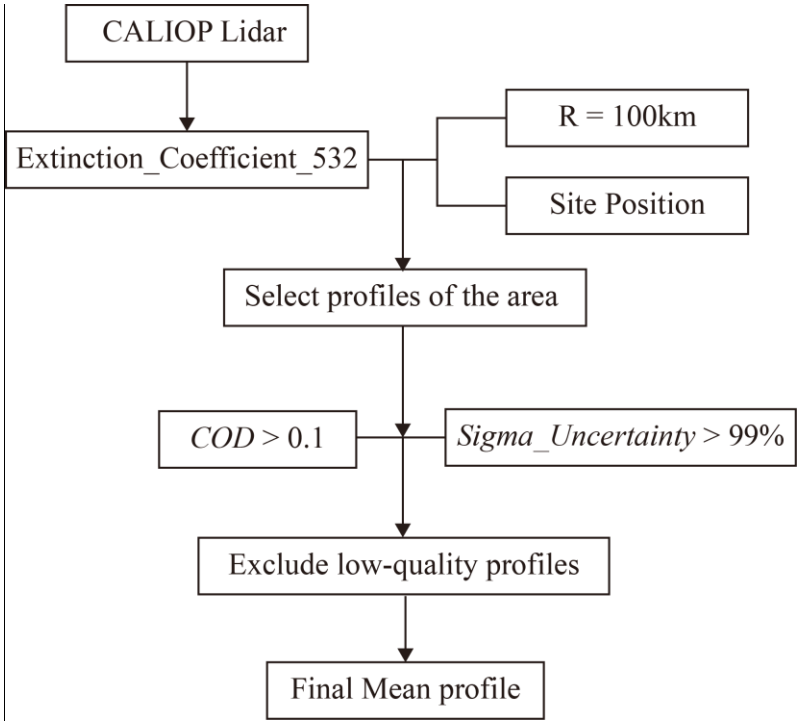

Figure 1. Flow chart of deriving aerosol vertical profile from CALIPSO data.

Figure 2. The aerosol classification scheme in four seasons from 2011 to 2015 using AE, SSA and FMF data from AERONET at sites in Beijing. The scatter plots of different colors is the distribution of aerosol types with different physic-optics characteristics in four seasons.

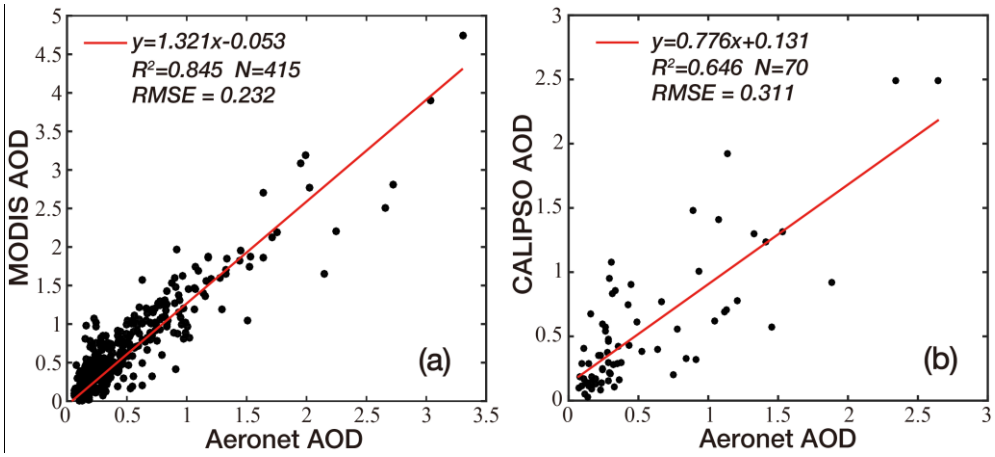

Figure 3. Scatter plots of AERONET AOD vs. MODIS AOD (a), and AERONET AOD vs. CALIPSO AOD (b) for the period of 2011 to 2015 in Beijing.

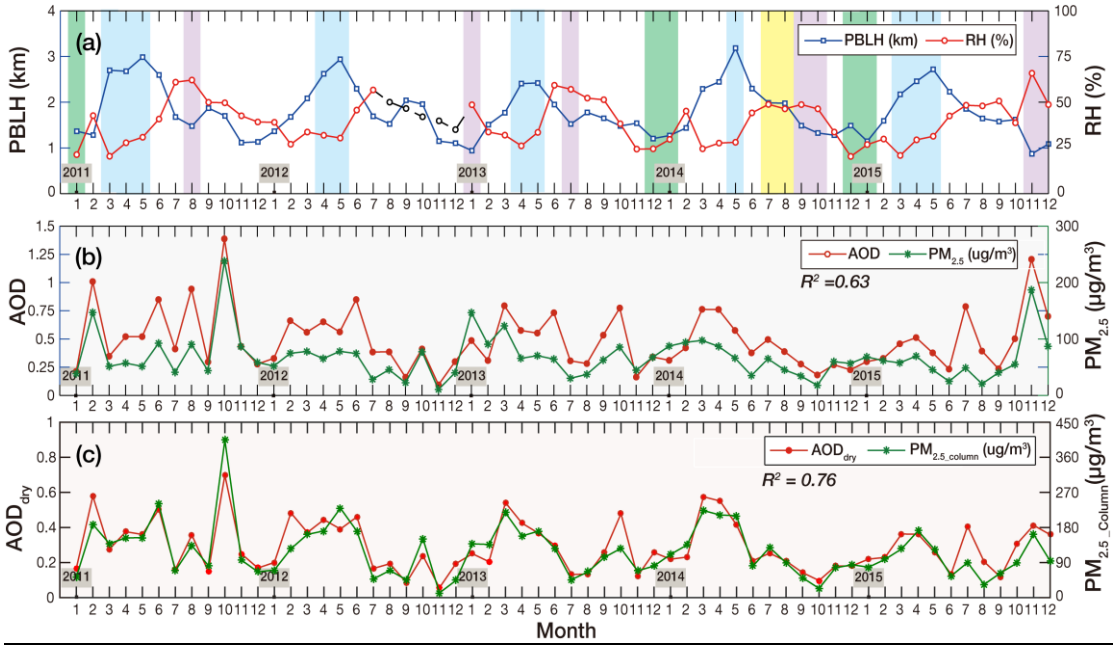

Figure 4. Comparison of monthly averaged RH and PBLH (a), AOD and $PM_{2.5}$ (b), AOD_{dry} and $PM_{2.5\_column}$ (c) at 14:00 LT for the period of 2011 to 2015 in Beijing. The blue, purple, green and yellow bands in (a) are for high PBLH and low RH, low PBLH and high PBLH, low PBLH and low RH, high PBLH and high RH, respectively.

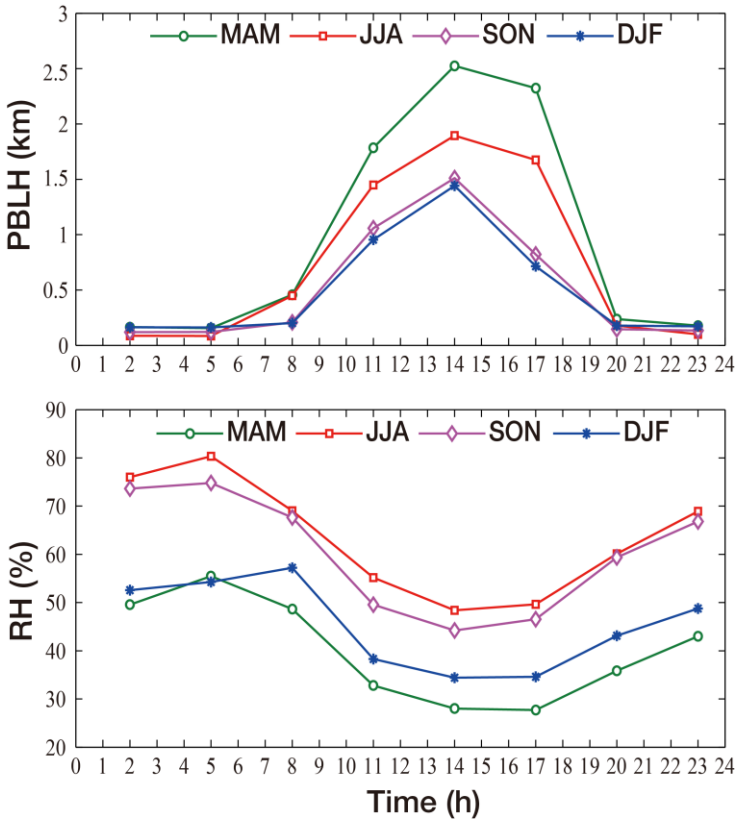

Figure 5. Diurnal variations of multi-year (2011-2015) averaged RH and PBLH over four seasons in Beijing.

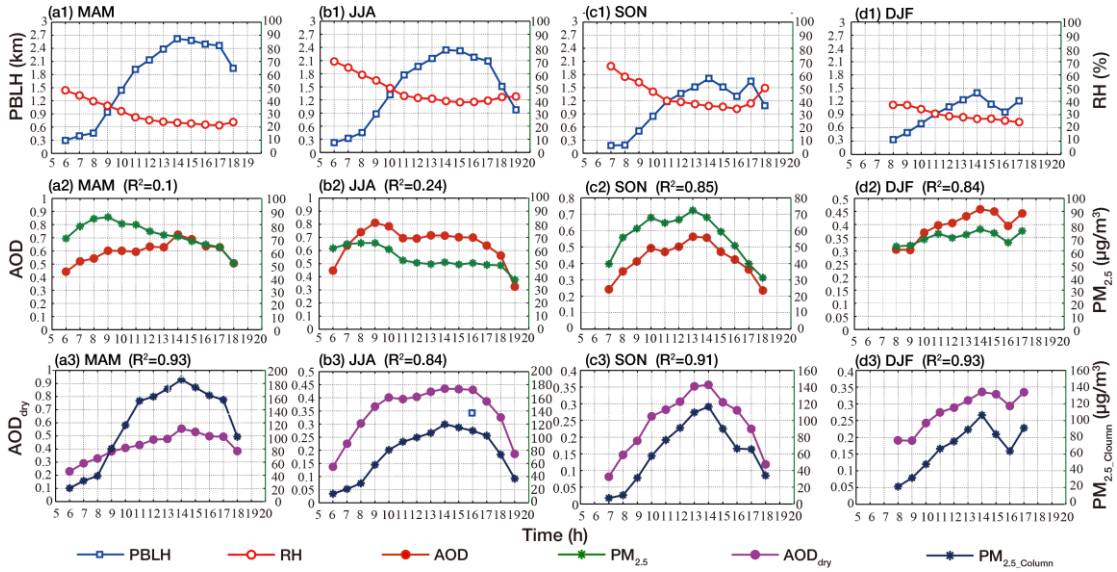

Figure 6. Comparison of multi-year (2011-2015) averaged RH and PBLH (a1~d1), AOD and $PM_{2.5}$ (a2~d2), AOD_{dry} and $PM_{2.5\_column}$ (a3~d3) by time of day in different seasons. The columns represent four seasons and the rows represent three different variables.

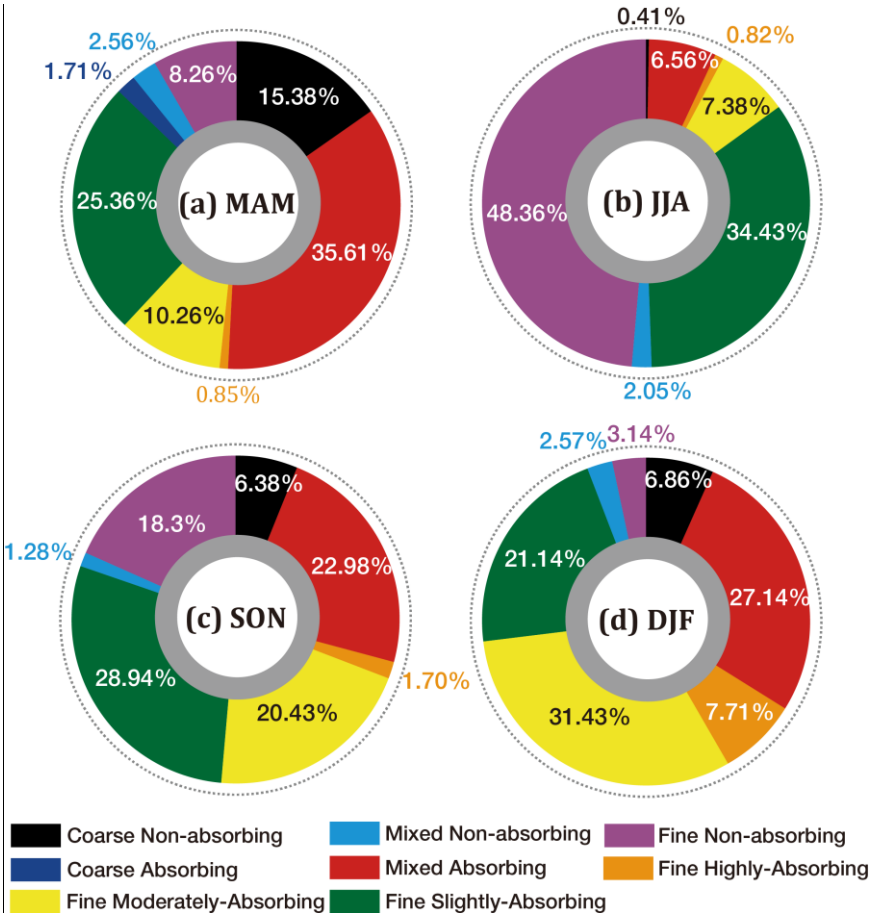

Figure 7. The frequency distribution of aerosol types over four seasons for the period of 2011 to 2015 in Beijing.

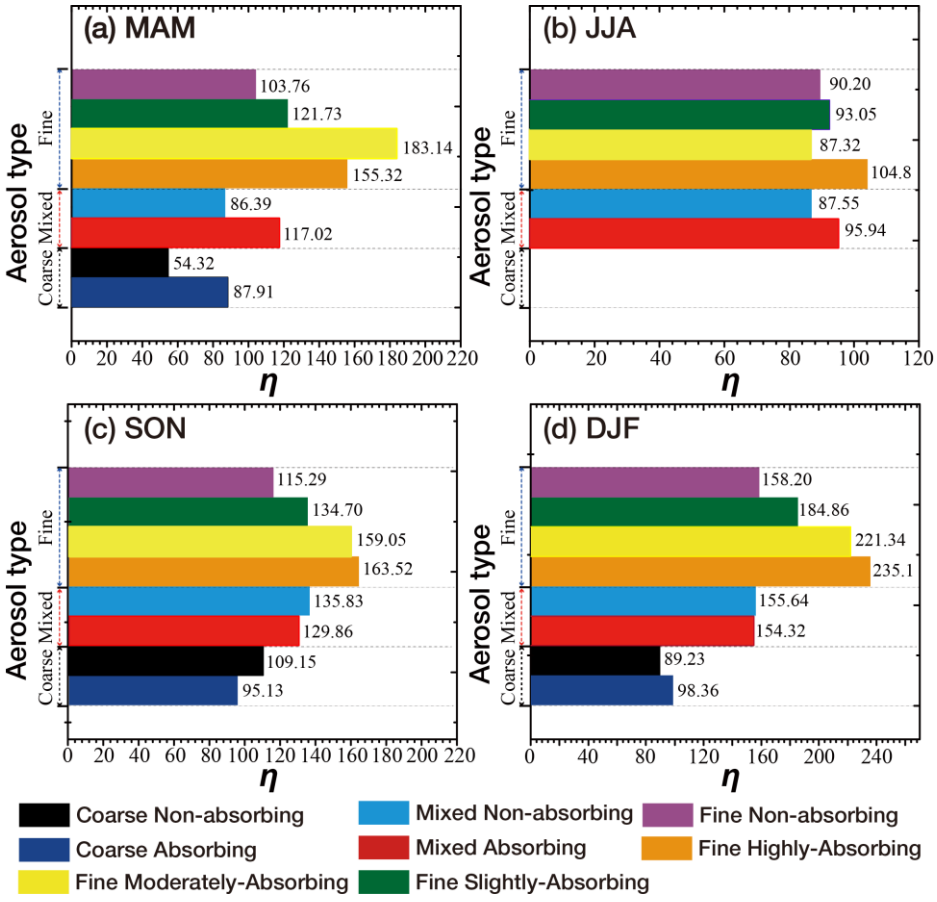

Figure 8. The variation of η with the aerosol type in four seasons for the period of 2011 to 2015.

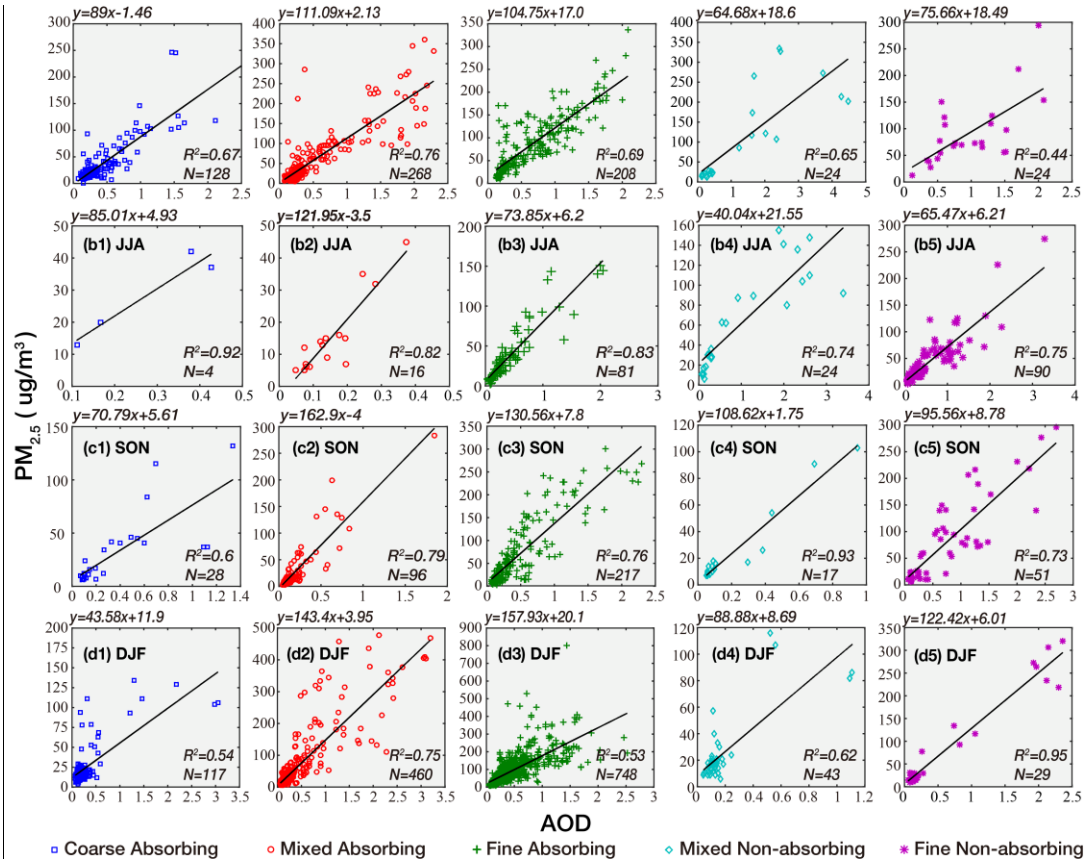

Figure 9. Scatter plots between AERONET AOD and $PM_{2.5}$ concentrations in four different seasons for five different types of aerosols. The first to 5th columns represent the aerosol types of coarse absorbing, mixed absorbing, fine absorbing, mixed non-absorbing, and fine non-absorbing, respectively. The colors also represent different aerosol types. The rows represent four seasons.

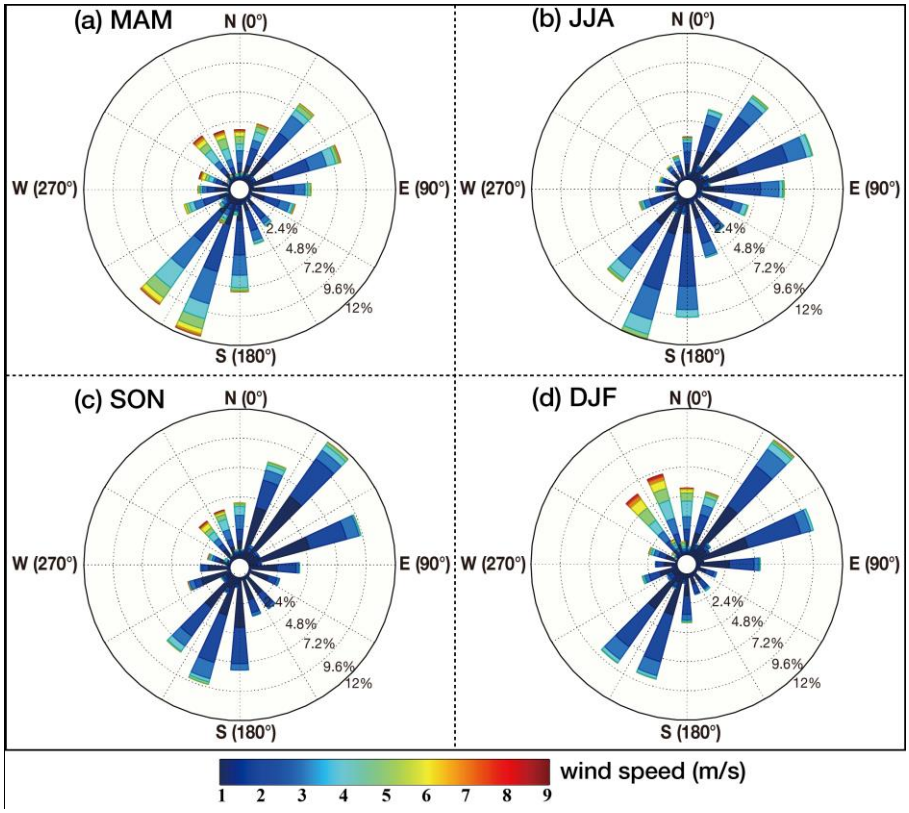

Figure 10. Wind rose of Beijing in four seasons for the period of 2011 to 2015

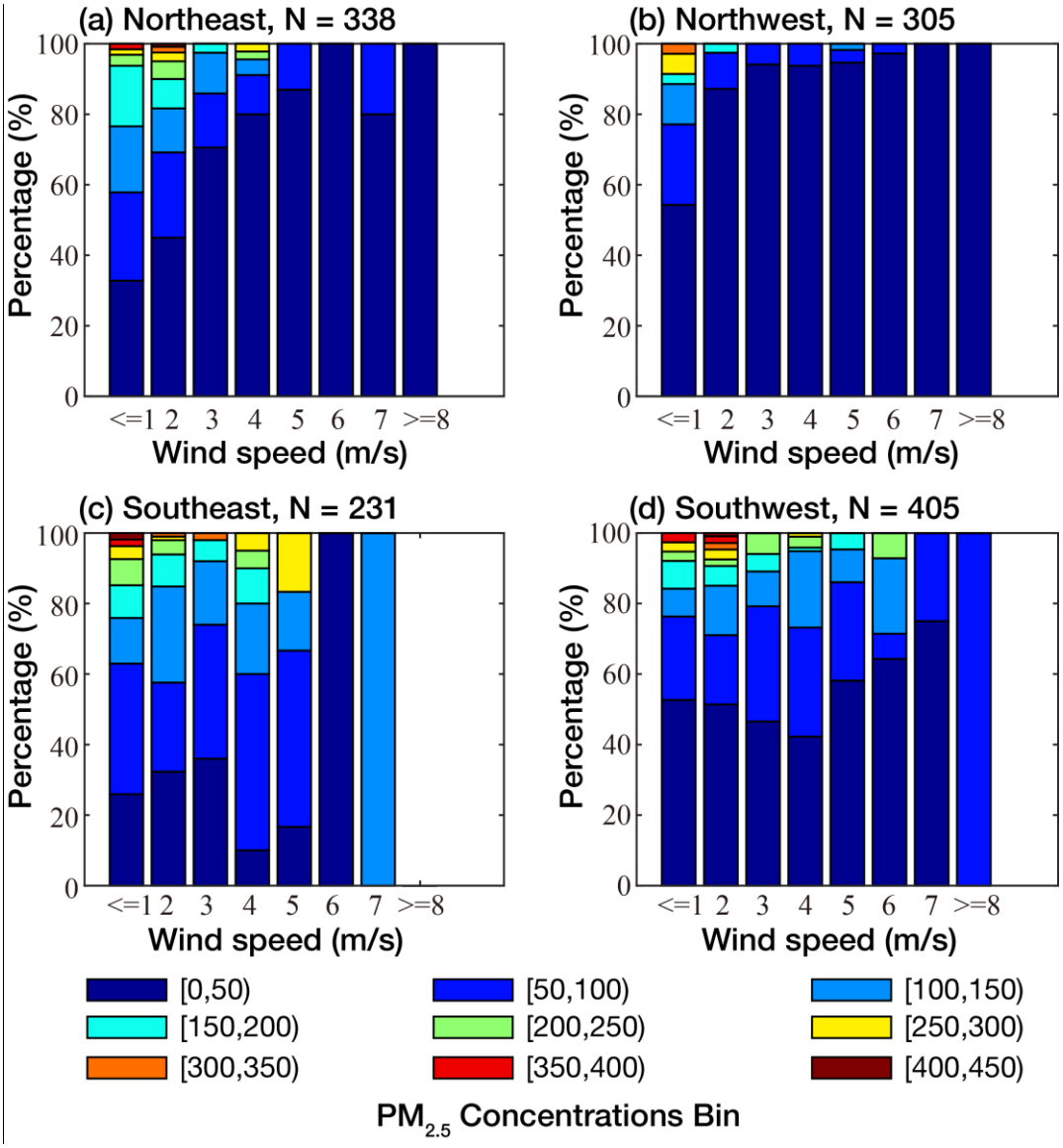

Figure 11. The relative distribution of $PM_{2.5}$ within different value ranges at Beijing for different surface wind speed in different wind direction.

5

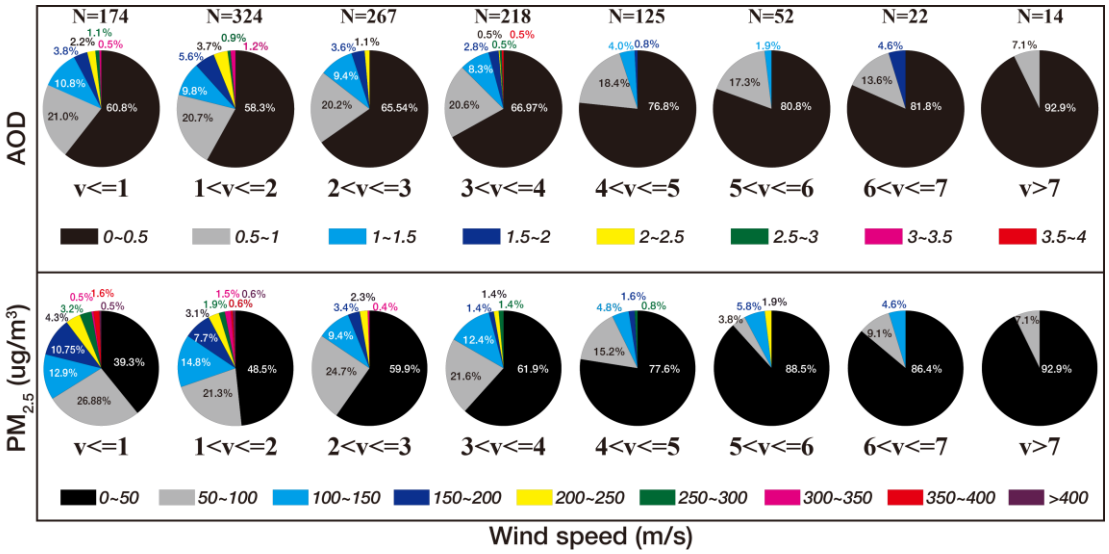

Figure 12. The relative distribution of AOD (upper panel) and $PM_{2.5}$ (lower panel) within different value ranges at Beijing for different surface wind speed ranges from 2011 to 2015. v and N represent the wind speed and samples respectively. The colors represent the value ranges of AOD (upper panel) and $PM_{2.5}$ (lower panel).

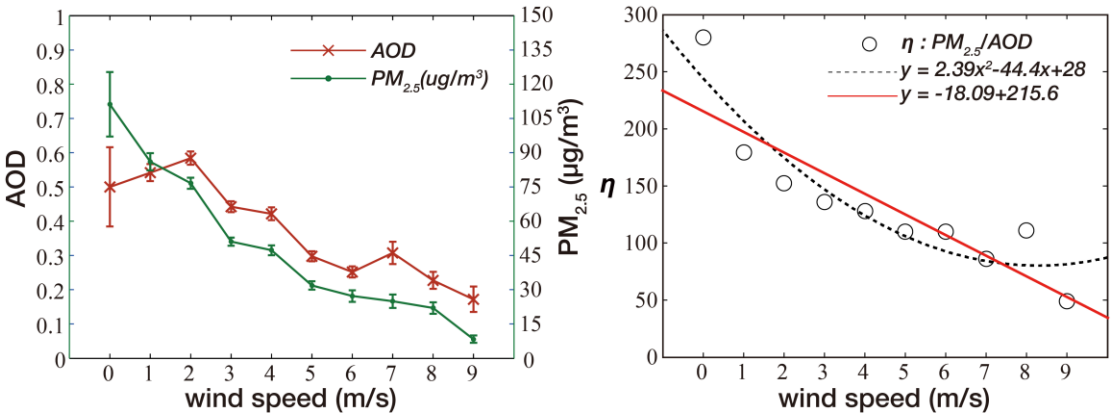

Figure 13. Variation of averaged AOD, $PM_{2.5}$ (left panel) and η (right panel) with the surface wind speed.

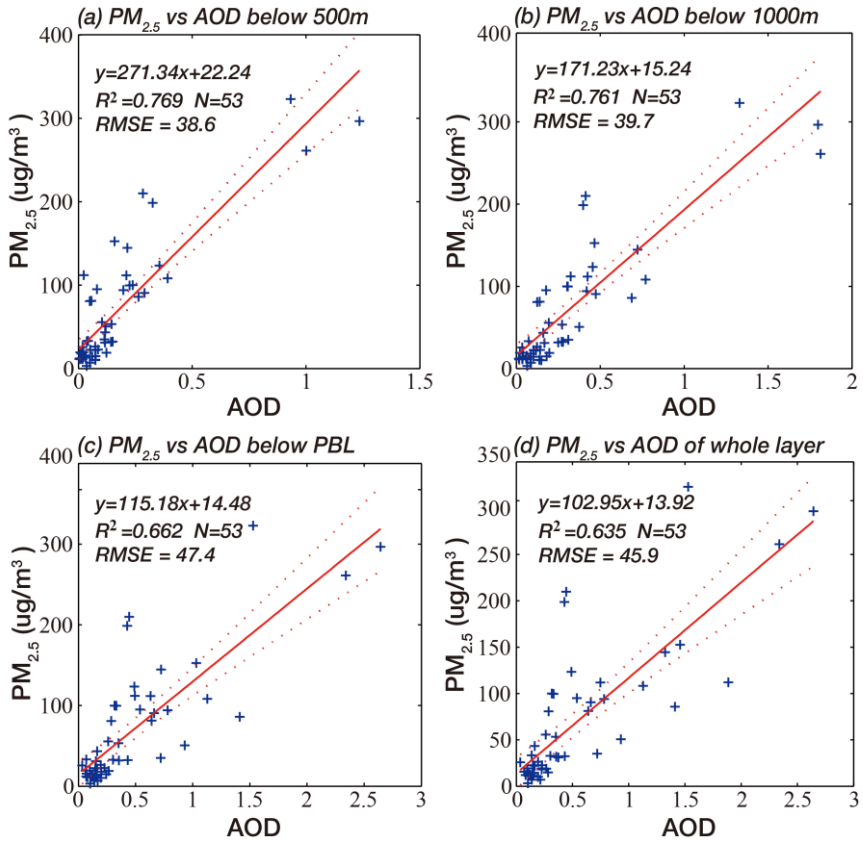

Figure 14. Scatter plots of stratified AOD vs. $PM_{2.5}$ concentrations. The red solid line is the linear fitting regression lines. It shows the relationship between (a) AOD below 500m, (b) AOD below 1000m, (c) AOD below PBL and (d) AOD of the whole atmosphere and $PM_{2.5}$ concentrations.